九州大学学術情報リポジトリ
Kyushu University Institutional Repository

Analyses of Surface Interaction Between Endothelial Cells and Poly(2-methoxyethyl acrylate)

エムディ，アジズル，ハク

https://hdl.handle.net/2324/5068193

出版情報：Kyushu University, 2022, 博士（工学）, 課程博士
バージョン：
権利関係：

Doctoral Dissertation 2022

Analyses of Surface Interaction Between Endothelial Cells and Poly(2-methoxyethyl acrylate)

九州大学

Masaru Tanaka Lab
Department of Chemistry and Biochemistry
Graduate School of Engineering
Kyushu University, Japan

Md Azizul Haque

DEDICATION

I would like to dedicate this thesis to my parents and my daughter who are always sacrificing their happiness from their own position for us

Table of Contents

Abstract

The cellular interaction with the biomaterials depends on several factors including protein adsorption, cell-substrate interaction, and cell-cell interaction. Cell adhesion strength to the substrate is a vital element to explain the biocompatibility of synthetic polymer biomaterials. In addition, cell attachment behavior on substrates also be regulated by the chemical and physical properties of the surface of biomaterials. Poly(2-methoxyethyl acrylate) (PMEA) is an FDA approved biocompatible polymer which is used as an antithrombogenic coating polymer in many sophisticated medical devices like artificial heart and lung, stents, catheter, and dialyzers etc. It is established that the water molecules interacting with PMEA can be classified into three types: free water, freezing-bound water (intermediate water), and non-freezing water. Intermediate water plays an important role to be an excellent biomaterial. PMEA can reduce the platelet adhesion by suppressing the adsorption and conformational change of fibrinogen. Recently, it was reported that non-blood cells can adhere to the coated surface of PMEA and its analogues through both integrin dependent and independent cell adhesion mechanism. However, there is no sufficient work of interaction analyses of endothelial cells and platelet PMEA analogues polymers. The present study was designed to investigate the interaction behavior of human umbilical vein endothelial cells (HUVECs) to the PMEA analogous polymer. Moreover, we have examined the HUVECs adhesion strength, HUVEC-HUVEC adhesion strength, platelet adhesion strength and number of platelet adhesion on both polymer and HUVECs monolayer, HUVEC migration analysis. We also observed the hydration state of the polymer-water interfaces. Based on our results, we indicated that the PMEA can be used as coating materials in construction of artificial small diameter blood vessel. We focus on how blood components and HUVECs interaction to biocompatible polymers in this thesis studies and whole the thesis work was separated in five following sections.

In **Chapter 1**, previous works and knowledges concerning biomaterials have been described in brief.

In **Chapter 2,** we stated HUVECs and platelet interaction analysis on PMEA analogous polymers. In this study, we extensively investigated HUVEC–polymer and platelet–polymer interaction behavior by measuring the adhesion strength using single-cell force spectroscopy. Furthermore, the hydration layer of the polymer interface was observed using frequency-modulation atomic force microscopy. We found that endothelial cells can attach and spread on the PMEA surface with strong adhesion strength compared to other analogous polymers. We confirmed that HUVECs attachment and platelet adhesion are regulated by the amount of intermediate water. In contrast, we found that the hydration layers on the PMEA analogous polymers are closely related to their platelet adhesion behavior. Based on our results, it can be concluded that PMEA is a promising candidate for the construction of artificial small-diameter blood vessels owing to the presence of intermediate water and a hydration layer on the interface.

In **Chapter 3**, we reported that the confluent monolayer of HUVECs on PMEA plays a major role in mimicking the inner surface of native blood vessels. We extensively investigated the cell-polymer and cell-cell interactions by measuring adhesion strength using single-cell force spectroscopy. In addition, attachment, and migration of HUVECs on PMEA-analogous substrates were detected, and the migration rate was estimated. Moreover, the bilateral migration of HUVECs between two adjacent surfaces was observed. Furthermore, the outer surface of HUVEC was examined using frequency-modulation atomic force microscopy (FM-AFM). Hydration was found to be an indication of a healthy glycocalyx layer. The results were compared with the hydration states of individual PMEA-analogous polymers to understand the adhesion mechanism between

the cells and substrates in the interface region. HUVECs could attach and spread on the PMEA surface with stronger adhesion strength than self-adhesion strength, and migration occurred over the surface of analogue polymers. We confirmed that platelets could not adhere to HUVEC monolayers cultured on the PMEA surface. Our findings show that PMEA can mimic original blood vessels through an antithrombogenic HUVEC monolayer and is thus suitable for the construction of artificial small-diameter blood vessels.

In **Chapter 4**, we have discussed the cell attachment behavior on biocompatible polymer brush surfaces rather the coating methods. We have investigated the HUVECs attachment ability, proliferation, and growth on grafted PMEA analogous brush system and bare gold surfaces. Immunocytochemical analysis reveals the cell morphology like cell area, circularity, aspect ratio and number of focal adhesions. In addition, HUVECs adhesion strength also measured. It was found that the polymer brush system increases the cell adhesion strength for some PMEA analogues compared to coating. We found that the elevation of adhesion strength comes due to the controlled height and grafting density (σ =0.1 chain/nm^2) of brush system and more focal adhesion formation of attached cells. Therefore, it can be said that polymer brush is an alternative of polymer coating in order to use it as a blood contacting surface.

In **Chapter 5**, the summary and future perspective of this study were described.

Chapter 1

Introduction

1.1 Overview of cardiovascular disease and its treatment

1.1.1Cardiovascular disease and its origins

Cardiovascular disease (CVD) is considered as the most common and leading cause death of around the world and the number of deaths is increasing more rapidly than before[1]. CVD is a group of diseases associated with heart and vascular disease, including coronary heart disease (CHD), cerebral arterial disease (CAD), and peripheral arterial diseases (PAD)[2,3]. Among all of them, CHD is the deadliest disease where the arteries of the heart cannot deliver enough oxygen-rich blood to the heart due to narrowed or blocked the blood vessels. The blockage of arteries is called atherosclerosis, in which fatty plaque accumulates on the arterial wall which blocks the blood flow to downstream tissues. Atherosclerosis can provoke several morphological changes such as stenosis, occlusion, or dilation, causing malperfusion of end-organs or rupture of vascular walls[4,5]. Usually, larger coronary arteries on the surface of the heart are affected by coronary artery disease whereas, coronary microvascular disease affects the tiny arteries in the heart muscle. The CVD occurrence is mostly related to changes in dietary habits, reduced exercise, increased working time, depression, national health care deficiencies and the occurred financial crisis[6–8].

Developing of atherosclerosis is significantly increased if the following symptoms appear

- Smoking: it makes stain on heart, damage the lining of arteries, and increase risk of blood clots.
- High blood pressure (hypertension): it puts a strain on your heart and can lead to CHD.

- High cholesterol: a fat made by the liver from the saturated fat
- High levels of lipoprotein (a): a risk factor for cardiovascular disease and atherosclerosis.
- Not enough regular exercise: inactivity increases fatty deposition in arteries.
- Diabetes: Blood sugar lead diabetes that double the risk of developing CHD.
- Thrombosis: a blood clot in a vein or artery that leads to a heart attack.

The following risk factors for developing atherosclerosis include:

- Obesity or overweight
- Family history of CHD

– the risk is increased for a person who have a male relative age under 55 years and women relative age under 65 years with CHD

1.1.2 Treatments of Cardiovascular disease

There are many treatments are available to treat CVD that can support to manage the symptoms and reduce the risk of further problems. Hence, all form of CVD can be managed effectively with a combination of lifestyle changes, medicine and, in some advanced cases, surgery. Therefore, an effective treatment can reduce the symptoms of CHD and improve the heart functioning. In brief-

- **Changing lifestyle:**
  - Stopping smoking quickly reduces risk of having a heart attack in future
  - Eating more healthily and doing regular exercise also reduce the future risk of heart disease.

- **Medicine:**

There are many different medicines are used to treat CHD. Usually, they either aim to reduce blood pressure or widen your arteries. Although, some heart medicines have side effects,

- Blood-thinning medicines: by thinning patients' blood and preventing it clotting.

  Common blood-thinning medicines include:

  - low-dose aspirin
  - clopidogrel
  - rivaroxaban
  - ticagrelor
  - prasugrel

- Statins: cholesterol-lowering medicine

  Examples include:

  - atorvastatin
  - simvastatin
  - rosuvastatin
  - pravastatin

- Beta blockers
- Nitrates
- Angiotensin-converting enzyme (ACE) inhibitors

- Angiotensin-2 receptor blockers (ARBs)
- Calcium channel blockers
- Diuretics

- **Procedures and surgery**

Depending on the level seriousness of CVD, or level of narrowed blood vessels as the result of a build-up of atheroma (fatty deposits) or if the symptoms cannot be controlled using medicines, then interventional procedures or surgery may be needed to open or bypass blocked arteries.

- **Coronary angioplasty**

Coronary angioplasty is sometime called in other name such as percutaneous coronary intervention (PCI), percutaneous transluminal coronary angioplasty (PTCA) or balloon angioplasty. Angioplasty is strategic procedure for someone with angina, or an urgent treatment if the CVD symptoms have become unstable or as an emergency treatment during a heart attack. During the procedure, small balloon is inserted to push the fatty tissue in the narrowed artery outwards. This allows the blood to flow more easily. A metal stent (a wire mesh tube) is usually placed in the artery to hold it open. Drug-eluting stents can also be used. These release medicines to stop the artery narrowing again. Sometimes blood compatible coating is used on the stents or other implanted device to escape from further thrombus formation on it[9,10].

- **Coronary artery bypass graft**

Sometimes, an artery that supplies blood to the chest wall is used and diverted to one of the heart arteries. This allows the blood to bypass (get around) the narrowed sections of coronary arteries.

Coronary artery bypass grafting (CABG) is also known as bypass surgery, cardiac bypass, or coronary artery bypass surgery. CABG is performed on patients with narrowed or occluded arteries. A blood vessel is inserted (transplanted) between the aorta and a part of the coronary artery beyond the narrowed or occluded area. The arteries that supply blood to the chest wall are used and may be sent to one of the arteries in the heart. This allows blood to bypass (avoid) the narrow part of the coronary arteries.

- **Heart transplant**

A heart transplant may be needed if the heart is severely damaged and medications or other treatments are ineffective, or if the heart is unable to pump enough blood around the body (heart failure). Heart transplantation involves replacing a damaged or malfunctioning heart with a healthy donor's heart. In contrast, the number of cardiac donors and surgery successfulness is very limited and rare.

1.2 Construction of native blood vessel

Blood vessels are compact and closed circulatory systems that penetrate to the most of the body’s tissues. Blood vessels are organized according to their working roles and size as either veins, capillaries or arteries[11]. Large vessels (arteries and veins) are responsible to provide efficient fluid transport to distant sites, while the small vessels (capillaries and arterioles) allow an optimal

exchange of nutrients, oxygen and waste within organs and tissues. Therefore, requirements of the design property and construction approaches are totally different for large vessels than small diameter vessels. In addition, a blood vessel is organized as three concentric layers: the tunica intima, the media and the adventitia where each of these layer is responsible for their independent but essential function: the intima, composed of endothelial cells (ECs), responsible for the anti-thrombogenic aspect; the media, composed of smooth muscle cells (SMCs), responsible for mechanical strength; and the adventitia, composed of fibroblasts (FBs), a collagen-rich connective tissue which maintains the structure, otherwise the blood vessel would be weak and fragile. These layers are trapped in a highly organized extracellular matrix (ECM) mainly composed of type I collagen, type III collagen and elastin. Shown in **Figure 1.1 (A)**. A short description is presented in the following sections.

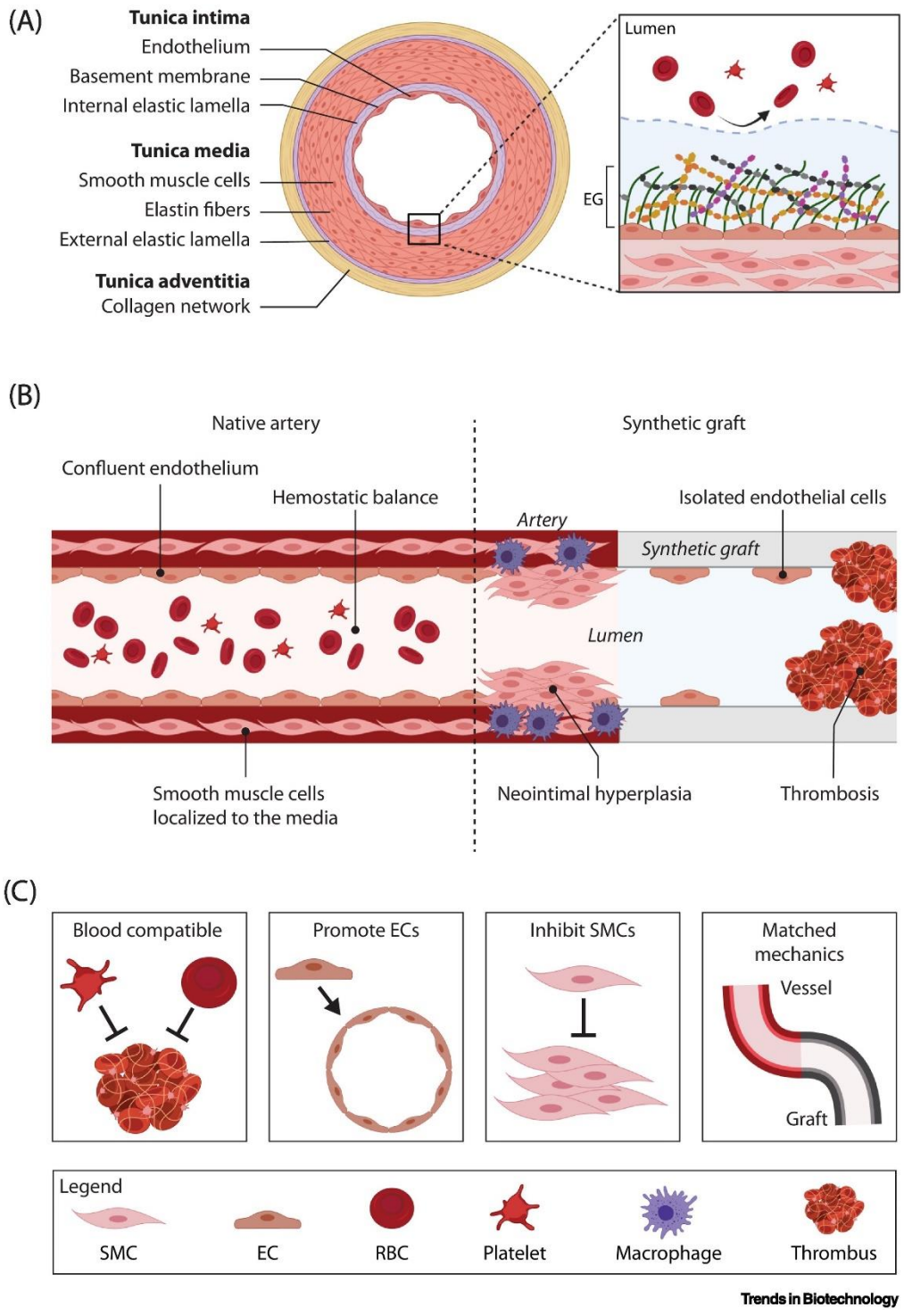

Figure 1.1. Anatomy of vascular graft, failure modes and design criteria[12].

(A) General structure of an artery. (B) Factors contributing to the failure of synthetic vascular grafts. The delayed formation of an endothelium leaves the hydrophobic graft surface exposed.

Blood plasma proteins rapidly adsorb to the exposed graft, followed by platelet adhesion and activation, which results in the formation of a platelet-rich thrombus. The biologically incompatible graft material provokes an immune response, resulting in macrophage infiltration and expression of inflammatory cytokines that drive smooth muscle cells to over-proliferate, developing neointimal hyperplasia. (C) Criteria for the rational design of artificial blood vessels. Image not to scale. Abbreviations: EC, endothelial cell; EG, endothelial glycocalyx; RBC, red blood cell; SMC, smooth muscle cell[12].

1.2.1 Intima

The intima is composed of ECs, a basal lamina, and a cell-free sub-endothelial space. The ECs monolayer of the intima forms a tight barrier between the lumen of the vessel and the vessel wall (Carabasi and Svigals, 2001). The blood and blood component are in direct contact with this ECs layer. Thus, ECs play then key roles in biological processes such as coagulation, inflammation, barrier function, blood flow regulation and synthesis/degradation of ECM components (Cines et al., 1998; Fauvel-Lafève, 1999). A thin layer of elastin and type IV collagen, called as internal elastic lamina (IEL), are responsible to hold the intima and the next layer media together (Tucker and Mahajan, 2018). The key role of the internal elastic lamina is associated with elasticity of the vascular wall to maintain blood pressure, even though current evidence ensured the multifunctional role.

1.2.2 Media

The main components of media are smooth muscle cells (SMC) along with collagen (type I and type III)[13]. These cells have a compressive phenotype that allows the contraction or expansion of the vessels[13,14]. The SMCs and collagen fibers are organized concentrically along with the axis of the vessel.

1.2.3 Adventitia

Adventitia is the outer layer of blood vessel wall. It is composed of fibroblasts surrounded in a loose collagen matrix. The adventitia is mainly composed of connective tissues such as type I and type II collagen, which prevents excessive dilation and contraction of blood vessels. The mechanical properties of blood vessels, such as tensile strength, are provided by the presence of these collagen fibers[11]. In the caliber of the aorta, a thin layer of outer elasticity is observed between the inner and outer patients.

1.3 Artificial vascular grafts

1.3.1 Artificial large diameter blood vessel

Large diameter (10-30 mm) synthetic grafts have been primarily developed due to the lack of alternative autologous grafts and sufficient patency. In 1954 Becky reported the first successful synthetic vascular graft transplantation into humans using polyester (polyethylene terephthalate: PET, known as Dacron) vascular grafts[15]. Since then, numerous trials, including various materials, PET (Dacron®), extended polytetrafluoroethylene (EPTFE), and polyurethane (PU), are now clinically approved[16]. These elements are mechanically and biologically compatible with local blood vessels. In addition to constant material improvements, ancillary changes have been developed, such as a combination of heparin on a bright surface to add anticoagulant function and a ring attachment to prevent the graft from falling. These improvements contribute to the long-term patency of medium-caliber (5-10 mm) grafts[17]. As a result, synthetic vascular grafts show satisfactory results in the repair of large and medium caliber vascular grafts.

1.3.2 Necessity of artificial small diameter blood vessel

Due to aging, lack of physical exercise or changing of lifestyle causes increasing the number of CVD patients along with CHD, CAD and PAD[18]. In advanced cases, the patient requires surgical revascularization such as coronary artery bypass grafting (CABG) or peripheral artery bypass

grafting. An established medical surgery involves inserting a vascular graft to bypass the blood around the blockage. At present days, the grafts clinically used for these small-diameter (<6 mm) implantation rely exclusively on autologous grafts because no suitable small-diameter synthetic grafts are currently permitted for clinical use due to their much lower patency rate than autologous grafts[19]. In blood vessel bypass surgery, autologous blood vessels, such as the internal thoracic or saphenous vein, are commonly used. Usually, the saphenous vein from the leg or internal mammary artery from the chest wall are collected as autologous grafts. However, autologous grafts also have some limitation including insufficient obtainability, invasive to harvesting, poor quality, inappropriate thickness (too thin or too thick), severe systemic atherosclerosis, or patient whose blood vessels have already been surgically removed in previous case[20,21]. Although, still now autologous vessels considered as the gold standard for vascular grafts, however, there are some unescapable complications occurred that can lead to failure of transplanted graft and may require additional graft for replacement[20,22]. In addition, veins used for arterial bypass have mismatched mechanical properties, are predisposed to accelerated atherosclerosis, and ~50% fail within 10 years[23]. Therefore, there is an urgent need for alternative practical small-diameter vascular grafts. In addition, other clinical diseases such as congenital cardiac anomalies and lower extremity arterial occlusion also create a great demand for vascular grafts [24].

1.4. Current strategy to develop artificial small diameter blood vessel

It must be considered that appropriate autologous vascular grafts are not always available due to the seriousness of the patient's health and collecting procedures. Therefore, developing artificial small-diameter blood vessels (ASDBVs) with suitable mechanical and biological properties comparable to natural blood vessels is a vital issue in medical science[25]. Artificial small-diameter vascular grafts may provide an excellent solution for CVD associated problem, but their design

and manufacture remain a challenge[26]. In recent decades, not only researchers but also companies have started investigations and already developed various materials and methods to fabricate ASDBVs in vitro[27–32]. Although they have not gotten yet fulfilled all requirements for ASDBVs that can mimic the native blood vessel in terms of functionality.

It is important to note that blood vessels' size (arteries, veins, and capillaries) is different from each other, and their construction and functions are also diverse. Indeed, large vessels are arranged for efficient transport over long distances while small vessels are organized for optimal exchange of oxygen, nutrients, and wastes. Therefore, it is not surprising that the requirements and design approaches for engineering large or small vessels are completely different. So, researchers are mainly focused on understanding the structural components of a blood vessel, increasing cells adhesion and tissue cohesion[33–42]. On the other hand, biocompatibility of construction materials and biological reaction to the blood components such as platelet adhesion, protein adsorption, and thrombus formation are also crucial issues to develop ASDBVs. Hence, all of these concepts are vital for the comprehensible design of biomaterials and the choice of an appropriate cellular source to give the blood vessel structural stability and facilitate its in vivo integration. Therefore, researchers have outlined various considerations in the development of small-diameter vascular grafts, including material choice (natural, synthetic polymer or biopolymer, or composites), surface modifications techniques to enhance biocompatibility, endothelialization to get anti-thrombogenic monolayer, and mechanical properties of the graft, that are currently being implanted. In addition, surface structure and biological activity of the inner surface of the vascular graft should be favorable to cell adhesion, growth, and proliferation. Some researcher gave an idea as five pillars of artificial small-diameter blood vessels (ASDBVs) engineered in vitro shown in Figure 2[43]. In addition, a general overview of biological, chemical, mechanical, and structural

considerations in the design and modification of small-diameter vascular grafts has shown in Figure 3 [53].

Figure 1.2. The five pillars of artificial small-diameter blood vessels (ASDBVs) engineered in vitro[43].

1.4.1 Biomaterial Selection

Various materials have been used to construct synthetic vascular graft including synthetic polymer biopolymer, and hybrid polymer. synthetic polymer can be categorized as degradable or non-degradable polymer. Non-degradable polymers were among the first materials used as a source for the production of vascular grafts that have been employed in bypass surgeries. Dacron based vascular graft was used in vitro with successful ECs seeding including collagen and fibronectin coating [44]. In addition, polyurethane coating-based Dacron was also used as vascular graft to improve cell attachment properties[45]. In contrast, ePTFE based vascular graft was investigated through endothelialization, plasma modification, anti-platelet properties inclusion. Sometimes, a combination of Dacron and ePTFE also used to get good patency rate[46–48].

Degradable polymers have been used as an alternative source to produce ASDBVs. These materials can be significantly degraded over time to form an accurate ECM[49]. Most commonly degradable materials used are polycaprolactone (PC), poly-lactic acid (PLA), poly (lactide-co-glycolide) (PLGA), polyglycolic acid (PGA), poly-l-lactic acid (PLLA), and polyglycerol sebacate (PGS)[49,50] .

For example, PGA shows rapid degradation time which can influence its biomechanical properties[49,50]. To solve it PLA is used along with to control the polymerization. Another material, PGS and PLA can be fully degraded within 30 days and over years respectively[49–51]. The stiffer behavior of PLA improves the endothelialization and patency rates. In addition, PCL, a hydrophobic material, showed long degradation time and can keep its initial biomechanical properties[49,50]. On the other hand, significant adverse reactions have been reported regarding their use. One major drawback is ineffective cell seeding and proliferation due to the lack of RGD-binding motifs[52]. As a results, platelet aggregation, clot formation, and lumen occlusion happened due to lack of ordered and monolayer endothelium[1].

Besides degradable and non-degradable polymer some natural biopolymer also been used as structural or coating materials to enhance endothelialization, migration and proliferation. The most common used biopolymers are collagen, fibrin, hyaluronan, silk and chitosan. Sometimes this biopolymer used alone or combined with other degradable or nondegradable polymer under the term of hybrid polymers such as PCL/Collagen, PET/PU/PCL, PU/PET, PU/PCL, PU/ collagen etc.

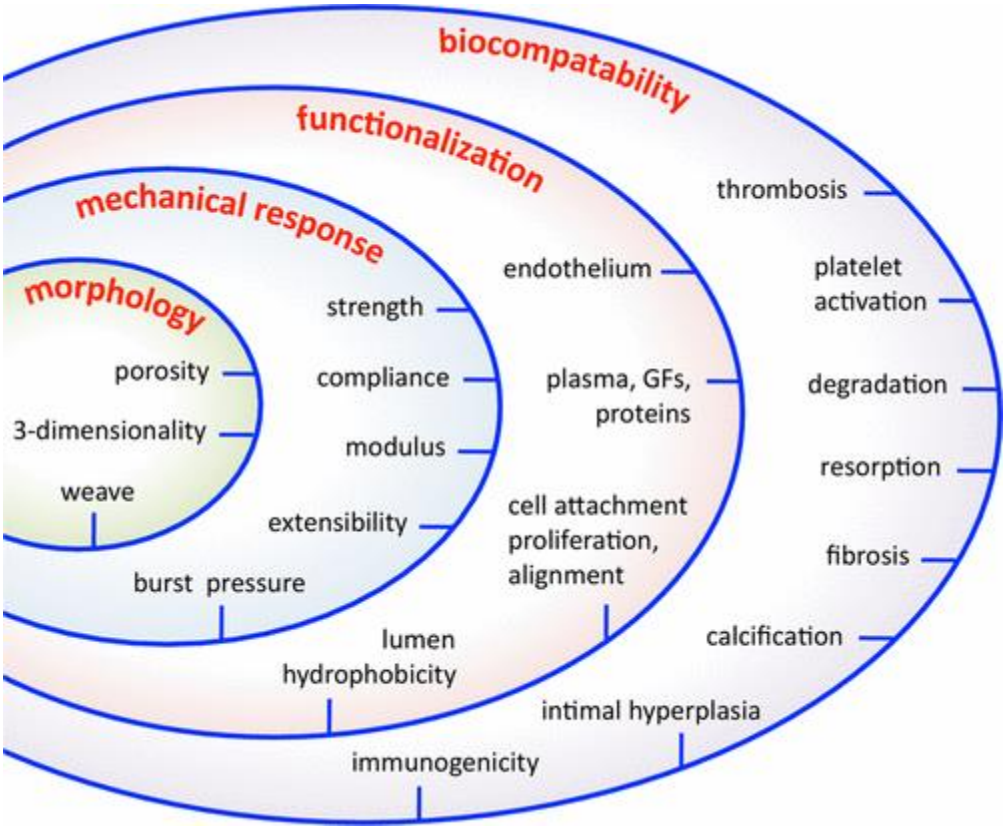

Figure1.3 General overview of biological, chemical, mechanical, and structural considerations in the design and modification of small-diameter vascular grafts[53].

1.4.2 Cell selection

Cell selection is a vital task in order to construct the artificial vascular grafts. Cell choice depends on the desire place of application and properties of native vessels. Thus, the selection of cells may be different. Moreover, in comparison of cell-seeded and un-seeded, cell-seeded vascular grafts have greater patency than unseeded grafts[54–56]. ECs are a crucial component of the blood vessel that provides an interface between the blood and the blood vessel wall[57].

However, there is no doubt that a stable confluent endothelium lining may act as completely antithrombogenic surface and can prevent the development of pseudo intimal hyperplasia and inflammatory response by releasing nitric oxide (NO) and prostacyclin (PGI2) to regulate platelet adhesion and activation; and producing tissue-type plasminogen activator (t-PA) to degrade fibrin

material and dissolve the blood clot[56,58]. However, such an endothelial cells (ECs) layer does not form spontaneously at the surface of a vascular implant in humans in vivo. Subsequently, researcher has proposed pre-seeding of ECs or progenitor cells prior to implantation in order to increase the patency of synthetic vascular graft[58,59] . However, poor cells adhesion ability under flow condition indicates low compatibility[60]. Consequently, polymers with antifouling and antithrombogenic properties with strong endothelial cell attachment abilities are desirable for researchers to develop artificial small-diameter blood vessels (ASDBVs) that can mimic native blood vessels.

1.4.3 Fabrication methods

Several fabrication methods are listed in literature which are considered as promising for manufacturing ASDBVs similar mechanical properties. In this section, we will briefly describe different ways of grafts fabricating.

- TESA Approach: developing vascular grafts utilizing cell sheets without support of vascular scaffolds[61].
- Paste extrusion and expansion: polymers by means of a mixing, extrusion, heating, and expanded stretching process, which yielded a microporous structure that was beneficial for tissue adhesion in vascular grafts[43].
- Electrospinning: degradable polymers or natural derived biomaterials are used to produce scaffolds[43,61,62].
- Braiding: a process of winding three or more fiber yarns in a specific pattern along the direction of fabric formation[43].
- Casting: a polymer is dissolved in a solvent along with porogen[62].

- Thermally induced phase separation (TIPS): phase separate a polymer–solvent or polymer–solvent–non-solvent homogeneous solution by cooling it to a low temperature to introduce polymer-rich and polymer-lean phases[43].
- Hydrogels as grafts: construction of ASDBV grafts using biocompatible hydrogels with tubular shape[43].
- Three Dimensional (3D) Bioprinting: complex structures and materials can be produced efficiently using degradable/nondegradable polymer[43,62,63].
- Four-Dimensional (4D) Bioprinting: 4D produced scaffolds show superiority over 3D bio printed scaffolds and termed as "smart" where "materials that can change their physical or chemical properties in a control and functional manner upon exposure to an external stimulus"[63,64].
- Combination of fabrication methods: Sometimes a combination of fabrication methods are applied to get better performance[43].

1.4.4 Mechanical Properties

- **Fatigue Properties and Elastic Modulus:** Young's modulus (the stress/strain ratio in the linear region of the tensile stress–strain curve) defines the stiffness of the material, even though its value may depend on the rate of elongation, and it is critically important for the application of SDBV grafts[43].
- **Nonlinear Elasticity:** Nonlinear elasticity, including the so-called toe region, is a very important property of native blood vessels. Human blood vessels show a low circumferential Young's modulus (usually 20–50 kPa) at the beginning of radius expansion, which indicates good flexibility[43].

- **Compliance Measurements:** a measure of the elastic deformation of a material in response to pressure, compliance can be calculated according to ANSI guidelines,

$$\%\ compliance\ per\ 100mmHg = \frac{(R_{P1} - R_{P2})/R_{p1}}{P1 - P2} \times 10^4$$

where P_1 is the lower pressure value, P_2 is the higher-pressure value (in mmHg), and R_{P1} and R_{P2} are the vessel inner diameters at the respective pressures[65].

- **Burst Pressure Measurements:** the maximum pressure that a vascular vessel can withstand before an acute leak occurs and it fails. This is expressed as, f= Pd/2t, where f, P, d, and t are the maximum force, burst pressure, diameter, and wall thickness, respectively[43]. Since f is a finite entity, the burst pressure decreases as the diameter increases and the wall thickness decreases. However, for a small-diameter graft, the burst pressure could be much higher than the blood pressure.

- **Suture Retention Strength (SRS):** a term that measures the adhesion of an implant to surrounding tissue. It is a key issue for surgery as its resistance to the stresses associated with implantation can only be established by determining the force necessary to pull a suture through the wall[66].

1.4.5 Characterization Techniques:

Along with proper manufacturing process of ASDVGs specific evaluation tests also important and must be performed before their final application. These tests include

- histological analysis,
- biochemical and DNA quantification,

- cytotoxicity assay,
- platelet adhesion test,
- biomechanical analysis,
- cell adhesion strength measurement
- cell-cell interaction, and
- implantation in animal models in order to assess effectively functionality of the vascular grafts.

Although the above methods are considered as primary assessment tests that should be performed to assess the biocompatibility of the manufactured ASDBVs. Moreover, the performance of cytotoxicity and the platelet adhesion assays is of major importance. Compared to large blood vessels, ASDBVs are characterized by tendency of platelet aggregation and thrombus formation including static and flow condition. According to ISO 10993-4 (Selection of Tests for Interactions of Blood), new biomaterials must be evaluated by the examination of material-induced thrombosis (thrombogenicity) and considered as one of the key requirements. Biomaterial's thrombogenicity evaluation test includes test of platelet adhesion, activation and spreading on biomaterial surfaces in static condition. In dynamic test systems, material samples that are in contact with flowing blood, platelet adhesion and thrombus formation can be analyzed qualitatively with microscopic techniques (e.g., scanning electron microscopy) Furthermore, seeding and formation of confluent monolayer of ECs should be properly assessed in ASDVGs to ensure the efficient endothelium.

1.5 Thrombogenicity and Biocompatibility

Thrombogenicity of a material surface can be defined as the ability of thrombus formation on or in a blood-contacting medical devices or other surface including artificial vascular graft. On the other hand, the word "biocompatibility" denotes how cordially the body responses to implants and biomaterials when it comes together in direct contact[67]. Biomaterials undergo tissue and animal processing before being used in human body to ensure their stability and effectiveness[68]. According to Williams, the ability of an implant substance to work in vivo without eliciting harmful local or systemic responses in the body is known as biocompatibility[69].

1.5.1 Mechanism of thrombus formation

The major factors of failure in non-autologous small-diameter grafts are acute thrombogenicity, intimal hyperplasia and infection. The lack of an intact endothelium is central to the main failure modes of artificial grafts. A healthy endothelium is coated in a layer of glycoproteins and proteoglycans, collectively known as the glycocalyx, which resists thrombus formation by preventing platelets and red blood cells adhering to endothelial cells[70]. In comparison, synthetic materials are highly unable to recover the protective endothelial cell layer are prone to increased rates of blood clotting, the dominant mode of acute failure in artificial grafts. Their rough, hydrophobic surfaces generally cause higher blood cell interactions and protein adsorption, driving accelerated clot formation[71]. Intimal hyperplasia is a significant factor of long-term patency. Although the exact mechanism is still unclear, excessive proliferation of smooth muscle cells is deemed to be a cause. Thrombus formation inside the synthetic graft shown in **Figure 1.1 (B)** and on the medical device surface shown in **Figure 1.4.**

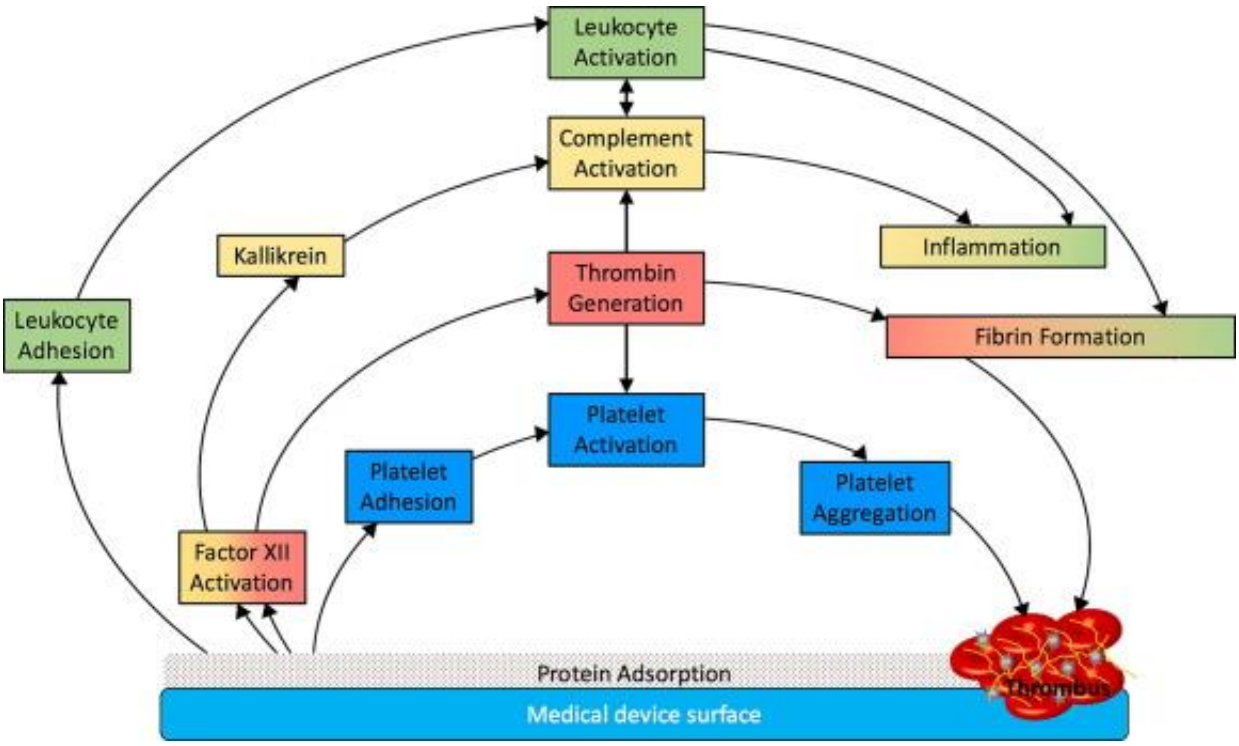

Figure 1.4. Blood-contacting medical device associated thrombosis. Protein adsorption on the surface of medical devices induces platelet adhesion, activation and aggregation. Factor XII adsorbed to the surface undergoes autoactivation, and the resulting factor XIIa converts PR kallikrein to kallikrein and initiates coagulation and thrombin generation. In addition to inducing fibrin deposition on the surface, thrombin promotes platelet activation. Platelet aggregates deposited on the surface are stabilized by fibrin strands to form a platelet-fibrin thrombus. Kallikrein, thrombin and other coagulation enzymes activate complement, inducing a local inflammatory response. Leukocytes also adhere to the surface where they become activated and can contribute to both inflammation and thrombosis[72].

1.5.2 Antithrombogenic mechanism of blood compatible polymer

Use of non-fouling polymers to modify the device surfaces is relatively widely adopted to improve the blood compatibility of the surfaces. When polymers are used in clinical practice, they gradually tend to expose some unexpected inherent flaws and shows the compatibility level. Since

blood compatibility is a premise for biocompatibility, we naturally turn our attention to the blood compatibility of polymers first. According to Whitesides, four molecular-level features of chemical groups that incorporated on the protein adsorption-resistant surfaces: (i) hydrophilic, (ii) including hydrogen-bond acceptors, (iii) without hydrogen-bond donors, (iv) overall electrically neutral[73]. Currently, the steric repulsion theory and hydration theory are relatively popular where steric repulsion theory is often used to explain the blood compatibility of polymers with high chain mobility whereas in hydration theory, water plays the key role in blood compatibility since water is the first blood component to interact with foreign surfaces. In this theory, polymer's polar groups interact with water, forming hydration layers that prevent proteins from penetrating the polymer layer.

1.5.3 Intermediate water concept towards biocompatibility

Poly(2-methoxyethyl acrylate) (PMEA), an FDA approved antithrombogenic synthetic polymer, using as coating materials of various medical devices such as stent, artificial lung, catheters etc[9]. Because of its intermediate water (IW, loosely bound water) content, PMEA shows antithrombogenic behavior. Now it is established that IW is a measure of biocompatibility and blood compatibility[10,74]. In consequence, we have investigated the relationship between polymers' hydration states and their blood compatibility using a variety of thermal and spectroscopic measurements on PMEA. It is now established that the hydration layers of the PMEA consist of three types of water depending on the interaction state. According to their crystallization behaviors, they are termed as non-freezing water (NFW), freezing-bound water, and freezing water or free water (FW). Next, this freezing bound water named as Intermediate Water (IW). From the differential scanning calorimetry (DSC) measurement, (i) the NFW does not crystallize even at −100 °C and so nondetectable in the DCS thermogram, (ii) freezing-bound water crystallizes at

ca. −40 °C (cold crystallization) and melts below 0 °C, (iii) FW melts at ca. 0 °C (a representative DSC thermogram of hydrated PMEA is shown **Figure 1.5a)**[75]**.** The existence of the three types of water is also reflected in their different dynamic behaviors. According to the ^{2}H-NMR and ^{13}C-NMR spectra of hydrated PMEA: (i) NFW exhibits low mobility due to a strong interaction with the PMEA chain, (ii) the mobility of freezing-bound water is higher than that of NFW, (iii) FW has the highest mobility due to its location far from the PMEA chain[76]. By investigating the process of water sorption into the PMEA film with time-resolved, in situ, attenuated total reflection infrared (ATR-IR) spectroscopy, Morita et al. revealed three different O–H stretching vibration [ν(O–H)] bands in the process, which can be assigned to the three hydrated water (shown in **Figure 1.5b**)[77,78]. The ν(O–H) band of NFW is at approximately 3600 cm^{-1}, which usually appears at the wavenumber of water molecules isolated from hydrogen-bonds or hydrogen-bonded to carbonyl groups. The ν(O–H) band of freezing-bound is at around 3400 cm^{-1} and FW has a broad vibration band ranged from 3400 to 3200 cm^{-1} which resembles that of bulk water[75,77].

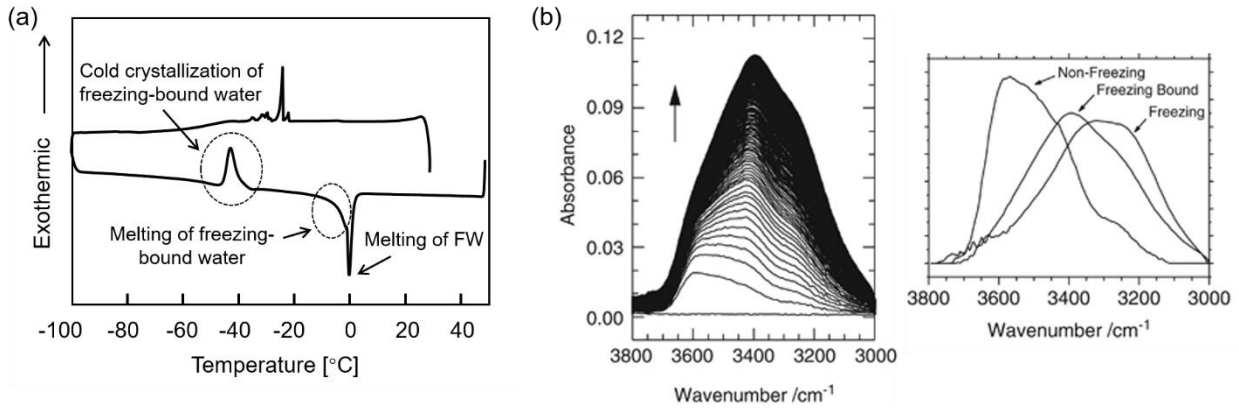

Figure 1.5. (a) A representative DSC thermogram of hydrated PMEA. (b) Time-resolved ATR-IR spectra of the sorption process for liquid water into a PMEA film (left) and pure spectra and of NFW, freezing-bound water, and FW (right) calculated using alternating least squares from the left of (b). The left and right of (b) referred to literature[77,78].

DSC measurement is easy to operate, sample preparation is simple, and results are straight forward compared to the ^{2}H-NMR, ^{13}C-NMR, and ATR-IR measurement. Therefore, we selected DSC measurement for further investigations to analyze the composition of hydration layers, or hydration states, of a number of well-known blood-compatible and non-blood-compatible polymers. By comparing the obtained and reported DSC results, it is found that the freezing bound water is present in blood compatible polymers, such as synthetic type: poly (ethylene glycol) (PEG), poly(2-methacryloyloxyethyl phosphorylcholine) PMPC, polyvinylpyrrolidone, poly(methylvinyl ether), poly(tetrahydrofurfuryl acrylate), and natural type: gelatin, albumin, cytochrome c, and hyaluronan, alginate, DNA, RNA, while barely in non-blood-compatible polymers[75,79]. Consequently, we proposed that freezing-bound water plays a key role in the blood compatibility of polymers.

Table 1.1. Features of three types of hydrated water[80].

Bonding Strength	Type of water	Freezability	ATR-IR peak top of OH stretching region (cm− 1)	NMR correlation time τc (s)	Surface force
Scarcely bound water	Freezing water or Free water	Melting at 0 ◦C	3400–3200	10^{-12}–10^{-11}	No interaction
Loosely bound water	Freezing bound water or Intermediate water	Freezing and melting below 0 ◦C	3400	10^{-10}–10^{-9}	Repulsion at a long range (2–4 nm)
Tightly bound water	Non-freezing bound water	Non-freezing below 0 ◦C	3600	10^{-8}–10^{-6}	Repulsion at a short range (<1 nm)

Based on the characteristics of each water shown in the DSC, NMR, IR and AFM results (summarized in Table 1.1), it is reasonable to assume that water deposits on the blood compatible polymer surface in the following order: NFW comes first, followed by freezing-bound water, and FW comes last. NFW interacts strongly with polymer chains, while freezing-bound water is

loosely bound to the polymer or NFW. FW is slightly affected by polymers and is freely exchanged with bulk water and results in a structure that resembles bulk water. The freezing-bound water can prevent the cells or proteins from directly contacting the polymer surface or NFW. Because freezing-bound water is so intermediated in terms of location and interaction strength with polymer when compared with NFW and FW, we refer to it as intermediate water (IW) instead[75].

According to the IR spectrum and quantum chemical calculations on PMEA, NFW mainly (85.6%) interacts with two carbonyl groups while IW interacts with the methoxy moiety in the side chain[77]. The chemical structure of a polymer can affect how water interacts with it, and as a result, blood compatibility may change. In fact, this inference has been demonstrated in studies of the hydration states and blood compatibility of a series of PMEA derivatives (the graphic conclusion is shown in **Figure 1.6**). To put it another way, generally, the higher the IW content, the better the blood compatibility of the polymer is. Hence, when designing the structure of a novel polymer, aiming at increasing the IW content to improve blood compatibility would be effective.

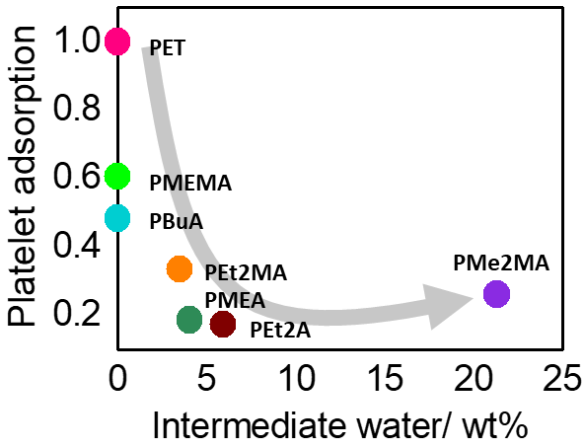

Figure 1.6. The correlation between IW water content (wt % IW) and the number of adhered platelets of PMEA derivatives[81].

In closing, a layer of IW can create a barrier that prevent the direct contact of bio-components on the surface of polymers or NFW, which plays a key role in the excellent blood compatibility of polymers. The presence of IW can also be regarded as an intrinsically common feature of blood-compatible polymers. Since DSC measurement can facilely and straightly detect the IW, it can be used to preliminarily judge polymers' blood compatibility. The content of IW is related to the polymer's blood compatibility. In general, the higher the content of IW, the better the blood compatibility. Therefore, IW can be employed to guide the development of novel blood-compatible polymers.

1.5.4 Biocompatibility in terms of cell adhesion ability and PMEA analogous polymer:

Up to the present time, there are many polymeric blood-compatible materials have been investigated including poly(2-methacryloyloxyethylphosphorylcholine)[82,83], poly(ethylene glycol)[84,85], and poly(2-oxazoline)s[86,87]. Among of these polymers, PMPC considered as one of the excellent biocompatible, anti-protein fouling and non-cell adhesion, polymers where phosphorylcholine group is present[88,89].

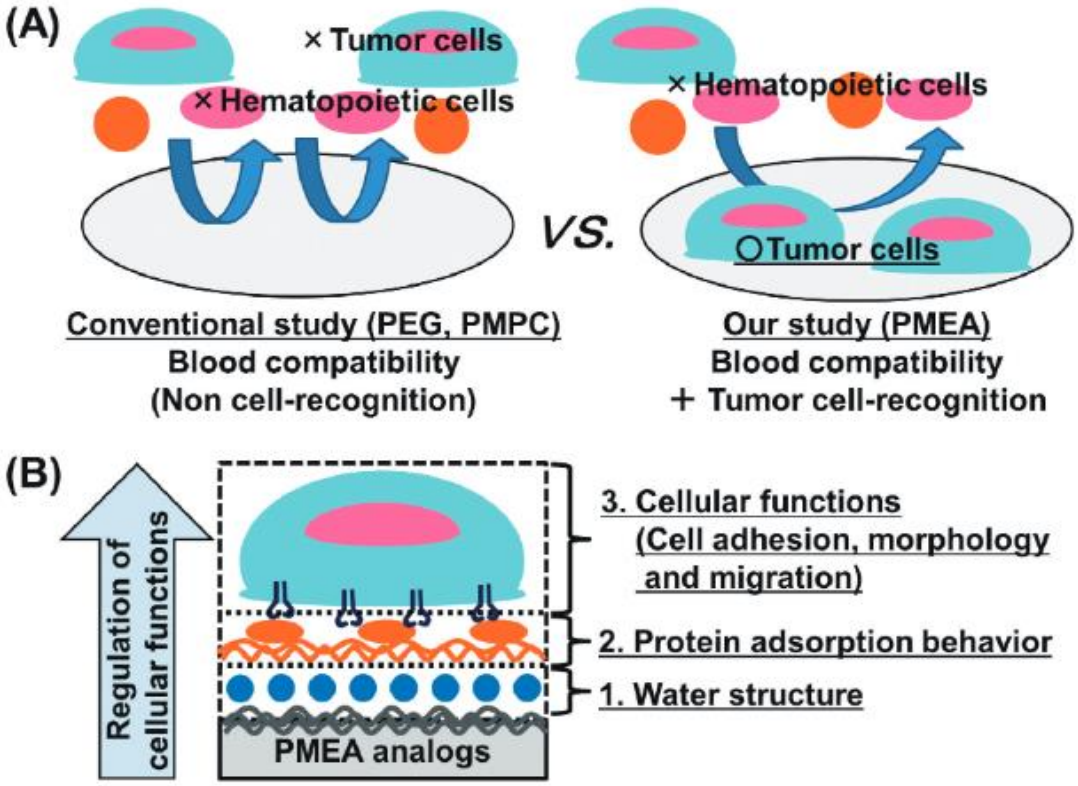

Figure 1.7 Regulation of blood compatibility and tumor cell-recognition on PMEA substrate. (A) Blood compatibility and tumor cell-recognition on PMEA and its analogs. On conventional blood compatible polymers such as PEG and PMPC, both hematopoietic cells and tumor cells cannot attach, that is, these polymers can express blood compatibility or non-cell recognition. In contrast, haematopoietically cannot attach but tumor cells can attach to PMEA and its analogs. In other word, PMEA analogs can express not only blood compatibility but also tumor cell-recognition. (B) Regulation of cellular functions. Using MEA analogs containing different amounts of intermediate water, water structure, protein adsorption behavior, and cellular functions such as cell adhesion, morphology, and migration can be sequentially regulated[90].

Cell adhesion is occurred by cell adhesion molecules (CAM), such as integrins. Integrin plays an important role in cell adhesion to the biocompatible substrates. If protein adsorption on the

substrates is suppressed, the cell adhesion is expected to be suppressed. Because integrin-dependent cell adhesion is weakened via the suppression of protein adsorption. The conventional polymeric materials such as PEG, and PMPC suppress protein adsorption as well as strongly suppress celladhesion[91–93]. In comparison to these polymeric surfaces, the cells can adhere to PMEA analogs through integrin independent adhesion if integrin-dependent cell adhesion is weakened due to protein adsorption suppression[94–96]. In integrin-independent adhesion, a direct interaction occurred between cells and PMEA analogs substrate surface[95,96].

1.6 Aim of this thesis

Due to the frequent thrombus formation inside the small diameter vascular graft, it is still challenging to use artificial vascular in human body. To date, there is no considerable satisfactory results in vivo or in clinical trial. Researchers are trying to construct artificial small diameter blood vessels using most possible strategies known until now and focusing on to develop new and effective techniques for this purpose. So many trials have done on developed synthetic small diameter graft, but the physical, mechanical, biocompatibility, blood compatibility, antithrombogenicity as well as similar functionality compared to native blood vessel does not attain yet. The main problem that already identified is thrombus formation or plaque deposition in inner part of artificial vessels. That means, platelets deposits on the surfaces over time. Some grafts were mechanically and physically fit but not shown proper functionality. However, some are shown good patency rate but to mechanically stable. Therefore, we have taken the challenges and set our aim to develop such kind surface which is able to prevent or suppress of thrombus formation and increase of endothelial cells adhesion to make a smooth endothelium inside the vascular graft.

According to our goal, primarily, we have focused on the antithrombogenic surface. Poly(2-methoxyethyl acrylate) (PMEA) is an FDA approved antithrombogenic synthetic polymer which is using as coating materials for various medical devices successfully. PMEA is water insoluble amorphous polymer and can be coated on any shapes.

As we described in previous section, in brief, Tanaka et al. found different water state on PMEA depending on the water molecules interaction with the PMEA polymer backbone and side chain by DSC measurement. Then categorized the water as Non-freezing Water (NFW), Intermediate water (IW), and Free Water (FW) or bulk water. NFW is strongly connected to polymer chain and FW stands far from polymer chain and shows highest mobility. Whereas IW is loosely connected to the methoxy moiety and only detectable at -40 ˚C during cold crystallization of DSC measurement. From several research on PMEA, it is established that PMEA surface is able to suppress the platelet adhesion due to the presence of IW. Furthermore, IW was found many other natural and synthetic polymer with diverse amount. Finally, it was concluded that IW play the key role to become the surface blood compatible by suppressing the adsorption and conformational change of platelet adhesive protein such as fibrinogen.

In addition, PMEA analogous polymer such as poly(3-methoxypropyl acrylate) (PMC3A), poly(n-butyl acrylate) (PBA), Poly(n-butyl methacryle$_{70}$-co-2-methacryloyloxyethyl phosphorylcholine$_{30}$) (PMPC), poly(2-methoxyethylmethacrylate) (PMEMA). Although analogous polymers have similar configuration and also have dissimilar characteristic including physical, morphological, biocompatibility, blood compatibility, platelet adhesion, cell adhesion and IW content. Some are good for cell adhesion but bad in terms of platelet adhesion and vice versa. Initially, all are the candidate for synthetic blood vessels depending on their characteristics and functionality. Therefore, in order to construct artificial small diameter blood vessels, we have

to find out the most suitable polymer form the analogous using effective investigation techniques. In this regard, based on the above problems and scopes, the research objectives of the thesis are included in the following features.

a) To find out the best polymer through the investigation of the effect of IW content on endothelial cells (HUVECs) adhesion strength and platelet adhesion strength, number of adhered cells and platelet on respective substrates for the evaluation of antithrombogenicity.

b) How to achieve antiplatelet property, like native blood vessel endothelium, on the substrates through HUVECs attachment, migration, and monolayer formation.

c) How to increase the cell adhesion as well as cell adhesion strength on polymer substrates using surface modification techniques other than spin coating methods

Our ultimate target is to construct artificial blood vessel using the superior features of our developed PMEA and its analogous polymer either as coating or as construction materials.

This thesis is divided into the following five chapters

In **chapter 1**, the details background of this research has stated including cardiovascular disease and its origin, possible treatments, necessity of artificial vascular graft, limitations of small diameter blood vessels, mechanism of thrombus formation, current construction strategy, thrombogenicity and biocompatibility, possible scope of using synthetic polymer such as PMEA analogous to construct small diameter blood vessels. Chapter has finished with the indication of research goals.

In **chapter 2**, the comparison study is presented where cell adhesion indicates the antithrombogenicity of PMEA analogous polymer. Also presented how IW regulates the cell

adhesion strength on polymer substrates.

In **chapter 3**, the possible mechanism of HUVECs monolayer formation on polymeric surfaces are presented along with platelet adhesion behavior on endothelium to mimic the native blood vessels.

Chapter 4 is consisting of endothelial cell adhesion, proliferation, and cytoskeleton on grafted polymer surfaces of Poly(2-methoxyethyl acrylate) (PMEA) analogs. Here, PMEA analogous polymer was grafted other than spin coating.

Finally, the conclusions of this thesis are summarized in **chapter 5**. Indication of future research and perspective also included along with the summary.

1.7 References

(1) Radke, D.; Jia, W.; Sharma, D.; Fena, K.; Wang, G.; Goldman, J.; Zhao, F. Tissue Engineering at the Blood-Contacting Surface: A Review of Challenges and Strategies in Vascular Graft Development. *Advanced Healthcare Materials* **2018**, *7* (15), e1701461. https://doi.org/10.1002/adhm.201701461.

(2) Carrabba, M.; Madeddu, P. Current Strategies for the Manufacture of Small Size Tissue Engineering Vascular Grafts. *Front Bioeng Biotechnol* **2018**, *6*, 41.

(3) Fiqrianti, I. A.; Widiyanti, P.; Manaf, M. A.; Savira, C. Y.; Cahyani, N. R.; Bella, F. R. Poly-L-Lactic Acid (PLLA)-Chitosan-Collagen Electrospun Tube for Vascular Graft Application. *J Funct Biomater* **2018**, *9* (2), 32.

(4) Copes, F.; Pien, N.; van Vlierberghe, S.; Boccafoschi, F.; Mantovani, D. Collagen-Based Tissue Engineering Strategies for Vascular Medicine. *Front Bioeng Biotechnol* **2019**, *7*, 166.

(5) Herrington, W.; Lacey, B.; Sherliker, P.; Armitage, J.; Lewington, S. Epidemiology of

Atherosclerosis and the Potential to Reduce the Global Burden of Atherothrombotic Disease. *Circ Res* **2016**, *118* (4), 535–546.

(6) Lima, D. B. de; Agustini, B. C.; Silva, E. G. da; Gaensly, F.; Cordeiro, R. B.; Fávero, M. L. D.; Brand, D.; Maraschin, M.; Bonfim, T. M. B. Evaluation of Phenolic Compounds Content and in Vitro Antioxidant Activity of Red Wines Produced from Vitis Labrusca Grapes. *Food Science and Technology* **2011**, *31*, 783–800.

(7) Noly, P.-E.; Ali, W. ben; Lamarche, Y.; Carrier, M. Status, Indications, and Use of Cardiac Replacement Therapy in the Era of Multimodal Mechanical Approaches to Circulatory Support: A Scoping Review. *Canadian Journal of Cardiology* **2020**, *36* (2), 261–269.

(8) Maniadakis, N.; Kourlaba, G.; Fragoulakis, V. Self-Reported Prevalence of Atherothrombosis in a General Population Sample of Adults in Greece; A Telephone Survey. *BMC Cardiovasc Disord* **2011**, *11* (1), 1–9.

(9) Tanaka, M.; Motomura, T.; Kawada, M.; Anzai, T.; Yuu Kasori; Shiroya, T.; Shimura, K.; Onishi, M.; Akira Mochizuki. Blood Compatible Aspects of Poly(2-Methoxyethylacrylate) (PMEA)-Relationship between Protein Adsorption and Platelet Adhesion on PMEA Surface. *Biomaterials* **2000**, *21* (14), 1471–1481.

(10) Tanaka, M.; Motomura, T.; Kawada, M.; Anzai, T.; Kasori, Y.; Shimura, K.; Onishi, M.; Mochizuki, A.; Okahata, Y. A New Blood-Compatible Surface Prepared by Poly (2-Methoxyethylacrylate) (PMEA) Coating -Protein Adsorption on PMEA Surface. *Japanese Journal of Artificial Organs* **2000**, *29* (1), 209–216. https://doi.org/doi.org/10.11392/jsao1972.29.209.

(11) Tennant, M.; McGeachie, J. K. Blood Vessel Structure and Function: A Brief Update on Recent Advances. *Australian and New Zealand Journal of Surgery* **1990**, *60* (10), 747–

753.

(12) Moore, M. J.; Tan, R. P.; Yang, N.; Rnjak-Kovacina, J.; Wise, S. G. Bioengineering Artificial Blood Vessels from Natural Materials. *Trends in Biotechnology*. Elsevier Ltd June 1, 2022, pp 693–707. https://doi.org/10.1016/j.tibtech.2021.11.003.

(13) Berillis, P. *Send Orders of Reprints at Reprints@benthamscience.Net The Open Circulation and Vascular Journal*; 2013; Vol. 6.

(14) Campbell, G. R.; Campbell, J. H. Smooth Muscle Phenotypic Changes in Arterial Wall Homeostasis: Implications for the Pathogenesis of Atherosclerosis. *Experimental and Molecular Pathology* **1985**, *42* (2), 139–162. https://doi.org/https://doi.org/10.1016/0014-4800(85)90023-1.

(15) Bakey, M. E.; de Bakey, M. E. Successful Resection of Aneurysm of Distal Aortic Arch and Replacement by Graft [Internet]. *J American Med Assoc* **1954**, *155*, 1398.

(16) Chlupác, J.; Filová, E.; Bačáková, L. Blood Vessel Replacement: 50 Years of Development and Tissue Engineering Paradigms in Vascular Surgery. *Physiological Research*. 2009, pp 119–140. https://doi.org/10.33549/physiolres.931918.

(17) Freeman, J.; Chen, A.; Weinberg, R. J.; Okada, T.; Chen, C.; Lin, P. H. Sustained Thromboresistant Bioactivity with Reduced Intimal Hyperplasia of Heparin-Bonded Polytetrafluoroethylene Propaten Graft in a Chronic Canine Femoral Artery Bypass Model. *Annals of Vascular Surgery* **2018**, *49*, 295–303.

(18) Wann-Hansson, C.; Wennick, A. How Do Patients with Peripheral Arterial Disease Communicate Their Knowledge about Their Illness and Treatments? A Qualitative Descriptive Study. *BMC Nurs* **2016**, *15* (1), 1–9.

(19) Veith, F. J. Gupta SK, Ascer E, White-Flores S, Samson RH, Scher LA, Towne JB,

Bernhard VM, Bonier P, Flinn WR, Astelford P, Yao JS, and Bergan JJ. *Six-year prospective multicenter randomized comparison of autologous saphenous vein and expanded polytetrafluoroethylene grafts in infrainguinal arterial reconstructions. J Vasc Surg* **1986**, *3*, 104–114.

(20) Aslani, S.; Kabiri, M.; Kehtari, M.; Hanaee-Ahvaz, H. Vascular Tissue Engineering: Fabrication and Characterization of Acetylsalicylic Acid-loaded Electrospun Scaffolds Coated with Amniotic Membrane Lysate. *J Cell Physiol* **2019**, *234* (9), 16080–16096.

(21) Braghirolli, D. I.; Helfer, V.; Chagastelles, P.; Dalberto, T.; Gamba, D.; Pranke, P. Electrospun Scaffolds Functionalized with Heparin and VEGF Increase the Proliferation of Endothelial Progenitor Cells. *Biomed Mater* **2017**, *12*, 025003.

(22) Gao, J.; Jiang, L.; Liang, Q.; Shi, J.; Hou, D.; Tang, D.; Chen, S.; Kong, D.; Wang, S. The Grafts Modified by Heparinization and Catalytic Nitric Oxide Generation Used for Vascular Implantation in Rats. *Regenerative Biomaterials* **2018**, *5* (2), 105–114.

(23) Caliskan, E.; de Souza, D. R.; Boening, A.; Liakopoulos, O. J.; Choi, Y.-H.; Pepper, J.; Gibson, C. M.; Perrault, L. P.; Wolf, R. K.; Kim, K.-B. Saphenous Vein Grafts in Contemporary Coronary Artery Bypass Graft Surgery. *Nature Reviews Cardiology* **2020**, *17* (3), 155–169.

(24) Drews, J. D.; Miyachi, H.; Shinoka, T. Tissue-Engineered Vascular Grafts for Congenital Cardiac Disease: Clinical Experience and Current Status. *Trends Cardiovasc Med* **2017**, *27* (8), 521–531.

(25) Baker, E. S.; Liu, T.; Petyuk, V. A.; Burnum-Johnson, K. E.; Ibrahim, Y. M.; Anderson, G. A.; Smith, R. D. Mass Spectrometry for Translational Proteomics: Progress and Clinical Implications. *Genome Med* **2012**, *4* (8), 1–11.

(26) Isenberg, B. C.; Williams, C.; Tranquillo, R. T. Small-Diameter Artificial Arteries Engineered in Vitro. *Circ Res* **2006**, *98* (1), 25–35.

(27) Gao, A.; Hang, R.; Li, W.; Zhang, W.; Li, P.; Wang, G.; Bai, L.; Yu, X. F.; Wang, H.; Tong, L.; Chu, P. K. Linker-Free Covalent Immobilization of Heparin, SDF-1α, and CD47 on PTFE Surface for Antithrombogenicity, Endothelialization and Anti-Inflammation. *Biomaterials* **2017**, *140*, 201–211. https://doi.org/10.1016/J.BIOMATERIALS.2017.06.023.

(28) Dahl, S. L. M.; Kypson, A. P.; Lawson, J. H.; Blum, J. L.; Strader, J. T.; Li, Y.; Manson, R. J.; Tente, W. E.; DiBernardo, L.; Hensley, M. T. Readily Available Tissue-Engineered Vascular Grafts. *Sci Transl Med* **2011**, *3* (68), 68ra9-68ra9.

(29) Browning, M. B.; Dempsey, D.; Guiza, V.; Becerra, S.; Rivera, J.; Russell, B.; Höök, M.; Clubb, F.; Miller, M.; Fossum, T. Multilayer Vascular Grafts Based on Collagen-Mimetic Proteins. *Acta Biomater* **2012**, *8* (3), 1010–1021.

(30) Heureux, N. L.; Dusserre, N.; Konig, G.; Victor, B. Keire P, Wight TN, Chronos NAF, Kyles AE, Gregory CR, Hoyt G, Robbins RC, McAllister TN. Human Tissue-Engineered Blood Vessels for Adult Arterial Revascularization. *Nat Med* **2006**, *12*, 361–365.

(31) Ma, Z.; Kotaki, M.; Yong, T.; He, W.; Ramakrishna, S. Surface Engineering of Electrospun Polyethylene Terephthalate (PET) Nanofibers towards Development of a New Material for Blood Vessel Engineering. *Biomaterials* **2005**, *26* (15), 2527–2536.

(32) Freed, L. E.; Engelmayr Jr, G. C.; Borenstein, J. T.; Moutos, F. T.; Guilak, F. Advanced Material Strategies for Tissue Engineering Scaffolds. *Advanced materials* **2009**, *21* (32-33), 3410–3418.

(33) van Wachem, P. B.; Beugeling, T.; Feijen, J.; Bantjes, A.; Detmers, J. P.; van Aken, W. G.

Interaction of Cultured Human Endothelial Cells with Polymeric Surfaces of Different Wettabilities. *Biomaterials* **1985**, *6* (6), 403–408.

(34) McAuslan, B. R.; Johnson, G. Cell Responses to Biomaterials I: Adhesion and Growth of Vascular Endothelial Cells on Poly (Hydroxyethyl Methacrylate) Following Surface Modification by Hydrolytic Etching. *J Biomed Mater Res* **1987**, *21* (7), 921–935.

(35) Wigod, M. D.; Klitzman, B. Quantification of in Vivo Endothelial Cell Adhesion to Vascular Graft Material. *J Biomed Mater Res* **1993**, *27* (8), 1057–1062.

(36) Brunstedt, M. R.; Ziats, N. P.; Rose-Caprara, V.; Hiltner, P. A.; Anderson, J. M.; Lodoen, G. A.; Payet, C. R. Attachment and Proliferation of Bovine Aortic Endothelial Cells onto Additive Modified Poly (Ether Urethane Ureas). *J Biomed Mater Res* **1993**, *27* (4), 483–492.

(37) McAuslan, B. R.; Johnson, G.; Hannan, G. N.; Norris, W. D.; Exner, T. Cell Responses to Biomaterials II: Endothelial Cell Adhesion and Growth on Perfluorosulfonic Acid. *J Biomed Mater Res* **1988**, *22* (11), 963–976.

(38) Absolom, D. R.; Hawthorn, L. A.; Chang, G. Endothelialization of Polymer Surfaces. *J Biomed Mater Res* **1988**, *22* (4), 271–285.

(39) Cenni, E.; Granchi, D.; Ciapetti, G.; Verri, E.; Cavedagna, D.; Gamberini, S.; di Leo, A.; Pizzoferrato, A. Cytokine Production and Adhesive Protein Expression by Endothelial Cells after Contact with Polyethylene Terephthalate. *Biomaterials* **1996**, *17* (21), 2071–2076.

(40) Storck, J.; Ab Del Razek, H.; Zimmermann, E. R. Effect of Polyvinyl Chloride Plastic on the Growth and Physiology of Human Umbilical Vein Endothelial Cells. *Biomaterials* **1996**, *17* (18), 1791–1794.

(41) Zhang, Y.; Anninos, P.; Norman, M. L. A Multispecies Model for Hydrogen and Helium Absorbers in Lyman-Alpha Forest Clouds. *The Astrophysical Journal* **1995**, *453* (2), L57.

(42) Cenni, E.; Granchi, D.; Ciapetti, G.; Verri, E.; Cavedagna, D.; Gamberini, S.; Cervellati, M.; di Leo, A.; Pizzoferrato, A. Expression of Adhesion Molecules on Endothelial Cells after Contact with Knitted Dacron. *Biomaterials* **1997**, *18* (6), 489–494.

(43) Wang, D.; Xu, Y.; Li, Q.; Turng, L. S. Artificial Small-Diameter Blood Vessels: Materials, Fabrication, Surface Modification, Mechanical Properties, and Bioactive Functionalities. *Journal of Materials Chemistry B*. Royal Society of Chemistry March 7, 2020, pp 1801–1822. https://doi.org/10.1039/c9tb01849b.

(44) Sugawara, Y.; Miyata, T.; Sato, O.; Kimura, H.; Namba, T.; Makuuchi, M. Rapid Postincubation Endothelial Retention by Dacron Grafts. *Journal of surgical research* **1997**, *67* (2), 132–136.

(45) Phaneuf, M. D.; Dempsey, D. J.; Bide, M. J.; Quist, W. C.; LoGerfo, F. W. Coating of Dacron Vascular Grafts with an Ionic Polyurethane: A Novel Sealant with Protein Binding Properties. *Biomaterials* **2001**, *22* (5), 463–469.

(46) Hytönen, J. P.; Leppänen, O.; Taavitsainen, J.; Korpisalo, P.; Laidinen, S.; Alitalo, K.; Wadström, J.; Rissanen, T. T.; Ylä-Herttuala, S. Improved Endothelialization of Small-Diameter EPTFE Vascular Grafts through Growth Factor Therapy. *Vascular Biology* **2019**, *1* (1), 1–9.

(47) Sipehia, R.; Liszowski, M.; Lu, A. In Vivo Evaluaton of Ammonia Plasma Modified EPTFE Grafts for Small Diameter Blood Vessel Replacement: A Preliminary Report. *Journal of Cardiovascular Surgery* **2001**, *42* (4), 537.

(48) Mall, J. W.; Philipp, A. W.; Rademacher, A.; Paulitschke, M.; Büttemeyer, R. Re-

Endothelialization of Punctured EPTFE Graft: An in Vitro Study under Pulsed Perfusion Conditions. *Nephrology Dialysis Transplantation* **2004**, *19* (1), 61–67.

(49) Ravi, S.; Qu, Z.; Chaikof, E. L. Polymeric Materials for Tissue Engineering of Arterial Substitutes. *Vascular* **2009**, *17* (1_suppl), 45–54.

(50) Ravi, S.; Chaikof, E. L. Biomaterials for Vascular Tissue Engineering. *Regenerative Med* **2010**, *5* (1), 107–120.

(51) Pashneh-Tala, S.; MacNeil, S.; Claeyssens, F. The Tissue-Engineered Vascular Graft—Past, Present, and Future. *Tissue Engineering Part B: Reviews* **2016**, *22* (1), 68–100.

(52) Tallawi, M.; Rosellini, E.; Barbani, N.; Cascone, M. G.; Rai, R.; Saint-Pierre, G.; Boccaccini, A. R. Strategies for the Chemical and Biological Functionalization of Scaffolds for Cardiac Tissue Engineering: A Review. *Journal of the Royal Society Interface* **2015**, *12* (108), 20150254.

(53) Hiob, M. A.; She, S.; Muiznieks, L. D.; Weiss, A. S. Biomaterials and Modifications in the Development of Small-Diameter Vascular Grafts. *ACS Biomaterials Science & Engineering* **2017**, *3* (5), 712–723. https://doi.org/10.1021/acsbiomaterials.6b00220.

(54) Kurobe, H.; Maxfield, M. W.; Breuer, C. K.; Shinoka, T. Concise Review: Tissue-Engineered Vascular Grafts for Cardiac Surgery: Past, Present, and Future. *Stem Cells Transl Med* **2012**, *1* (7), 566–571.

(55) Naito, Y.; Shinoka, T.; Duncan, D.; Hibino, N.; Solomon, D.; Cleary, M.; Rathore, A.; Fein, C.; Church, S.; Breuer, C. Vascular Tissue Engineering: Towards the next Generation Vascular Grafts. *Adv Drug Deliv Rev* **2011**, *63* (4–5), 312–323.

(56) Li, S.; Henry, J. J. D. Nonthrombogenic Approaches to Cardiovascular Bioengineering. *Annual Review of Biomedical Engineering* **2011**, *13* (1), 451–475.

https://doi.org/10.1146/annurev-bioeng-071910-124733.

(57) Kaushal, S.; Amiel, G. E.; Guleserian, K. J.; Shapira, O. M.; Perry, T.; Sutherland, F. W.; Rabkin, E.; Moran, A. M.; Schoen, F. J.; Atala, A. Functional Small-Diameter Neovessels Created Using Endothelial Progenitor Cells Expanded Ex Vivo. *Nat Med* **2001**, *7* (9), 1035–1040.

(58) Deutsch, M.; Meinhart, J.; Fischlein, T.; Preiss, P.; Zilla, P. ,. Clinical Autologous in Vitro Endothelialization of Infrainguinal EPTFE Grafts in 100 Patients: A 9-Year Experience. *Surgery* **1999**, *126* (5), 847–855.

(59) Bordenave, L.; Fernandez, Ph.; Rémy-Zolghadri, M.; Villars, S.; Daculsi, R.; Midy, D. In Vitro Endothelialized EPTFE Prostheses: Clinical Update 20 Years after the First Realization. *Clinical Hemorheology and Microcirculation* **2005**, *33* (3), 227–234.

(60) Feugier, P.; Black, R. A.; Hunt, J. A.; How, T. v. Attachment, Morphology and Adherence of Human Endothelial Cells to Vascular Prosthesis Materials under the Action of Shear Stress. *Biomaterials* **2005**, *26* (13), 1457–1466. https://doi.org/10.1016/j.biomaterials.2004.04.050.

(61) Mallis, P.; Kostakis, A.; Stavropoulos-Giokas, C.; Michalopoulos, E. Future Perspectives in Small-Diameter Vascular Graft Engineering. *Bioengineering*. 2020, p 160. https://doi.org/10.3390/bioengineering7040160.

(62) Li, Z.; Li, X.; Xu, T.; Zhang, L. Acellular Small-Diameter Tissue-Engineered Vascular Grafts. *Applied Sciences (Switzerland)*. MDPI AG July 1, 2019. https://doi.org/10.3390/app9142864.

(63) Gu, B. K.; Choi, D. J.; Park, S. J.; Kim, M. S.; Kang, C. M.; Kim, C. H. 3-Dimensional Bioprinting for Tissue Engineering Applications. *Biomaterials Research*. BioMed Central

Ltd. 2016. https://doi.org/10.1186/s40824-016-0058-2.

(64) Tamay, D. G.; Dursun Usal, T.; Alagoz, A. S.; Yucel, D.; Hasirci, N.; Hasirci, V. 3D and 4D Printing of Polymers for Tissue Engineering Applications. *Frontiers in Bioengineering and Biotechnology* **2019**, *7*.

(65) de Valence, S.; Tille, J. C.; Mugnai, D.; Mrowczynski, W.; Gurny, R.; Möller, M.; Walpoth, B. H. Long Term Performance of Polycaprolactone Vascular Grafts in a Rat Abdominal Aorta Replacement Model. *Biomaterials* **2012**, *33* (1), 38–47. https://doi.org/10.1016/j.biomaterials.2011.09.024.

(66) Chaparro, F. J.; Matusicky, M. E.; Allen, M. J.; Lannutti, J. J. Biomimetic Microstructural Reorganization during Suture Retention Strength Evaluation of Electrospun Vascular Scaffolds. *Journal of Biomedical Materials Research Part B: Applied Biomaterials* **2016**, *104* (8), 1525–1534. https://doi.org/https://doi.org/10.1002/jbm.b.33493.

(67) de Moraes Porto, I. C. C. Polymer Biocompatibility. Polymerization. *London: IntechOpen Ltd* **2012**.

(68) Williams, D. F. There Is No Such Thing as a Biocompatible Material. *Biomaterials* **2014**, *35* (38), 10009–10014.

(69) Williams, B. P. Biomaterials-Induced Sterile Inflammation, Mechanotransduction, and Principles of Biocompatibility Control, ACS Biomater. *Sci. Eng* **2017**, No. 3, 2–25.

(70) Moore, K. H.; Murphy, H. A.; George, E. M. The Glycocalyx: A Central Regulator of Vascular Function. *American Journal of Physiology-Regulatory, Integrative and Comparative Physiology* **2021**, *320* (4), R508–R518. https://doi.org/10.1152/ajpregu.00340.2020.

(71) Jaffer, I. H.; Fredenburgh, J. C.; Hirsh, J.; Weitz, J. I. Medical Device-Induced Thrombosis:

What Causes It and How Can We Prevent It? *Journal of Thrombosis and Haemostasis* **2015**, *13* (S1), S72–S81. https://doi.org/https://doi.org/10.1111/jth.12961.

(72) Jaffer, I. H.; Weitz, J. I. The Blood Compatibility Challenge. Part 1: Blood-Contacting Medical Devices: The Scope of the Problem. *Acta Biomaterialia*. Acta Materialia Inc August 1, 2019, pp 2–10. https://doi.org/10.1016/j.actbio.2019.06.021.

(73) Ostuni, E.; Chapman, R. G.; Holmlin, R. E.; Takayama, S.; Whitesides, G. M. A Survey of Structure− Property Relationships of Surfaces That Resist the Adsorption of Protein. *Langmuir* **2001**, *17* (18), 5605–5620.

(74) Tanaka, M.; Mochizuki, A.; Ishii, N.; Motomura, T.; Hatakeyama, T. Study of Blood Compatibility with Poly(2-Methoxyethyl Acrylate). Relationship between Water Structure and Platelet Compatibility in Poly(2-Methoxyethylacrylate-Co-2-Hydroxyethylmethacrylate). *Biomacromolecules* **2002**, *3* (1), 36–41. https://doi.org/10.1021/bm010072y.

(75) Tanaka, M.; Hayashi, T.; Morita, S. The Roles of Water Molecules at the Biointerface of Medical Polymers. *Polymer Journal*. July 2013, pp 701–710. https://doi.org/10.1038/pj.2012.229.

(76) Miwa, Y.; Ishida, H.; Saitô, H.; Tanaka, M.; Mochizuki, A. Network Structures and Dynamics of Dry and Swollen Poly(Acrylate)s. Characterization of High- and Low-Frequency Motions as Revealed by Suppressed or Recovered Intensities (SRI) Analysis of 13C NMR. *Polymer (Guildf)* **2009**, *50* (25), 6091–6099. https://doi.org/10.1016/j.polymer.2009.10.037.

(77) Morita, S.; Tanaka, M.; Ozaki, Y. Time-Resolved in Situ ATR-IR Observations of the Process of Sorption of Water into a Poly(2-Methoxyethyl Acrylate) Film. *Langmuir* **2007**,

23 (7), 3750–3761. https://doi.org/10.1021/la0625998.

(78) Tanabe, A.; Morita, S.; Tanaka, M.; Ozaki, Y. Multivariate Curve Resolution Analysis on the Multi-Component Water Sorption Process into a Poly(2-Methoxyethyl Acrylate) Film. *Applied Spectroscopy* **2008**, *62* (1), 46–50. https://doi.org/10.1366/000370208783412555.

(79) Sato, K.; Kobayashi, S.; Kusakari, M.; Watahiki, S.; Oikawa, M.; Hoshiba, T.; Tanaka, M. The Relationship between Water Structure and Blood Compatibility in Poly(2-Methoxyethyl Acrylate) (PMEA) Analogues. *Macromolecular Bioscience* **2015**, *15* (9), 1296–1303. https://doi.org/10.1002/mabi.201500078.

(80) Tanaka, M.; Morita, S.; Hayashi, T. Role of Interfacial Water in Determining the Interactions of Proteins and Cells with Hydrated Materials. *Colloids and Surfaces B: Biointerfaces* **2021**, *198*. https://doi.org/10.1016/j.colsurfb.2020.111449.

(81) Sato, K.; Kobayashi, S.; Sekishita, A.; Wakui, M.; Tanaka, M. Synthesis and Thrombogenicity Evaluation of Poly(3-Methoxypropionic Acid Vinyl Ester): A Candidate for Blood-Compatible Polymers. *Biomacromolecules* **2017**, *18* (5), 1609–1616. https://doi.org/10.1021/acs.biomac.7b00221.

(82) Ishihara, K.; Kozaki, Y.; Inoue, Y.; Fukazawa, K. Biomimetic Phospholipid Polymers for Suppressing Adsorption of Saliva Proteins on Dental Hydroxyapatite Substrate. *Journal of Applied Polymer Science* **2021**, *138* (6), 49812.

(83) Shi, X.; Cantu-Crouch, D.; Sharma, V.; Pruitt, J.; Yao, G.; Fukazawa, K.; Wu, J. Y.; Ishihara, K. Surface Characterization of a Silicone Hydrogel Contact Lens Having Bioinspired 2-Methacryloyloxyethyl Phosphorylcholine Polymer Layer in Hydrated State. *Colloids and Surfaces B: Biointerfaces* **2021**, *199*, 111539.

(84) Mabry, K. M.; Lawrence, R. L.; Anseth, K. S. Dynamic Stiffening of Poly (Ethylene

Glycol)-Based Hydrogels to Direct Valvular Interstitial Cell Phenotype in a Three-Dimensional Environment. *Biomaterials* **2015**, *49*, 47–56.

(85) Ye, K.; Wang, X.; Cao, L.; Li, S.; Li, Z.; Yu, L.; Ding, J. Matrix Stiffness and Nanoscale Spatial Organization of Cell-Adhesive Ligands Direct Stem Cell Fate. *Nano Lett* **2015**, *15* (7), 4720–4729.

(86) Jana, S.; Uchman, M. Poly (2-Oxazoline)-Based Stimulus-Responsive (Co) Polymers: An Overview of Their Design, Solution Properties, Surface-Chemistries and Applications. *Progress in Polymer Science* **2020**, *106*, 101252.

(87) Lorson, T.; Luebtow, M. M.; Wegener, E.; Haider, M. S.; Borova, S.; Nahm, D.; Jordan, R.; Sokolski-Papkov, M.; Kabanov, A. v; Luxenhofer, R. Poly (2-Oxazoline) s Based Biomaterials: A Comprehensive and Critical Update. *Biomaterials* **2018**, *178*, 204–280.

(88) Ishihara, K.; Aragaki, R.; Ueda, T.; Watenabe, A.; Nakabayashi, N. Reduced Thrombogenicity of Polymers Having Phospholipid Polar Groups. *J Biomed Mater Res* **1990**, *24* (8), 1069–1077.

(89) Goda, T.; Konno, T.; Takai, M.; Moro, T.; Ishihara, K. Biomimetic Phosphorylcholine Polymer Grafting from Polydimethylsiloxane Surface Using Photo-Induced Polymerization. *Biomaterials* **2006**, *27* (30), 5151–5160.

(90) Tanaka, M.; Kobayashi, S.; Murakami, D.; Aratsu, F.; Kashiwazaki, A.; Hoshiba, T.; Fukushima, K. Design of Polymeric Biomaterials: The “Intermediate Water Concept.” *Bulletin of the Chemical Society of Japan*. Chemical Society of Japan 2019, pp 2043–2057. https://doi.org/10.1246/bcsj.20190274.

(91) Zhang, F.; Li, G.; Yang, P.; Qin, W.; Li, C.; Huang, N. Fabrication of Biomolecule-PEG Micropattern on Titanium Surface and Its Effects on Platelet Adhesion. *Colloids and*

Surfaces B: Biointerfaces **2013**, *102*, 457–465.

(92) Iwasaki, Y.; Tabata, E.; Kurita, K.; Akiyoshi, K. Selective Cell Attachment to a Biomimetic Polymer Surface through the Recognition of Cell-Surface Tags. *Bioconjug Chem* **2005**, *16* (3), 567–575.

(93) Bretland, A. J.; Lawry, J.; Sharrard, R. M. A Study of Death by Anoikis in Cultured Epithelial Cells. *Cell Prolif* **2001**, *34* (4), 199–210.

(94) Hoshiba, T.; Nemoto, E.; Sato, K.; Orui, T.; Otaki, T.; Yoshihiro, A.; Tanaka, M. Regulation of the Contribution of Integrin to Cell Attachment on Poly(2-Methoxyethyl Acrylate) (PMEA) Analogous Polymers for Attachment-Based Cell Enrichment. *PLoS ONE* **2015**, *10* (8). https://doi.org/10.1371/journal.pone.0136066.

(95) Hoshiba, T.; Nikaido, M.; Tanaka, M. Characterization of the Attachment Mechanisms of Tissue-Derived Cell Lines to Blood-Compatible Polymers. *Advanced Healthcare Materials* **2014**, *3* (5), 775–784. https://doi.org/10.1002/adhm.201300309.

(96) Hoshiba, T.; Yoshihiro, A.; Tanaka, M. Evaluation of Initial Cell Adhesion on Poly (2-Methoxyethyl Acrylate) (PMEA) Analogous Polymers. *Journal of Biomaterials Science, Polymer Edition* **2017**, *28* (10–12), 986–999. https://doi.org/10.1080/09205063.2017.1312738.

Chapter 2

Cell adhesion strength indicates the antithrombogenicity of Poly(2-methoxyethyl acrylate) (PMEA): Potential candidate for artificial small-diameter blood vessel

Graphical Abstract

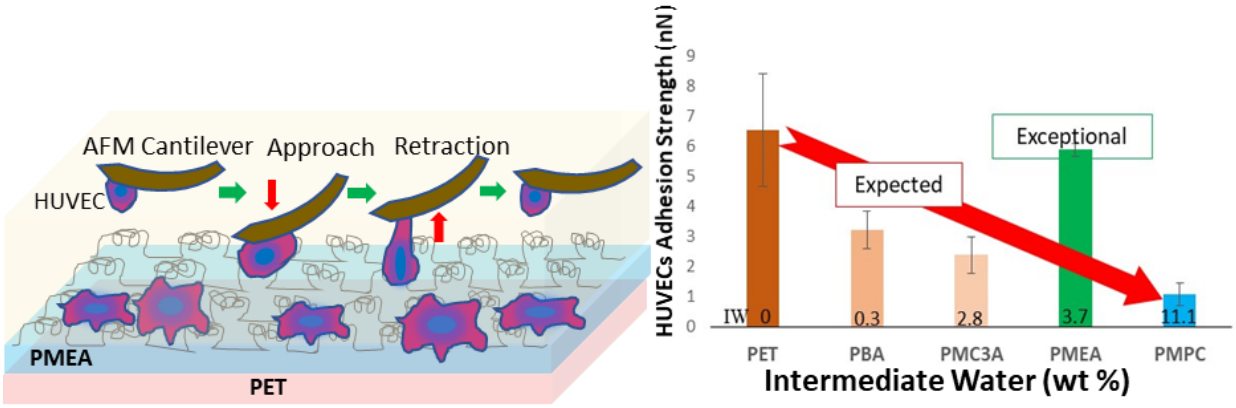

Abstract:

Poly (2-methoxyethyl acrylate) (PMEA) is an US FDA-approved biocompatible polymer, although there is insufficient work on human umbilical vein endothelial cells (HUVECs) and platelet interaction analysis on PMEA analogous polymers. In this study, we extensively investigated HUVEC–polymer and platelet–polymer interaction behavior by measuring the adhesion strength using single-cell force spectroscopy. Furthermore, the hydration layer of the polymer interface was observed using frequency-modulation atomic force microscopy. We found that endothelial cells can attach and spread on the PMEA surface with strong adhesion strength compared to other analogous polymers. We confirmed that HUVECs attachment and platelet adhesion are regulated by the amount of intermediate water (IW). We found that the hydration layers on the PMEA analogous polymer are closely related to their weak platelet adhesion behavior. Based on our results, it can be concluded that PMEA is a promising candidate for the construction of artificial small-diameter blood vessels owing to the presence of IW and a hydration layer on the interface.

Keywords: PMEA; HUVEC; platelet; interaction; hydration.

2.1 Introduction

In the modern era, owing to the unique properties of biocompatible polymers, they have been widely used in organ transplantation, tissue engineering scaffolds, development of medical devices, drug delivery systems, and biomedical healthcare sensors [1,2]. These biomaterials can be used in different ways, sometimes as a coating material or as an entire system made of the material itself to maintain the physiological and mechanical properties. Once biomaterials come in contact with the components of the living body, such as cells or proteins, they collaborate in distinctive ways. In particular, cells interact with the biomaterial interface through the extracellular matrix, which controls cell functions such as viability, growth rate, mobility, and protein secretion [3,4]. Therefore, cell adhesion study is one of the major concerns for biomaterials to become a perfect candidate for in vivo application in the human body. Consequently, cell adhesion capacity controls cell morphology, such as cell survival, proliferation, migration, and differentiation [5–7]. In contrast, platelet adhesion, as well as blood component adherence to the bio-polymeric substrate, is also a vital phenomenon to become surface blood compatible [8].

Cardiovascular diseases (CVDs) are a threat to human health. Approximately 17.9 million people died of CVDs in 2019, which is 32% of the world's total deaths, and this number is expected to increase to 23.6 million by 2030 [9]. In CVDs, blood vessels are mostly blocked or narrowed by atherosclerosis or thrombosis. Atherogenesis is initiated by endothelial dysfunction, and its movement leads to vessel damage and blocking, which causes thrombosis of the arterial wall as well as injury and dysfunction of tissues and organs [10,11]. Consequently, researchers are focusing on to effective ways to reduce the causes of CVDs as well as the appropriate treatments of insured vessels, particularly for small-diameter blood vessels.

As an effective treatment, vascular graft transplantation with synthetic vascular grafts is an

alternative option to replace injured vessels along with angioplasty, atherectomy, and stent insertion [12]. Currently, the available commercial artificial blood vessels are mostly made of polyethylene terephthalate (PET), polytetrafluoroethylene (PTFE), and dracon, which are used in large-diameter vessel transplants [13]. However, small-diameter vascular grafts are still under evaluation owing to thrombus formation inside the tube after implantation [14,15]. This implies that the interfaces of these synthetic polymers do not meet the requirements for transplantable grade or biocompatibility. Thus, the interfacial properties must be changed according to the compatibility state. Hence, an alternative method for changing the properties of the biopolymer interface is surface modification. Various surface modification techniques have been used to functionalize the interface of substrates for cell attachment, growth, migration, rapid endothelization, and long-term anticoagulation [9,16,17]. Polymer coating is an effective approach for functionalizing biomaterial surfaces. It is well established that functionalization with poly(ethylene glycol) and zwitterionic polymers, including poly(2-methacryloyloxyethyl phosphorylcholine) (PMPC), suppresses biofilm formation, immune responses to the biomaterial surfaces, and the adhesion of platelets [18–20]. Therefore, polymers with antifouling and antithrombogenic properties and strong endothelial cell attachment ability are desirable for scientists to obtain artificial small-diameter blood vessels (ASDBV).

Poly(2-methoxyethyl acrylate) (PMEA) is an FDA-approved biocompatible polymer that is used as an antithrombogenic coating polymer in several sophisticated medical devices such as artificial hearts and lungs, stents, catheters, and dialyzers[8,21]. A remarkable characteristic of PMEA is its unique interaction with water molecules, which play a dominant role in the biological environment and are detected using differential scanning calorimetry (DSC)[22], infrared spectroscopy[23], nuclear magnetic resonance[24], and several other approaches. Using DSC

measurements, Tanaka et al. classified water molecules interacting with PMEA into three types: free water (FW), freezing-bound water (intermediate water; IW), and non-freezing water (NFW)[25]. IW plays an important role in surface biocompatibility. In a previous study, it was found that PMEA can reduce protein adsorption and platelet adhesion by suppressing the conformational change of fibrinogen[8,26]. Recently, it has been reported that non-blood cells can attach to the coated surface of PMEA and its analogous through integrin-dependent and integrin-independent mechanisms[27]. We also observed that integrin-independent cell attachment occurred on the PMEA-coated surface. Therefore, it is possible to find a suitable polymer that can be used to develop an implant biomaterial, such as an artificial blood vessel, if we can investigate human umbilical vein endothelial cells (HUVECs) and human platelet adhesion behavior (survival, proliferation, migration, differentiation, and interaction strength) on the surface of PMEA analogs.

HUVECs have been acknowledged as a useful model for research on the human endothelium[28]. HUVECs are an excellent model for the study of vascular endothelial properties and the main biological pathways involved in endothelial function, although this model does not represent all endothelial cell types found in an organism [29]. In contrast, the endothelium acts as a barrier between the blood and organs, and at the same time, is responsible for the transfer of nutrients, hormones, and white blood cells, as well as anti-inflammatory responses [30]. Moreover, blood pressure, flow, and coagulation are regulated by this organ [31]. In addition, HUVECs are also effective in studying hemodynamic interactions between the endothelium layer and atherosclerotic plaque formation because they allow exposure of endothelial cells (ECs) to shear stress controlling flow conditions, and therefore, represent blood flow conditions as in vivo [32]. Furthermore, ECs play a role in angiogenesis and platelet binding to substrates and endothelial monolayers under flow conditions [33].

To develop a transplantable ASDBV (<6 mm), the construction materials should have the following properties: (1) biocompatibility to prevent an immune reaction against the artificial vessel, (2) cytophilic properties that enable endothelial and smooth muscle cells to migrate, and (3) properties that prevent thrombus formation [34]. To meet these requirements, it is important to investigate HUVECs integration into the construction polymer. In a previous study, Sato et al. reported the compatibility of PMEA with the adhesion and proliferation of endothelial and smooth muscle cells [34]. Hoshiba et al. investigated the adhesion of the cancer cell line HT-1080, a fibrosarcoma cell line, on PMEA, analogous to single-cell force microscopy [27]. HUVECs are the key cells in native blood vessels and have an important influence on the development of artificial blood vessels as the same confluent layer over the synthetic surface. However, there is no significant study on the interaction between the polymer surface and HUVECs by force measurement. In contrast, a recently published report describes the design of a biocompatible elastomer using a PMEA-silica composite to obtain a tough and tube-like structure of ASDBV compared to the native vessel [35–37]. They reported that the mechanical properties of the PMEA-silica composites are comparable to those of native blood vessels and that the antithrombotic properties do not change with a slight increase in silica adhesion, although there is no evidence of endothelial cell adhesion ability.

In this study, the surface interaction of HUVECs on PMEA and its analogous was quantitatively investigated by force measurement for the development of ASDBVs. We also compared platelet adhesion behavior and time profiles of initial cell attachment. Furthermore, we observed the hydration states of the polymer interfaces using frequency-modulation atomic force microscopy (FM-AFM). Finally, we related the results of single-cell force spectroscopy (SCFS) and FM-AFM to characterize HUVECs attachment and platelet adhesion mechanisms on PMEA

analogous surfaces.

2.2 Materials and Methods

2.2.1 Chemicals and materials

Polyethylene terephthalate (PET) was purchased from Mitsubishi Plastic Inc. (Tokyo, Japan). Poly(2-methoxyethyl acrylate) (PMEA, Mn = 26.9 kg/mol, Mw/Mn = 2.73), poly(3-methoxypropyl acrylate) (PMC3A, Mn = 20.8 kg/mol, Mw/Mn = 3.83), poly(n-butyl acrylate) (PBA, Mn = 62.8 kg/mol, Mw/Mn = 1.41) were synthesized according to a previous report[38]. Poly(n-butyl methacryle$_{70}$-co-2-methacryloyloxyethyl phosphorylcholine$_{30}$) (PMPC, Mw = 600 kg/mol) was donated by NOF Corporation, Japan. Tissue culture polystyrene (TCPS) was purchased from IWATA, Japan. Fibronectin was obtained from Wako Pure Chemical Industries (Osaka, Japan). Human whole blood for the platelet adhesion test was purchased from Tennessee Blood Survices (USA) and collected in a vacuum blood collection tube (Venoject II, Terumo Co., Japan) containing 3.2% sodium citrate as an anticoagulant. Human whole blood was collected within a week of blood collection. Blocking reagent was purchased from Nacalai Tesque (Kyoto, Japan). All other reagents and solvents were obtained from Kanto Chemical Co. (Tokyo, Japan).

2.2.2 Fabrication of polymer-coated substrates

PET was used as a substrate for coating. One side of the PET sheet (thickness = 120 μm) was indicated as coating side. Prior to coating, PET sheet was cut into a circle with a diameter of 14 mm. After cutting the PET substrate using hand press cutting tool from the A4 size PET sheet, it may catch some dust. To clean the dust, each PET substrate was dipped in toluene 2-3 times and then dried in air. The whole cleaning process need only 5-10 s for each substrate. PMEA, PMC3A, and PBA were dissolved in Toluene (0.5 wt/vol%) to make a polymer solution. PMPC was dissolved in methanol at the same concentration. PMEA analogue polymer solutions (26.2 μL/cm^2)

were spin-coated on the PET substrates using a Mikasa Spin Coater MS-A100 at a constant rate of 3000 rpm for 40 s, ramped down for 4 s, and thereafter dried for at least for 24h in a vacuum dryer at 25 °C. The stability of prepared films was confirmed by the contact angle measurement after immersed in water.

2.2.3 Contact angle (CA)

CA represents the wettability of studied polymers. CA measurements were per-formed using milli Q water. The CA values of PMEA analogous surfaces were calculated using two methods: (1) sessile drop of water and (2) air bubble in water at 25 °C using a DropMaster DMo-501SA (Kyowa Interface Science Co., Tokyo, Japan). In the sessile drop method, a 2 μL water droplet was placed on the polymer surface for 60 s, and the CAs were measured using photographic images. The droplet method was executed by placing 2 μL of water droplets on the five positions of each substrate. We did the measurement three times with three different substrates. So total number of images is 15 for droplet method. In the captive bubble method, PMEA analogous substrates were immersed in Milli-Q water for 24 h. Thereafter, 2 μL of air bubbles were injected beneath the substrate surfaces located in water, and the CAs were measured using photographic images. Finally, the CA at 30 s was counted as the CA of the substrate.

2.2.4 Endothelial cell culture

Endothelial cells were used for all experiments described in this article. Commercially available human umbilical vein endothelial cells (HUVEC, Lonza, Cologne, Germany) were cultured under static cell culture conditions (37 ℃, 5 vol% CO_2) in polystyrene-based cell culture flasks. Cells were used for 4 to 6 passages and cultured in endothelial basal medium (EBM-2) supplemented with endothelial growth medium (EGM-2) Single Quots® kit and 2 vol% FBS (Lonza, Cologne, Germany). Prior to the experiments, cells were detached from the culture dish

using 0.25% trypsin/EDTA solution (Thermo Fisher Scientific, Rockford, IL, USA). The HUVECs solution was centrifuged at 1200 rpm for 3 min to isolate HUVECs from the old medium. Initial cell counting was performed using a hemocytometer to adjust the cell density.

2.2.5 Cell attachment and proliferation assay

Cell attachment and proliferation assays were performed using 24 well plate (IWATA, Japan). Initially, the 24 well plate was coated with PMPC (0.5 wt/vol%) and stored for drying. The pre-coated polymer substrates were thereafter fixed in 24 well plate using glue on the back side of each substrate. The substrates were then cured under ultraviolet (UV) light for 30 min. Phosphate-Buffered Saline (PBS) was then added to the well and stored it in incubator for 1 h at 37 °C. Afterwards, PBS was removed, culture media were added and incubated under the same conditions for another 1 h at 37 °C. HUVECs were seeded on the substrates at 1 x 104 cells/cm2 in serum-containing media and allowed to adhere and proliferate on the surface of the substrates for 1 d, 3 d, 5 d and 7 d. The culture media was changed in every two days for 3 d, 5 d and 7 d. After cell cultivation, at specific time intervals, the cells were counted using a microplate analyzer from the standard curve prepared by the colorimetric WST-8 assay (Dojindo Laboratories, Kumamoto, Japan).

2.2.6 Immunocytochemical analysis

Before starting the experiment, the prepared substrates were preconditioned, as in the cell attachment and proliferation assays. HUVECs (5×10^3 cells/cm^2) were thereafter seeded on each polymer-coated substrate (φ = 14 mm) and incubated for 1, 24, and 72 h. After culturing for specific times, the cells were fixed using preheated (37 ˚C) 4% (w/v) paraformaldehyde (Fujifilm Wako Pure Chemical Corporation, Osaka, Japan) and stored outside for 10 min. Thereafter, 1% (v/v) Triton X-100 (Fujifilm Wako Pure Chemicals Co., Ltd., Osaka, Japan) in PBS (−) was added

to increase plasma membrane permeability. After washing, the sections were blocked for 30 min. The substrates were thereafter treated with mouse monoclonal anti-human vinculin antibody (VIN-11-5; Sigma-Aldrich, St. Louis, MO, USA)(1:200) diluted in PBS (−) for 90 min at room temperature, and subsequently treated with Alexa Fluor 568-conjugated anti-mouse IgG (H + L) antibody(1:1000 dilution), Alexa Fluor 488-conjugated phalloidin (1:1000 diluted), DAPI (4,6-diamidino-2-phenylindole (1:1000 diluted)) (all from Thermo Fisher Scientific, Waltham, MA, USA), and all diluted in 10% blocking solution in PBS, treated for 1 h at room temperature. After performing these steps, stained cells were fixed on glass slides. Fluorescence images were captured using a confocal laser scanning microscope (CLSM) (FV-3000; Olympus, Tokyo, Japan). The cell area and circularity were evaluated quantitatively using ImageJ software (version 1.53C, Bethesda, MD, USA).

2.2.7 HUVECs- polymer interaction by SCFS

The PMEA analogous substrates were exposed under UV for 30 min and thereafter incubated with PBS for 1 h at 37 °C. Subsequently, EGM-2 medium was added to the substrate and freshly detached cells (passage: 5–6) were injected. In contrast, the tip-less cantilever TL-CONT (spring constant k = 0.2 N/m, NANOSENSORS) was coated by fibronectin with human fibronectin solution (1 mg/mL) for 20 min at room temperature. A single HUVEC was captured with a tipless cantilever for 10 min of holding time (set point: 2 nN) (Supporting information Figure S1). The Z-lengths for cell was 100 µm the vertical displacement range of the AFM. We have found that the HUVEC cells is around 20 µm in size and cell was detached around 70-90 µm. The force curves between the cell and the substrate were recorded using an atomic force microscope AFM (CellHesion, JPK) equipped with a cell-attached tipless cantilever (set point: 2 nN, approach rate: 5.0 µm/s, holding time: 120 s, retraction time: 15 µm/s) (Supporting information Figure S3). The

set point for measuring the cell adhesion strength was determined from the relationship between the set points and the cell adhesion strength of HUVECs attached to the PMEA-coated PET substrate[39]. In brief, we have selected contact time 120 s and set point 2 nN after investigating different contact time (60, 120, 240 and 300 s) at different setpoint (0.5, 1, 2, 3, and 5 nN). We have found a linear relationship between contact time and adhesion force and set point and adhesion force. HUVECs is very slow doubling time (24-36 h). So, we fixed contact time 120 s because of initial contact is not happened earlier due to slow doubling time. On the other hand, we realized that at fixed set point 2 nN and 120 s contact time, HUVECs shows considerable adhesion force. The adhesion force was defined as the maximum force for the detachment of the cell from the substrate, corresponding to the force at the minimum point of the retraction curve. Adhesion work was estimated as the amount of work required to detach the cell from the substrate, corresponding to the area enclosed by the baseline and retraction curve[40].

2.2.8 Human platelet adhesion test

The antithrombotic properties of the hybrids were evaluated using the human platelet adhesion test. Human platelet adhesion tests were performed according to our previously reported procedure [41]. In brief, human whole blood was centrifuged at 400g for 5 min to collect platelet-rich plasma (PRP). The residue was also centrifuged at 2500g for 10 min to collect platelet-poor plasma (PPP). Plasma solution containing platelets was prepared by adjusting the seeding density to 4×10^7cells/cm^2 by mixing PRP and PPP obtained from fresh human whole blood. The plasma solution (200μL) was placed on each polymer substrate cut into 8×8 mm squares, and the substrate was incubated at 37°C for 1 h. After 1 h of incubation, each substrate was rinsed with PBS(−), and then, the platelets adhered to the substrates were fixed by immersing in 1%glutaraldehyde in PBS(−) for 2h at 37°C. Finally, each substrate was rinsed with PBS(−) and pure water and then

dried. The number of adhered platelets was counted by scanning electron microscopy (SEM).

2.2.9 Platelet–polymer substrate interaction by SCFS

Prior to this experiment, PMEA analogous substrates were exposed under UV for 30 min and thereafter incubated with PBS for 1 h at 37 °C. The supplied fresh blood was centrifuged at 400 g for 5 min to obtain platelet-rich plasma (PRP), and the remaining blood was centrifuged at 2500 g for 10 min to obtain platelet-poor plasma (PPP). PPP was thereafter added to the substrate, and freshly collected platelets (PRP-10 µl) were injected into the PPP. Meanwhile, the tip-less cantilever TL-CONT (spring constant k = 0.2 N/m, NA-NOSENSORS) was treated with human fibronectin solution (1 mg/mL) for 10 min. A single platelet was captured with a tipless cantilever for holding time of 5 min (set point: 2 nN) (Supporting information Figure S3). The Z-lengths for platelet was 50 µm to en-sure a complete separation of cells. The average size of platelet is 1.5-3µm and detached around 7-10 µm. The force curves between the platelet and the substrate were recorded using an AFM (CellHesion, JPK) equipped with a platelet-attached tipless cantilever (set point: 2 nN, approach rate: 1.0 µm/s, holding time: 10 s, retraction time: 5 µm/s) (Supporting information Figure S4).

2.2.10 FM-AFM of single HUVEC surface

Frequency Modulation AFM (FM-AFM) is a powerful tool for investigating weak interactions on interfaces using the frequency shift associated with cantilever oscillation to detect interactions on a probe. In FM-AFM, the cantilever acts as the oscillator in an active circuit. The frequency of the cantilever changes due to the force interaction between the cantilever tip and substrate at constant amplitude. Frequency changes are detected by an FM demodulator.

FM-AFM was performed using an SPM-8100FM (Shimadzu Co., Japan) in water at 23 °C. A PPP-NCHAuD cantilever (typical spring constant, k = 42 N/m, NanoWorld AG) was used. The

resonance frequency in water was approximately 140 kHz, and the z-direction scan was performed with a force limit of 2 V, which corresponds to a frequency shift of ca. 400 Hz. The amplitude of the cantilever oscillation was maintained constant at approximately 2 nm.

2.2.11 Statistical analyses

Data are expressed as mean ± standard deviation (SD) of at least three independent trials. The significance of the differences between the means of the individual groups was assessed by one-way analysis of variance followed by the Tukey–Kramer multiple comparison test using Origin Pro ver. 2019b (Northampton, MA, USA). Statistical significance was set at $p < 0.05$. Curve fitting was performed using the Origin Pro ver. 2019b (Northampton, MA, USA).

2.3 Results and Discussion

2.3.1 Physicochemical properties of PMEA analogous coated surface

Figure 2.1 shows the chemical structures of the polymers investigated. Previously, it was clearly demonstrated that PMEA analogous polymer (PMEA, PMC3A, and PBA) contained three different types of water: FW, IW, and NFW[41–44]. Based on this analysis, the physicochemical properties, including molecular weight (Mn), glass transition temperature (T_g), amount of FW, IW, NFW, and equilibrium water content (EWC), are summarized in (Table 2.1). The amount of each water content (FW, IW, NFW, and EWC) and T_g changed in the following order: PBA < PMC3A < PMEA and PMEA > PMC3A > PBA, respectively. It is also reported that the hydrophilicity of the side chain of a polymer was linked to hydrated water and cell attachment behavior[45]. In contrast, the surface morphologies of PMEA analogous coated PET substrates were investigated using transmission electron microscope (TEM) and AFM previously. TEM observations indicated that the thickness of the spin-coated film was approximately 70–80 nm[46], and AFM topographic analysis identified the microphase-separated structure as polymer- and water-rich domains of

specific coated substrates[47] in which the water-rich domain worked to reduce the adsorption of fibrinogen on PMEA. In addition, because of the strong effect of the physicochemical properties of the biopolymer interface, the surface type was confirmed by CA measurements in dry and hydrated states. The CA of each coated substrate was measured using both sessile drop and captive air bubble methods (Table 2.2). The results were recorded for 60 s and presented herein at exactly 30 s. In the sessile drop measurements, the CA decreased in the following sequence: PMPC > PBA > PET > PMC3A > PMEA, whereas results from captive air bubbles exhibited different trends as PMPC > PMEA > PMC3A > PBA > PET at 30 s and 24 h of soaking. These results revealed that proper coating of each polymer on the PET substrate and hydration caused a structural change in the coated surface for specific coated substrates. No significant changes were observed for the PET substrates.

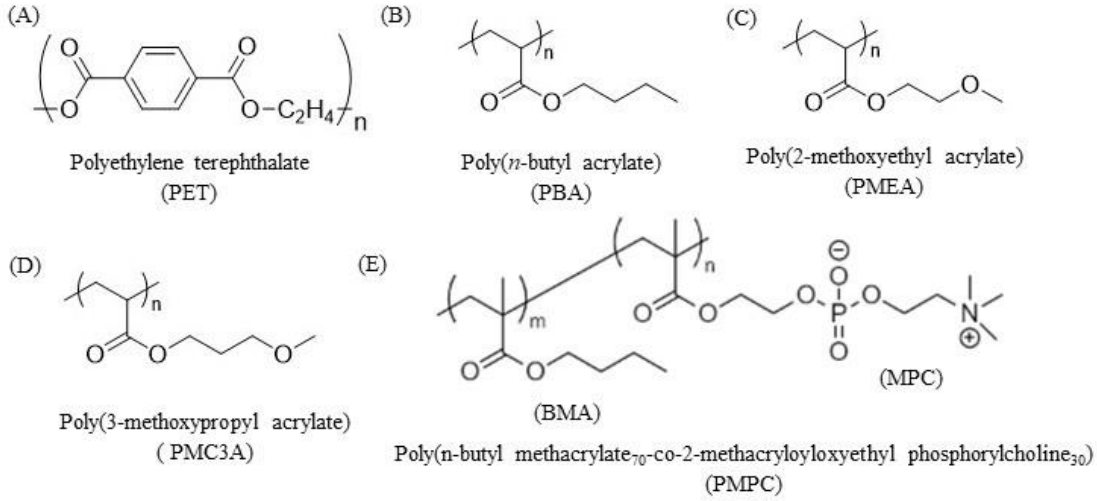

Figure 2.1. Chemical structure of (A) polyethylene terephthalate (PET); (B) poly(n-butyl acrylate) (PBA); (C) poly(2-methoxyethyl acrylate) (PMEA); (D) poly(3-methoxypropyl acrylate) (PMC3A), and (E) poly(*n*-butyl methacrylate$_{70}$-co-2-methacryloyloxyethyl phosphorylcholine$_{30}$) (PMPC).

Table 2.1: Characterization of PMEA analogous polymer.

Polymers	M_n (Kg/mol)	M_w/M_n	T_g dry [a)] (˚C)	T_g wet[a)] (˚C)	IW[a,b)] (wt.%)	NFW [a,b)] (wt.%)	FW [c)] (wt.%)	EWC[d)] (wt%)
PBA	62.8	1.41	-47	-48	0.31	0.45	0.54	1.3
PMEA	26.9	2.73	-35	-51	3.7	2.5	2.5	8.7
PMC3A	20.8	3.83	-48	-58	2.8	3.1	1.7	7.6
PMPC	--	--	--	--	11.11	33.33	--	--

[a]Measured by DSC performed at a rate of 5 ˚C/min, [b]intermediate water (IW), [c]non-freezing water (NFW), and [d]equilibrium water content (EWC)

Table 2.2: CAs on the polymer surface*

Polymers	CA [deg]		
	Sessile water drops	Captive air bubble	
	(30 s)	(30 s)	24 h
PET	73.3 (±0.9)	125.5 (±2.2)	125.4 (±0.5)
PBA	83.8 (±1.9)	126.7 (±2.8)	125.0 (±1.7)
PMEA	44.3 (±2.1)	134.0 (±0.9)	132.9 (±1.8)
PMC3A	52.1 (±0.5)	126.9 (±1.0)	127.8 (±0.7)
PMPC	108.9 (±0.5)	152.4 (±2.9)	150.0 (±3.8)

* 2 μL water droplet in air (sessile drop) and 2 μL air bubble in water (Captive bubble). The data represent the means ± SD (n = 5)

2.3.2 Cell attachment and proliferation assay

Toward the design of biomaterials, particularly ASDBVs, the ability of attachment, sustainability, and proliferation of endothelial cells on the coated substrate is one of the significant factors. From the anatomy of native blood vessels, it is known that blood vessels consist of three distinct layers: tunica extema or adventita, tunica media, and tunica intima, which is the most inner layer[48]. Therefore, the endothelial cells are attached to this inner part, where blood is directly in contact with these cells and blood flows over there. Consequently, endothelial cells play a vital role in blood vessel compatibility. In this regard, we performed cell attachment and proliferation assays of HUVECs and attached cell morphology to evaluate whether the coated surface was viable, as shown in **Figure 2 (a–b)**. Initially, we seeded HUVECs on the substrate and evaluated the number of cells attached and proliferated after 1, 3, 5, and 7 days of culture. Thereafter, we observed that after 24 h of culture time, more than 50% of the seeding density (5 x 10^3 cells/cm2)

of HUVECs adhered to PMEA, PBA, and PET. It indicates that the number of adhered cells on these polymers are almost similar to each other. Whereas PMC3A showed comparatively lower number of HUVECs adhered on its surfaces which is 42% if its seeding density. In contrast, PMPC and TCPS exhibited very low and high (127%) cell attachments, respectively, of negative and positive controls. As the culture time increased, days 3 to 5 HUVECs proliferated gradually on PMEA, PBA, and PET. However, almost all cells had died on PMPC owing to lack of adherence, and the number of cells increased on TCPS, similar to the trend observed in previous studies. On the other hand, HUVECs number were increased more than two- and three-fold on PMEA, PMC3A, and PET respectively, whereas PBA exhibited low amplification. The number of HUVECs on the substrates at day 7 decreased in the following order: TCPS > PET > PMEA > PMC3A > PBA > PMPC. However, the differences among PMEA, PMC3A, and PBA were not significant, even on day 7. Therefore, we performed further investigations using SCFS as a more quantitative and short-time investigation.

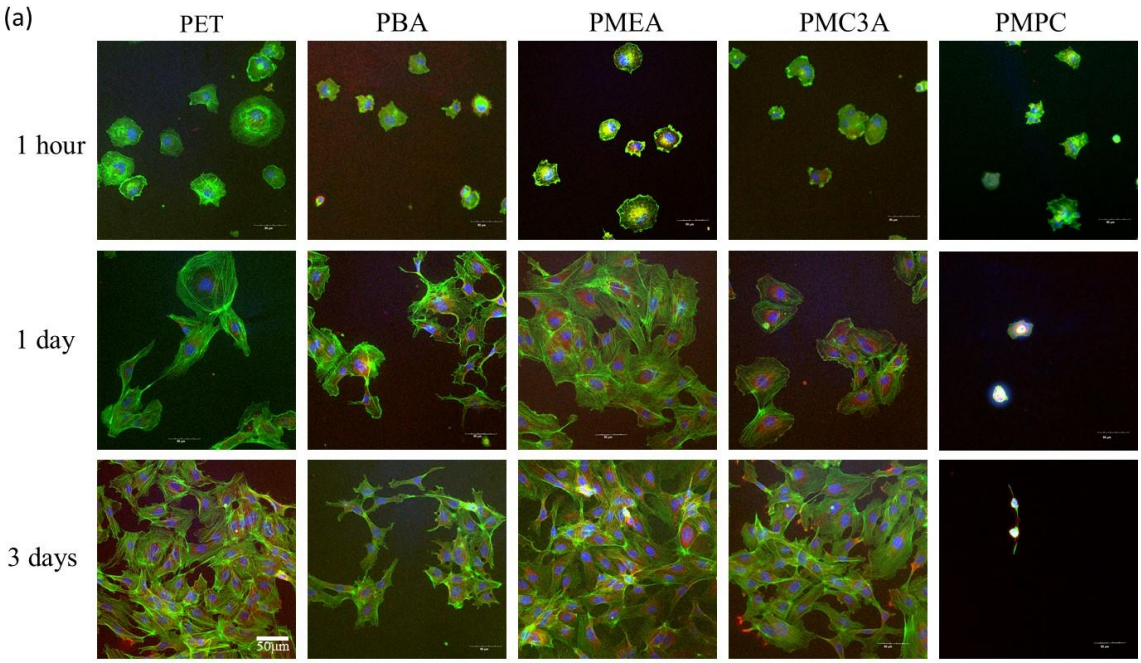

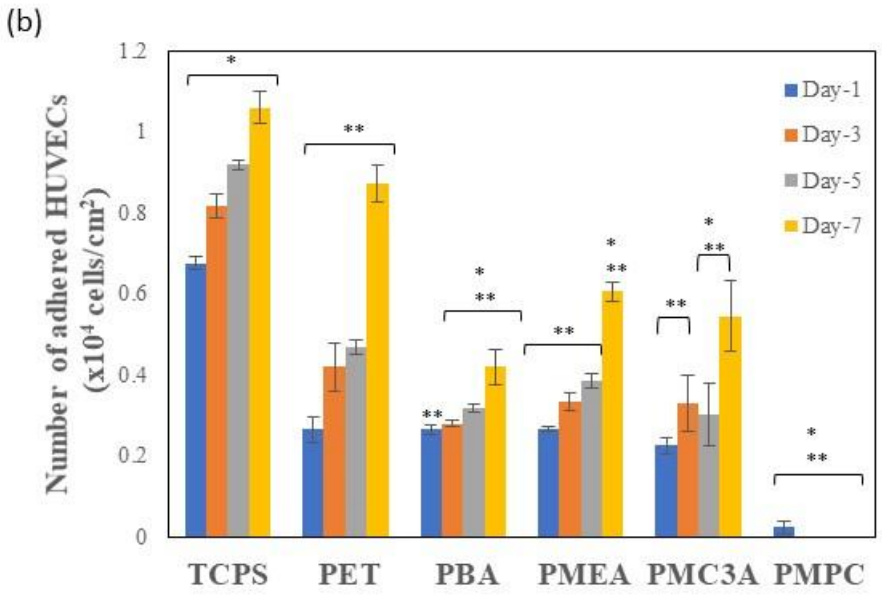

Figure 2.2. (a) CLSM images of PMEA analogous-coated substrates. Blue: cell nuclei; green: vinculin; red: actin fibers. White bar indicates 50 μm. (b) Number of adhered HUVECs on PMEA analogous coated substrates at 1, 3, 5, and 7 d. The data represent the mean ± SD (n = 3), **p < 0.05 compared with TCPS and *p < 0.05 compared with PET.

2.3.3 Measurement of cell -substrate interaction behavior by SCFS

One of the vital features before the construction of ASDBV is to obtain knowledge of the degree of adhesion strength of cell-substrate interactions at the interface of the synthetic polymers. When the blood flows inside the blood vessel, particularly over the layer of endothelial cells, it creates a certain shear force that can wash out the cells from the substrate surface if the adhesion strength is not sufficiently strong. Moreover, different cells have different interaction behaviors for specific surfaces, which may be strong or weak. In addition, cell types and surface characteristics are responsible for this phenomenon. Furthermore, surface modification with the investigation of substrate surface morphology such as roughness, hydrophilicity and hydrophobicity, bound water content influences the cell adhesion strength[39]. Protein adsorption on the substrates also regulates the cell adhesion ability[49]. There is other possibility of tuning cell adhesion by chemical

functionalization as in the case of neural cells where adhesion/repulsion has been controlled after suitable functionalization of metal electrodes[50]. Thus, quantitative investigation and comparison are required for the fabrication of an appropriate ASDBV. In this study, we evaluated the interaction strength between the cell membrane and PMEA-analogous substrates using SCFS. The SCFS measurement, which uses a single cell as a probe for the AFM cantilever, provides insights into the magnitude of the initial interaction force of a single cell in contact with the substrates[40]. In brief, AFM observation is considered as a multipurpose technique including imaging and detection of tiny interaction forces in few pN level between two surfaces. SCFS mode of AFM technique may detect the interaction between single living cells and substrate or single cell, one on the substrate, and other one is adhered on the cantilever with the help of cell adhering protein coating[51].

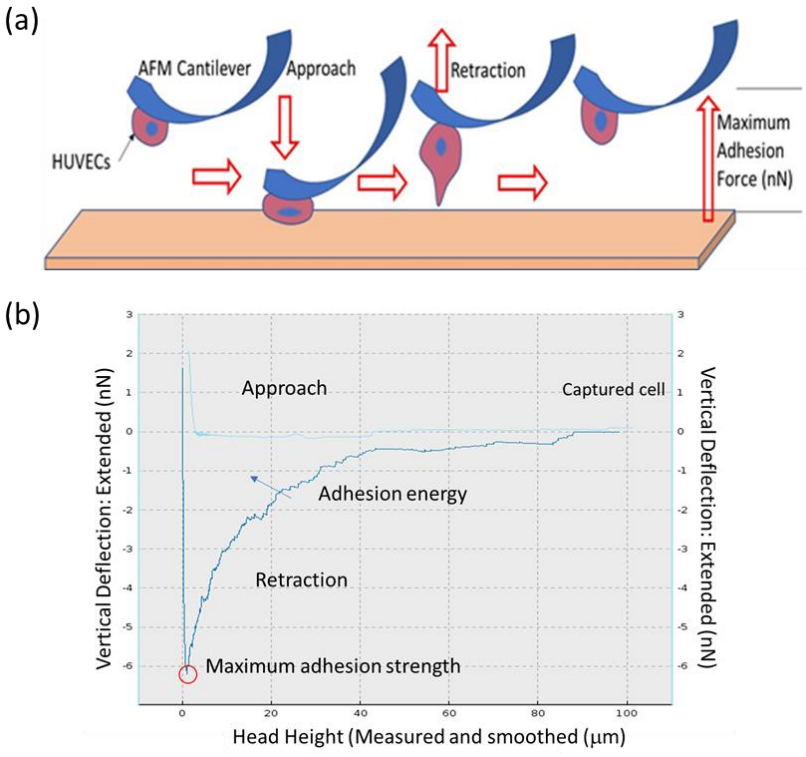

Figure 2.3. Schematic of (a) cell–substrate interaction measurement (b) A force–distance (F-D)

curve recorded with the CellHesion AFM technique.

An animation is presented in **Figure 2.3** to illustrate how cell-substrate interaction was measured and (b) A force–distance (F-D) curve recorded with the CellHesion AFM technique. In brief, the cantilever was coated with fibronectin, and a single cell was captured and approached the measured substrate. Here, an interaction occurred between these two surfaces. After a while, the cantilever was retracted, and the data were represented as the force–distance curve. The SCFS results are shown in **Figure 2.4**. We found that HUVECs adhered to PMEA more strongly than to other analogous. The adhesion strength and energy were similar to those of TCPS and PET. In contrast, PBA exhibited a low adhesion strength and energy for HUVECs adhesion. The adhesion on PMC3A was lower, but larger than that on PMPC.

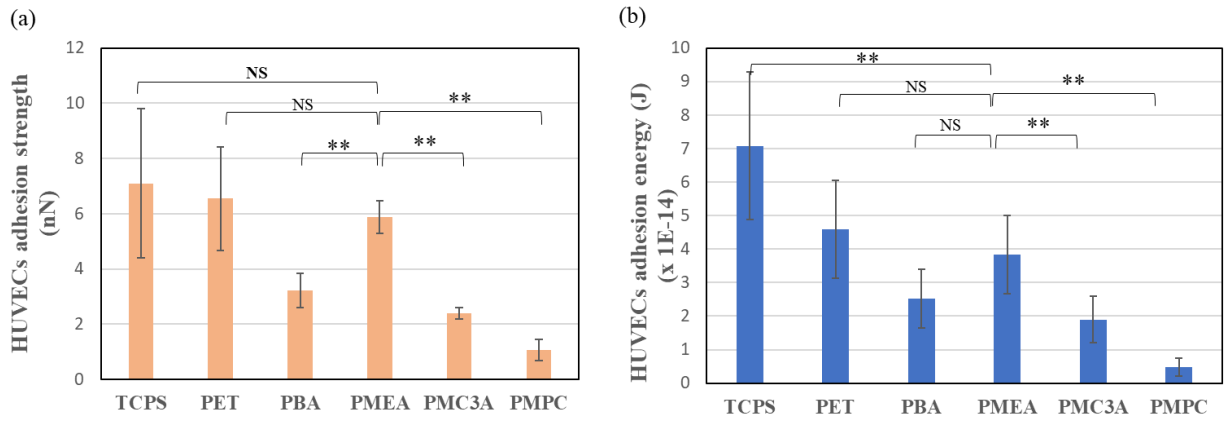

Figure 2.4. (a) HUVECs adhesion strength and (b) adhesion energy on various polymer substrate. The data represent the mean ± SD ($n > 10$), $^{**}p < 0.05$ compared with PMEA.

Generally, cells adhere to the polymeric interface through cell-binding proteins. In serum-containing media, fibronectin, a cell adhesion protein, is responsible for cell adhesion through integrin, which is known as integrin-dependent cell adhesion[52]. However, it has been reported that integrin-independent cell adhesion may occur on PMEA through direct interactions between the cell membrane and the polymer surface[27]. In this case, protein adsorption on the PMEA surface

was inhibited because of the presence of a hydration layer, where IW portion is the key factor. In our previous study, we observed that cells could adhere to the PMEA surface without FBS proteins[26,27]. Endothelial cells, such as HUVECs, are more likely to adhere to fibronectin than fibrinogen through the RGD sequence, which is known as a universal binding site[53–55]. In our study, PMEA-analogous polymer exhibited different adherences to HUVECs because of its surface characteristics and morphology. At hydrated condition the PMEA analogous polymer shows microphase separation and the protein adsorption behavior is different for each phase of each polymer. We are saying that protein adsorption regulates the cell adhesion and we tried to find how strong the cell adhesion on each substrate by SCFS. From our previous investigations, more fibronectin adhered on water rich domain whereas fibronectin and fibrinogen adsorption are similar on polymer rich region[49]. Fibronectin is responsible for cell adhesion and fibrinogen enhance the platelet adhesion. Furthermore, it is reported that PMEA contains 3.7% IW, whereas PMC3A and hydrated PBA contain 2.7% and 0.1% IW, respectively. It was also reported that more than 3%IW is required to become the surface better hemocompatibility for poly(ethylene glycol), poly(meth)acrylates, aliphatic carbonyls, and poly(lactic-co-glycolic acid) surfaces.[56]. Therefore, owing to the different IW content, the cell adhesion number varied in our tested polymers.

2.3.4 Human platelet adhesion test

A platelet adhesion number test was performed under static conditions to evaluate the non-thrombogenic properties of PMEA-analogous polymer. The morphology and number of attached platelets were investigated using SEM. Several platelets attached to the PET surface were also observed. A similar trend was observed for PBA-coated surfaces. On the other hand, PMEA, PMC3A, and PMPC exhibited few platelet adhesions. Moreover, the platelets attached to PMEA, PMC3A, and PMPC appeared mostly circular, unbranched, and distributed far away. The platelet

area was also small, at approximately 2–5 μm. This implies that activation levels I to II, regularly I for PMPC and PMEA, were observed. In contrast, almost all of the attached platelets on PET and PBA exhibit activation levels of II to III. This implies that platelet spreading and proliferation occurred on the surface. The attached platelet area at approximately 5–10 μm has several branches.

However, we still do not know how strongly or loosely the platelets adhere to the surface. As previously mentioned, shear stress affects adherent cells and platelet adhesion inside native blood vessels.

Furthermore, to investigate the platelet adhesion strength on PMEA-analogous polymers more quantitatively, we also used SCFS for platelets (Figure 2.6a). Similarly, platelet adhesion energy was calculated for each substrate. This adhesion energy represents the area under the retraction curve of the force curves obtained from the SCFS (Figure 2.6b). This reveals the total work done to detach platelets from their adherent state. A higher energy indicates a greater spread of platelets and strong adhesion to the substrates. We found that the adhesion force between platelets and PET has the highest interaction strength among all the polymers. The second highest level was platelet-PBA. Owing to the lack of IW in the chemical structures of PET and PBA, platelet adhesion protein adsorption increased. Therefore, platelets attached and denatured on these surfaces within a short time, and during retraction of the cantilever, more force is needed to detach the platelets from the surfaces. PMEA and PMC3A exhibited similar strengths, but lower strength compared to PET and PBA, whereas PMPC exhibited the lowest adhesion force. Moreover, the platelets were loosely attached to PMPC, PMEA, and PMC3A. These results also confirmed platelet adhesion on the test polymers under static conditions. In addition, we have observed the oscillation in approach and retraction curve which is little complicated to understand. It can be clarified as the experiment was conducted using platelet poor plasma (PPP) collected from whole human blood and single platelet.

In PPP, the blood proteins density is still high and may create sublayer which influence the movement of cantilever resulting oscillation happen in approach and retraction curve at 10 μm above from the polymer interface. However, the practical interaction of platelet-polymer and detachment happened within 10 μm because of the small size of single platelet. Most of the measurement related to platelet adhesion force and adhesion energy shows similar tendency.

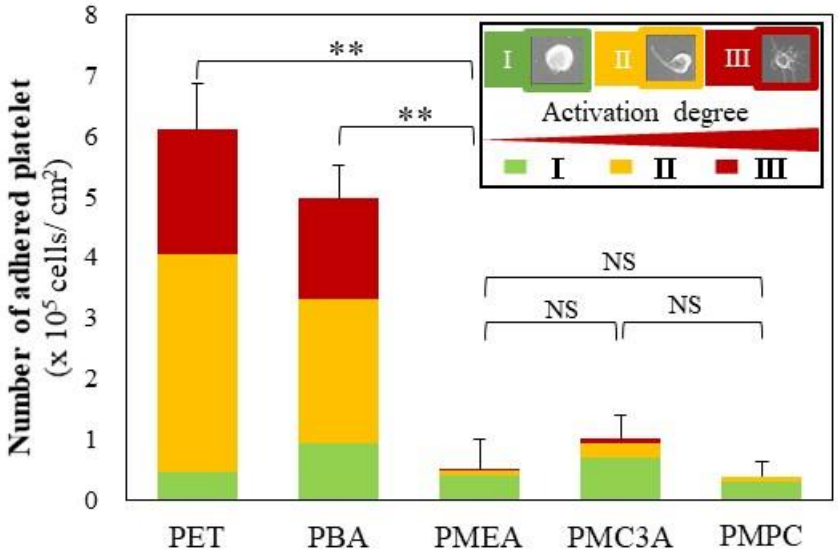

Figure 2.5. Summary of the human platelet adhesion experiments. Number of the adhered platelets on the coatings of the PMEA, PMC3A, PBA, PMPC, and bare PET. The data represent the means ± SD, n = 15, **: $p < 0.01$ (vs PET).

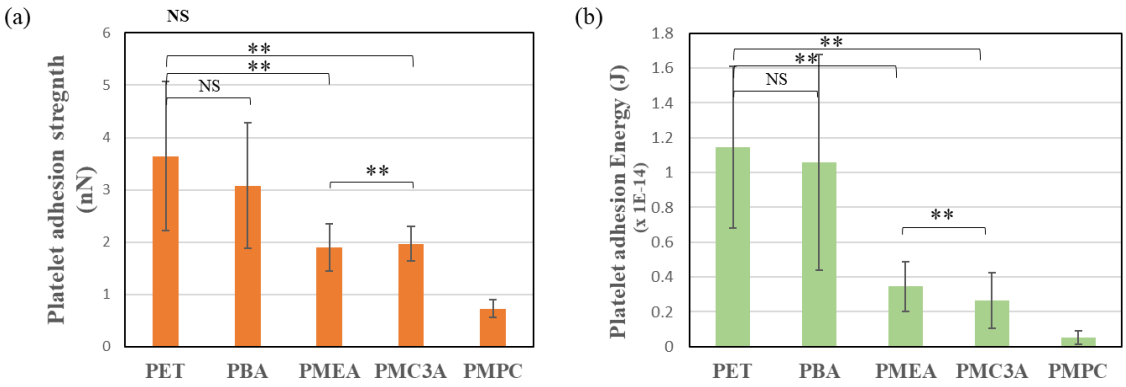

Figure 2.6. Comparison of (a) platelet adhesion strength and (b) adhesion energy on different polymer substrates. The data represent the mean ± SD ($n > 5$), $^{**}p < 0.05$ (vs PET).

To determine the mechanism of platelet adhesion behavior, we previously reported that platelet adhesion is regulated by the amount of blood serum proteins or adhesion proteins that adhere to the polymer surface[8,38,41]. Fibrinogen and fibronectin are responsible for platelet adhesion. Fibrinogen is the plasma protein responsible for platelet adhesion[57], and it has been reported that the γ-chain of fibrinogen is related to the adhesion and activation of platelets, leading to thrombogenesis[57,58]. However, some synthetic polymers suppress platelet adhesion by suppressing fibrinogen adhesion[58]. The reason behind this property was attributed to the hydration layer formed at the interface. This hydration layer acts as a barrier between the serum protein and polymer surface. When synthetic polymers are exposed to the culture medium, PBS, or water, they adsorb water molecules at various positions in their chemical structures[8,47,59].

We initially indicated that Tanaka et al. reported that hydrated PMEA and its analogous contains IW. However, not all polymers are associated with these water molecules. All natural biopolymers were found to comprise IW on their surface, such as heparin, chondroitin sulfate, and DNA (RNA). Recently, it has been established that IW is a key factor in surface biocompatibility[42]. Sato et al. found different amounts of IW in hydrated PMEA analogous. They also reported that these hydrated PMEA analogous suppressed platelet adhesion by suppressing protein adsorption

and deformation by increasing the amount of IW. Our platelet-substrate interaction study also demonstrated that the amount of IW might play a key role in expressing the blood compatibility of polymeric materials. If we order our polymer as IW content, we observed a similar tendency that platelet adhesion was suppressed as the IW increased, and the percentages of IW of the test polymers are listed in **Table 2.1**. Because PET and PBA do not contain any IW, serum proteins adhered to the surface. Consequently, the number of platelet adhesions was high. In contrast, PMPC, PMEA, and PMC3A exhibited low platelet counts on their surfaces. This is because IW exerts a repulsive effect against protein adsorption. Previously, we reported the spontaneous formation of numerous protrusions of the nanometer scale at the PMEA/phosphate-buffered saline (PBS) interfaces[47]. This result indicates the microphase separation of the polymer as polymer- and water-rich domains at the interfacial region[60]. Because of the partial imbroglio of the polymer chain in the bulk polymer phase, the mobility of the polymer chain is restricted at the interface, and phase separation occurs on the microscopic scale. The phase separation of a homopolymer at an interface is unique and makes an essential contribution to the blood compatibility of PMEA[61,62]. Our previous work also indicated that plasma protein fibrinogen exhibited adhesive interactions with the PMEA interface in polymer-rich domains, but repulsive interactions in water-rich domains[61]. In contrast, fibrinogen adhered to both the polymer- and water-rich domains on PBA, an analogous polymer of PMEA, exhibiting thrombogenic behavior. We considered that the differences between PMEA and PBA were caused by differences in polymer density and hydration structures, particularly in the water-rich domains[58].

To clarify the mechanism of protein adsorption and the platelet adhesion, the adhesion force between blood compatible polymer (PMEA, PBA) and proteins (BAS and fibrinogen) were measure by AFM in our previous investigation[63]. Here, Hayashi *et al*. showed that electrostatic

force may not be responsible for protein resistance of PMEA whereas PBA strongly adhered to proteins. He also found that the self-assembly monolayer (SAM) of ethylene glycol (EG) shows the water- mediated repulsion in surface force measurements that prevented platelet adhesion[64]. Furthermore, the charge neutrality of the terminal groups of the SAMs is necessary for suppression of protein adhesion as well as platelet compatibility. However, the local electrostatic interaction between the protein and SAM overcomes the water-induced repulsion, resulting in the adsorption of proteins and the adhesion of platelets[64].

2.3.5 FM-AFM observation of coated polymer surfaces

FM-AFM is a powerful tool for investigating weak interactions on interfaces using the frequency shift associated with cantilever oscillation to detect interactions on a probe. In our previous work[65], we reported FM-AFM observations of polymer-grafted Au substrates of PMEA, PMC3A, and PBA, and that PMEA and PMC3A exhibited a repulsive layer (mixed layer of polymer chains and hydration water) in water-rich domains. In contrast, PBA exhibited no repulsive layers in the water-rich domains. This difference may reflect the presence of IW on the interfaces. In this work, we performed FM-AFM to investigate the hydration states of spin-coated polymer films.

Figure 2.7(a–e) shows the results of FM-AFM (z–x scan) on each polymer/water interface, and Figure 2.7(f) shows the frequency shift (the intensity of the repulsion) as a function of distance from the interface obtained from the averaged cross section of the entire x-range. The repulsive layer is marked in blue and white, demonstrating the degree of frequency shift. The thickness of the repulsive layer on the PMPC was dramatically high at a thickness of approximately 20 nm. This thick hydration layer indicates a large amount of hydration at the PMPC/water interface and could be the reason for the extremely low HUVEC attachment and platelet adhesion. The

thicknesses of the other polymers were relatively small; however, a clear trend was observed. The repulsive layer thickness decreased in the order of PMPC > PMEA > PMC3A > PBA~PET. Interestingly, this trend is in accordance with the amount of hydrated water in the polymers (Table 2.1) and the trend of platelet adhesion (**Figures 2.5** and **2.6**). Therefore, we can expect that these repulsive layers on the spin-coated polymer films may originate from the mixed layer of polymer chains and hydration water on the interfaces, as well as our previous results obtained in the grafted polymer systems, and work to suppress platelet adhesion on the interfaces.

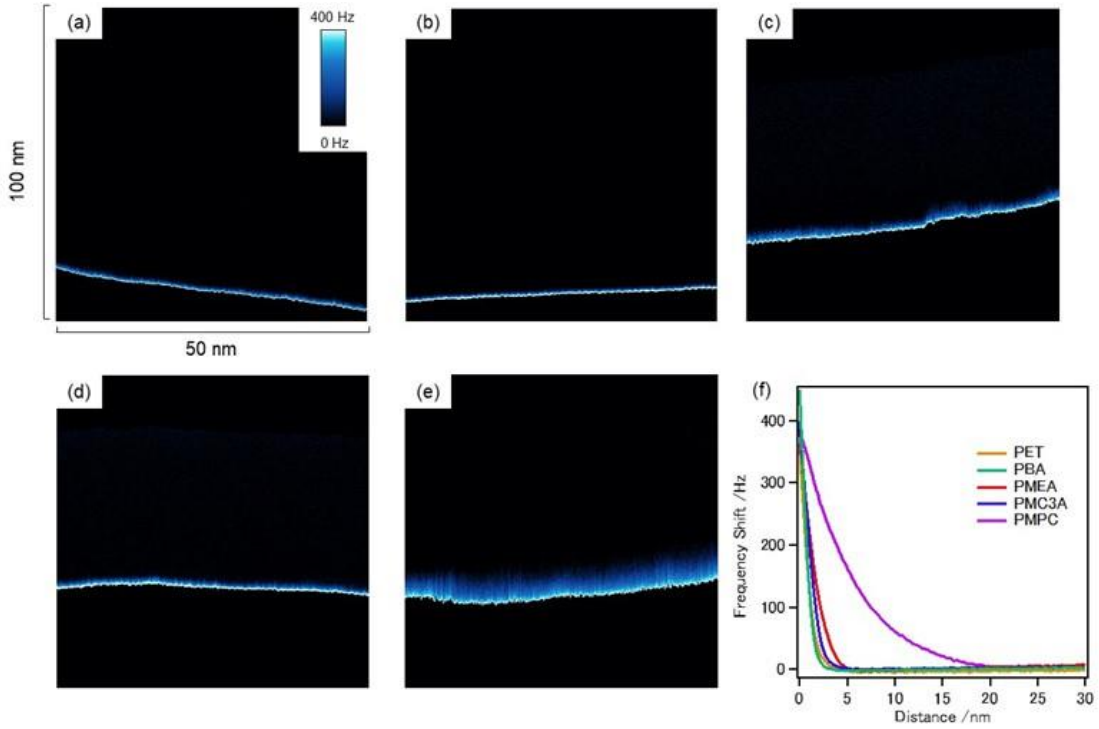

Figure 2.7. Images of FM-AFM z–x scan on (a)PET, (b) PBA, (c) PMEA, (d) PMC3A, and (e) PMPC. (f) Frequency shift-distance curves obtained from the averaged cross section of (a–e).

2.3.6 Relationship between IW and cell adhesion strength

Candidacy of PMEA as the construction material of the ASDBV depends in the relationship between IW and cell adhesion strength, as shown in (**Figure 2.8**). We confirmed that the HUVEC adhesion strength, number of adhered HUVECs and platelets on these substrates are related to the

IW content of each polymer. In this study, we investigated a PMEA-analogous polymer to find the most suitable polymer for use as a construction material for ASDBV development by the fulfilment of similar desired requirements of a native blood vessel. It is known that the native blood vessel has three layers: the adventitia or outer layer, which provides structural support and shape to the vessel; the tunica media, or a middle layer composed of elastic and muscular tissue that regulates the internal diameter of the vessel; and the tunic intima or an inner layer consisting of an endothelial lining that provides a frictionless pathway for blood movement[48]. Therefore, the surface of the artificial blood vessel should be biocompatible, nonthrombogenic, and have similar biochemical functions as native vessels.

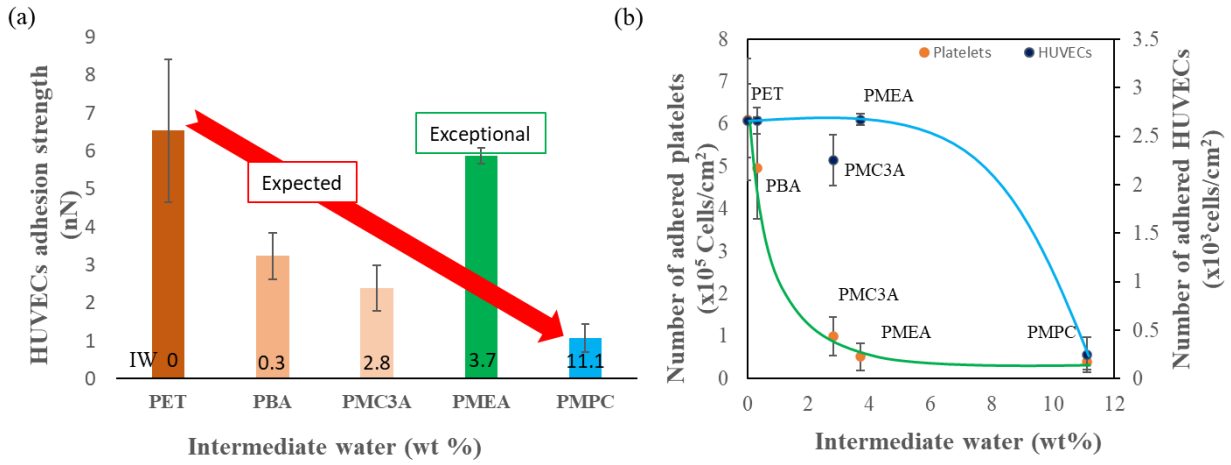

Figure 2.8. Effect of IW content on (a) HUVECs adhesion strength and (b) number of adhered platelets and HUVECs on PMEA analogous polymer.

First, we explicitly focused on the adhesion behavior of HUVECs on substrates. HUVECs attachment test reveals how the number of attached cells decreased with increasing the IW as shown in (Figure 2.8b). Similarly, HUVEC adhesion strength was more drastically enhanced on PMEA than on PMC3A or PBA. In addition, we compared platelet adhesion on the polymers. It

was clear from both the normal adhesion test and platelet adhesion strength measurements that PMEA and PMC3A effectively suppressed platelet adhesion, but PBA did not. These results indicate that PMEA is an excellent candidate as a construction material for ASDBV development because it possesses both cytophilic and antithrombotic properties. In contrast, PMC3A suppressed both platelets and HUVEC, but PBA did not suppress either.

Additionally, the hydration state of the hydrated polymer surface was examined using FM-AFM for the first time. The thickness of the repulsive layer observed for each polymer agreed well with the trend of platelet adhesion and the amount of water in the polymers. As it is expected that the repulsive layer contains polymer chains and hydration water, the presence of the repulsive layer indicates the presence of water molecules interacting with the polymer chains on the interface, that is, IW. This result is consistent with our previous results demonstrating that IW suppresses fibrinogen adsorption and platelet adhesion at material interfaces. In the case of cell attachment, cells generally attach to the polymeric interface via cell-binding proteins. In serum-containing media, fibronectin, a cell adhesion protein, is responsible for cell adhesion through integrin, which is known as integrin-dependent cell adhesion[52]. Our recent work revealed that fibronectin easily interacts with the surface of biomaterials and causes conformational changes, even on PMEA. Furthermore, it has been reported that integrin-independent cell adhesion may occur on PMEA through direct interactions between the cell membrane and polymer surface[27]. This indicates that the difference in the trend of HUVEC attachment on PMEA, PMC3A, and PBA should be explained by other factors, not only the hydration layer on the interfaces. However, the relationship between cell adhesion strength and IW implies antithrombogenic surfaces of PMEA in the fabrication of ASDBV.

2.3.7 Relationship between hydrophilicity of polymer and cell adhesion strength

Besides the relationship between IW and cell adhesion strength, we have developed the relationship between hydrophilicity of polymer and cell adhesion strength. Hydrophilicity is measured in terms of the contact angle of the water drops to the surface of each polymer. In case of PMPC copolymer, before hydration, the water contact angle is high due to hydrophobicity of BMA although the PMPC homopolymer brush water contact angle is 3°[66]. We have plotted the cell adhesion strength against the water contact angle of each polymer that measured on both 1) sessile drop and 2) captive air bubble methods (shown in Figure 9a and 9b).

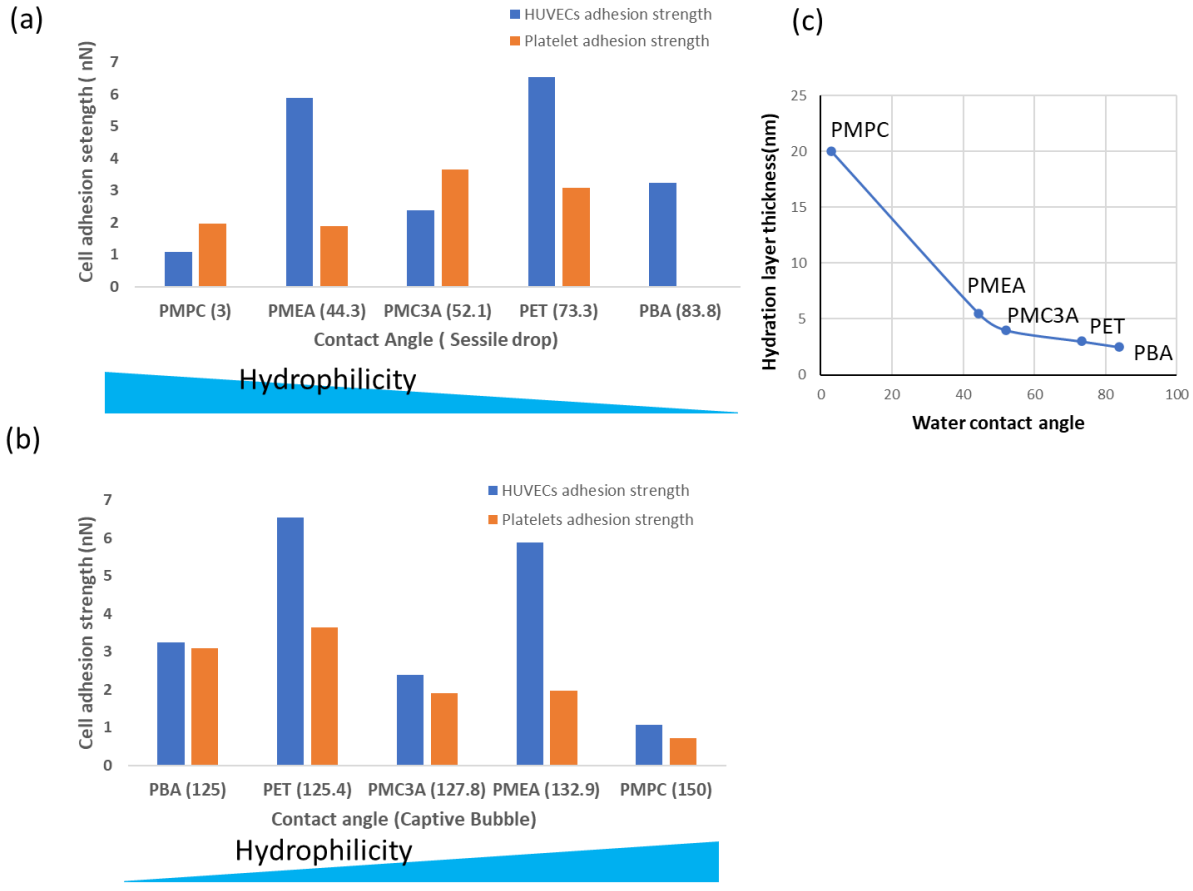

Figure 2.9. Effect of hydrophilicity of each polymer on HUVECs and platelets adhesion strength on PMEA analogous polymer (a) Sessile drop (b) Captive air bubble method.

In sessile drop method, we see that the order of hydrophilicity of studied polymer is PMPC>

PMEA>PMC3A>PET>PBA. PMPC is super hydrophilic whereas PMEA shows less surface hydrophilicity (Figure 2.9a) at initial stage. On the other hand, the order of hydrophilicity of studied polymer measured after 24 h of hydrated state by captive bubble methods is PBA ≈PET<PMC3A <PMEA<PMPC. As we know that protein adsorption is suppressed because of hydration layer formation on the surface of polymer. From FM-AFM observation, we have evaluated the thickness of hydration layer. If we compare the figure 2.9b with the thickness of hydration layer (shown in Figure 2.7f), we will find the same order as the order of contact angle (Figure 2.9c). This result reveals that at hydrate condition polymer change its hydrophobicity due to the IW content as well as EWC (Table 2.1).

Therefore, there is no direct relation between cell adhesion strength and contact angle, but it can be said that IW regulates the hydration layer; Hydration layer suppress the protein adsorption; low protein adsorption suppresses the platelet adhesion. In contrast, PMEA and PMC3A exhibits phase separation state where polymer rich and water rich domain present. These water rich domain accept fibronectin adsorption and denaturation and then cell can attach on that protein. Thus, PMEA shows suppress of platelet adhesion and increase of HUVECs attachments with strong interactions.

2.4 Conclusions

In conclusion, based on the conducted experiments, results, and discussion, the surface interactions of HUVECs were measured extensively. The IW content of PMEA analogous polymers influences the HUVEC adhesion strength and the number of adhered HUVECs and platelets on each substrate. It can be said that PMEA achieves the best outcomes among the analogues, such as low platelet adhesion and adhesion strength, high HUVECs attachment, proliferation, and high adhesion strength at the initial time. It can be suggested that PMEA can be

used as a construction material to develop ASDBV because of its nonthrombigenic behavior and strong adhesion of endothelial cells. Finally, in this work, we examined the potential of PMEA for use in ASDBV at the initial stage, based on the interaction between the polymer interface and platelets and HUVEC. The cell behavior in the next stage, that is, monolayer formation of HUVEC on PMEA (HUVEC–HUVEC interaction) and the antithrombogenic property of the HUVEC monolayer (HUVEC–platelet interaction), will be reported in the next series of studies.

2.5 References

(1) Ratner, B. D.; Hoffman, A. S.; Schoen, F. J.; Lemons, J. E. *Biomaterials Science: An Introduction to Materials in Medicine*; San Diego, California, 2004.

(2) Tsuruta, T. Contemporary Topics in Polymeric Materials for Biomedical Applications. *Advances in Polymer Science* **1996**, *126*, 1–55. https://doi.org/10.1007/3-540-60484-7_1.

(3) Kim, S. H.; Turnbull, J.; Guimond, S. Extracellular Matrix and Cell Signalling: The Dynamic Cooperation of Integrin, Proteoglycan and Growth Factor Receptor. *Journal of Endocrinology*. 2011, pp 139–151. https://doi.org/10.1530/JOE-10-0377.

(4) Guilak, F.; Cohen, D. M.; Estes, B. T.; Gimble, J. M.; Liedtke, W.; Chen, C. S. Control of Stem Cell Fate by Physical Interactions with the Extracellular Matrix. *Cell Stem Cell*. 2009, pp 17–26. https://doi.org/10.1016/j.stem.2009.06.016.

(5) Giancotti, F. G.; Ruoslahti, E. Integrin Signaling. *Science (1979)* **1999**, *285* (5430), 1028–1033. https://doi.org/10.1126/science.285.5430.1028.

(6) Anselme, K.; Bigerelle, M. Modelling Approach in Cell/Material Interactions Studies. *Biomaterials* **2006**, *27* (8), 1187–1199. https://doi.org/10.1016/j.biomaterials.2005.10.009.

(7) Harburger, D. S.; Calderwood, D. A. Integrin Signalling at a Glance. *Journal of Cell Science* **2009**, *122* (2), 159–163. https://doi.org/10.1242/jcs.018093.

(8) Tanaka, M.; Motomura, T.; Kawada, M.; Anzai, T.; Yuu Kasori; Shiroya, T.; Shimura, K.; Onishi, M.; Akira Mochizuki. Blood Compatible Aspects of Poly(2-Methoxyethylacrylate) (PMEA)-Relationship between Protein Adsorption and Platelet Adhesion on PMEA Surface. *Biomaterials* **2000**, *21* (14), 1471–1481.

(9) Radke, D.; Jia, W.; Sharma, D.; Fena, K.; Wang, G.; Goldman, J.; Zhao, F. Tissue Engineering at the Blood-Contacting Surface: A Review of Challenges and Strategies in Vascular Graft Development. *Advanced Healthcare Materials* **2018**, *7* (15), e1701461. https://doi.org/10.1002/adhm.201701461.

(10) Marchio, P.; Guerra-Ojeda, S.; Vila, J. M.; Aldasoro, M.; Victor, V. M.; Mauricio, M. D. Targeting Early Atherosclerosis: A Focus on Oxidative Stress and Inflammation. *Oxidative Medicine and Cellular Longevity*. 2019. https://doi.org/10.1155/2019/8563845.

(11) Libby, P.; Buring, J. E.; Badimon, L.; Hansson, G. K.; Deanfield, J.; Bittencourt, M. S.; Tokgözoğlu, L.; Lewis, E. F. Atherosclerosis. *Nature Reviews Disease Primers* **2019**, *5* (1), 56. https://doi.org/10.1038/s41572-019-0106-z.

(12) Mallis, P.; Kostakis, A.; Stavropoulos-Giokas, C.; Michalopoulos, E. Future Perspectives in Small-Diameter Vascular Graft Engineering. *Bioengineering*. 2020, p 160. https://doi.org/10.3390/bioengineering7040160.

(13) Xue, L.; Greisler, H. P. Biomaterials in the Development and Future of Vascular Grafts. *Journal of Vascular Surgery*. 2003, pp 472–480. https://doi.org/10.1067/mva.2003.88.

(14) Fang, J.; Li, S. Advances in Vascular Tissue Engineering. *Journal of Medical Biomechanics* **2016**, *31* (4), E333--E339. https://doi.org/10.3871/j.1004-7220.2016.04.333.

(15) Tara S; Rocco KA; Hibino N; Sugiura T; Kurobe H; Breuer CK; Shinoka T. Vessel Bioengineering. *Circulation Journal* **2014**, *78* (1), 12–19. https://doi.org/10.1253/circj.CJ-13-1440.

(16) Gao, A.; Hang, R.; Li, W.; Zhang, W.; Li, P.; Wang, G.; Bai, L.; Yu, X. F.; Wang, H.; Tong, L.; Chu, P. K. Linker-Free Covalent Immobilization of Heparin, SDF-1α, and CD47 on PTFE Surface for Antithrombogenicity, Endothelialization and Anti-Inflammation. *Biomaterials* **2017**, *140*, 201–211. https://doi.org/10.1016/J.BIOMATERIALS.2017.06.023.

(17) Weidenbacher, L.; Müller, E.; Guex, A. G.; Zündel, M.; Schweizer, P.; Marina, V.; Adlhart, C.; Vejsadová, L.; Pauer, R.; Spiecker, E.; Maniura-Weber, K.; Ferguson, S. J.; Rossi, R. M.; Rottmar, M.; Fortunato, G. In Vitro Endothelialization of Surface-Integrated Nanofiber Networks for Stretchable Blood Interfaces. *ACS Applied Materials and Interfaces* **2019**, *11*, 5740–5751. https://doi.org/10.1021/acsami.8b18121.

(18) Noy, J.-M.; Chen, F.; Akhter, D. T.; Houston, Z. H.; Fletcher, N. L.; Thurecht, K. J.; Stenzel, M. H. Direct Comparison of Poly(Ethylene Glycol) and Phosphorylcholine Drug-Loaded Nanoparticles In Vitro and In Vivo. *Biomacromolecules* **2020**, *21*, 2320–2333. https://doi.org/10.1021/acs.biomac.0c00257.

(19) Furuzono, T.; Ishihara, K.; Nakabayashi, N.; Tamada, Y. *Chemical Modifcation of Silk Fibroin with 2-Methacryloyloxyethyl Phosphorylcholine. II. Graft-Polymerization onto Fabric through 2-Methacryloyloxyethyl Isocyanate and Interaction between Fabric and Platelets*; 2000.

(20) Park, H. H.; Sun, K.; Seong, M.; Kang, M.; Park, S.; Hong, S.; Jung, H.; Jang, J.; Kim, J.; Jeong, H. E. Lipid-Hydrogel-Nanostructure Hybrids as Robust Biofilm-Resistant

Polymeric Materials. *ACS Macro Letters* **2019**, *8* (1), 64–69. https://doi.org/10.1021/acsmacrolett.8b00888.

(21) Suhara, H.; Sawa, Y.; Nishimura, M.; Oshiyama, H.; Yokoyama, K.; Saito, N.; Matsuda, H. Efficacy of a New Coating Material, PMEA, for Cardiopulmonary Bypass Circuits in a Porcine Model. *The Annals of Thoracic Surgery* **2001**, *71* (5), 1603–1608. https://doi.org/https://doi.org/10.1016/S0003-4975(01)02466-3.

(22) Hatakeyama, H.; Hatakeyama, T. Interaction between Water and Hydrophilic Polymers. *Thermochimica Acta* **1998**, *308* (1–2). https://doi.org/10.1016/s0040-6031(97)00325-0.

(23) Morita, S.; Tanaka, M.; Ozaki, Y. Time-Resolved in Situ ATR-IR Observations of the Process of Sorption of Water into a Poly(2-Methoxyethyl Acrylate) Film. *Langmuir* **2007**, *23* (7), 3750–3761. https://doi.org/10.1021/la0625998.

(24) Miwa, Y.; Ishida, H.; Saitô, H.; Tanaka, M.; Mochizuki, A. Network Structures and Dynamics of Dry and Swollen Poly(Acrylate)s. Characterization of High- and Low-Frequency Motions as Revealed by Suppressed or Recovered Intensities (SRI) Analysis of 13C NMR. *Polymer (Guildf)* **2009**, *50* (25), 6091–6099. https://doi.org/10.1016/j.polymer.2009.10.037.

(25) Tanaka, M.; Motomura, T.; Ishii, N.; Shimura, K.; Onishi, M.; Mochizuki, A.; Hatakeyama, T. Cold Crystallization of Water in Hydrated Poly(2-Methoxyethyl Acrylate) (PMEA). *Polymer International* **2000**, *49*, 1709–1713.

(26) Hoshiba, T.; Nikaido, M.; Tanaka, M. Characterization of the Attachment Mechanisms of Tissue-Derived Cell Lines to Blood-Compatible Polymers. *Advanced Healthcare Materials* **2014**, *3* (5), 775–784. https://doi.org/10.1002/adhm.201300309.

(27) Hoshiba, T.; Yoshihiro, A.; Tanaka, M. Evaluation of Initial Cell Adhesion on Poly (2-Methoxyethyl Acrylate) (PMEA) Analogous Polymers. *Journal of Biomaterials Science, Polymer Edition* **2017**, *28* (10–12), 986–999. https://doi.org/10.1080/09205063.2017.1312738.

(28) Medina-Leyte, D. J.; Domínguez-Pérez, M.; Mercado, I.; Villarreal-Molina, M. T.; Jacobo-Albavera, L. Use of Human Umbilical Vein Endothelial Cells (HUVEC) as a Model to Study Cardiovascular Disease: A Review. *Applied Sciences (Switzerland)* **2020**, *10* (3), 938. https://doi.org/10.3390/app10030938.

(29) Baudin, B.; Bruneel, A.; Bosselut, N.; Vaubourdolle, M. A Protocol for Isolation and Culture of Human Umbilical Vein Endothelial Cells. *Nature Protocols* **2007**, *2* (3), 481–485. https://doi.org/10.1038/nprot.2007.54.

(30) Onat, D.; Brillon, D.; Colombo, P. C.; Schmidt, A. M. Human Vascular Endothelial Cells: A Model System for Studying Vascular Inflammation in Diabetes and Atherosclerosis. *Current Diabetes Reports* **2011**, *11* (3), 193–202. https://doi.org/10.1007/s11892-011-0182-2.

(31) Schleger, C.; Platz, S. J.; Deschl, U. Development of an in Vitro Model for Vascular Injury with Human Endothelial Cells. *ALTEX-Alternatives to animal experimentation* **2004**, *21* (Supp2), 12–19.

(32) Vion, A. C.; Ramkhelawon, B.; Loyer, X.; Chironi, G.; Devue, C.; Loirand, G.; Tedgui, A.; Lehoux, S.; Boulanger, C. M. Shear Stress Regulates Endothelial Microparticle Release. *Circulation Research* **2013**, *112* (10), 1323–1333. https://doi.org/10.1161/CIRCRESAHA.112.300818.

(33) Fearon, I. M.; Gaça, M. D.; Nordskog, B. K. In Vitro Models for Assessing the Potential Cardiovascular Disease Risk Associated with Cigarette Smoking. *Toxicology in vitro : an international journal published in association with BIBRA*. 2013, pp 513–522. https://doi.org/10.1016/j.tiv.2012.08.018.

(34) Sato, C.; Aoki, M.; Tanaka, M. Blood-Compatible Poly(2-Methoxyethyl Acrylate) for the Adhesion and Proliferation of Endothelial and Smooth Muscle Cells. *Colloids and Surfaces B: Biointerfaces* **2016**, *145*, 586–596. https://doi.org/10.1016/J.COLSURFB.2016.05.057.

(35) Asai, F.; Seki, T.; Hoshino, T.; Liang, X.; Nakajima, K.; Takeoka, Y. Silica Nanoparticle Reinforced Composites as Transparent Elastomeric Damping Materials. *ACS Applied Nano Materials* **2021**, *4* (4), 4140–4152. https://doi.org/10.1021/acsanm.1c00472.

(36) Asai, F.; Seki, T.; Sugawara-Narutaki, A.; Sato, K.; Odent, J.; Coulembier, O.; Raquez, J. M.; Takeoka, Y. Tough and Three-Dimensional-Printable Poly(2-Methoxyethyl Acrylate)-Silica Composite Elastomer with Antiplatelet Adhesion Property. *ACS Appl Mater Interfaces* **2020**, *12* (41), 46621–46628. https://doi.org/10.1021/acsami.0c11416.

(37) Watanabe, K.; Miwa, E.; Asai, F.; Seki, T.; Urayama, K.; Nakatani, T.; Fujinami, S.; Hoshino, T.; Takata, M.; Liu, C.; Mayumi, K.; Ito, K.; Takeoka, Y. Highly Transparent and Tough Filler Composite Elastomer Inspired by the Cornea. *ACS Materials Letters* **2020**, *2* (4), 325–330. https://doi.org/https://doi.org/10.1021/acsmaterialslett.9b00520.

(38) Kobayashi, S.; Wakui, M.; Iwata, Y.; Tanaka, M. Poly(ω-Methoxyalkyl Acrylate)s: Nonthrombogenic Polymer Family with Tunable Protein Adsorption. *Biomacromolecules* **2017**, *18* (12), 4214–4223. https://doi.org/10.1021/acs.biomac.7b01247.

(39) Nishida, K.; Anada, T.; Kobayashi, S.; Ueda, T.; Tanaka, M. Effect of Bound Water Content on Cell Adhesion Strength to Water-Insoluble Polymers. *Acta Biomaterialia* **2021**, *134*, 313–324. https://doi.org/10.1016/J.ACTBIO.2021.07.058.

(40) Friedrichs, J.; Legate, K. R.; Schubert, R.; Bharadwaj, M.; Werner, C.; Müller, D. J.; Benoit, M. A Practical Guide to Quantify Cell Adhesion Using Single-Cell Force Spectroscopy. *Methods* **2013**, *60* (2), 169–178. https://doi.org/10.1016/j.ymeth.2013.01.006.

(41) Sato, K.; Kobayashi, S.; Kusakari, M.; Watahiki, S.; Oikawa, M.; Hoshiba, T.; Tanaka, M. The Relationship between Water Structure and Blood Compatibility in Poly(2-Methoxyethyl Acrylate) (PMEA) Analogues. *Macromolecular Bioscience* **2015**, *15* (9), 1296–1303. https://doi.org/10.1002/mabi.201500078.

(42) Tanaka, M.; Kobayashi, S.; Murakami, D.; Aratsu, F.; Kashiwazaki, A.; Hoshiba, T.; Fukushima, K. Design of Polymeric Biomaterials: The "Intermediate Water Concept." *Bull Chem Soc Jpn* **2019**, *92* (12), 2043–2057. https://doi.org/10.1246/BCSJ.20190274.

(43) Morita, S.; Tanaka, M.; Kitagawa, K.; Ozaki, Y. Hydration Structure of Poly(2-Methoxyethyl Acrylate): Comparison with a 2-Methoxyethyl Acetate Model Monomer. *Journal of Biomaterials Science, Polymer Edition* **2010**, *21* (14), 1925–1935. https://doi.org/10.1163/092050610X494613.

(44) Kobayashi, S.; Wakui, M.; Iwata, Y.; Tanaka, M. Poly(ω-Methoxyalkyl Acrylate)s: Nonthrombogenic Polymer Family with Tunable Protein Adsorption. *Biomacromolecules* **2017**, *18* (12), 4214–4223. https://doi.org/10.1021/acs.biomac.7b01247.

(45) Hancock, B. C.; Zografi, G. The Relationship Between the Glass Transition Temperature and the Water Content of Amorphous Pharmaceutical Solids. *Pharmaceutical Research:*

An Official Journal of the American Association of Pharmaceutical Scientists **1994**, *11* (4), 471–477. https://doi.org/10.1023/A:1018941810744.

(46) Hoshiba, T.; Orui, T.; Endo, C.; Sato, K.; Yoshihiro, A.; Minagawa, Y.; Tanaka, M. Adhesion-Based Simple Capture and Recovery of Circulating Tumor Cells Using a Blood-Compatible and Thermo-Responsive Polymer-Coated Substrate. *RSC Advances* **2016**, *6* (92), 89103–89112. https://doi.org/10.1039/c6ra15229e.

(47) Murakami, D.; Kobayashi, S.; Tanaka, M. Interfacial Structures and Fibrinogen Adsorption at Blood-Compatible Polymer/Water Interfaces. *ACS Biomaterials Science and Engineering* **2016**, *2* (12), 2122–2126. https://doi.org/10.1021/acsbiomaterials.6b00415.

(48) Tucker, W. D.; Arora, Y.; Mahajan, K. Anatomy, Blood Vessels. *In: StatPearls.* **2021**.

(49) Nishida, K.; Baba, K.; Murakami, D.; Tanaka, M. Nanoscopic Analyses of Cell-Adhesive Protein Adsorption on Poly(2-Methoxyethyl Acrylate) Surfaces. *Biomaterials Science* **2022**, *10* (11), 2953–2963. https://doi.org/10.1039/D2BM00093H.

(50) Mescola, A.; Canale, C.; Prato, M.; Diaspro, A.; Berdondini, L.; Maccione, A.; Dante, S. Specific Neuron Placement on Gold and Silicon Nitride-Patterned Substrates through a Two-Step Functionalization Method. *Langmuir* **2016**, *32* (25), 6319–6327. https://doi.org/10.1021/acs.langmuir.6b01352.

(51) Oropesa-Nuñez, R.; Mescola, A.; Vassalli, M.; Canale, C. Impact of Experimental Parameters on Cell–Cell Force Spectroscopy Signature. *Sensors (Switzerland)* **2021**, *21* (4), 1–11. https://doi.org/10.3390/s21041069.

(52) Hozumi, K.; Otagiri, D.; Yamada, Y.; Sasaki, A.; Fujimori, C.; Wakai, Y.; Uchida, T.; Katagiri, F.; Kikkawa, Y.; Nomizu, M. Cell Surface Receptor-Specific Scaffold Requirements for Adhesion to Laminin-Derived Peptide-Chitosan Membranes.

Biomaterials **2010**, *31* (12), 3237–3243. https://doi.org/10.1016/j.biomaterials.2010.01.043.

(53) Hersel, U.; Dahmen, C.; Kessler, H. RGD Modified Polymers: Biomaterials for Stimulated Cell Adhesion and Beyond. *Biomaterials* **2003**, *24* (24), 4385–4415. https://doi.org/10.1016/S0142-9612(03)00343-0.

(54) Tersteeg, C.; Roest, M.; Mak-Nienhuis, E. M.; Ligtenberg, E.; Hoefer, I. E.; de Groot, P. G.; Pasterkamp, G. A Fibronectin-Fibrinogen-Tropoelastin Coating Reduces Smooth Muscle Cell Growth but Improves Endothelial Cell Function. *Journal of Cellular and Molecular Medicine* **2012**, *16* (9), 2117–2126. https://doi.org/10.1111/j.1582-4934.2011.01519.x.

(55) Dejana, E.; Colella, S.; Languino, L. R.; Balconi, G.; Corbascio, G. C.; Marchisio, P. C. Fibrinogen Induces Adhesion, Spreading, and Microfilament Organization of Human Endothelial Cells in Vitro. *Journal of Cell Biology* **1987**, *104* (5), 1403–1411. https://doi.org/10.1083/jcb.104.5.1403.

(56) Bag, M. A.; Valenzuela, L. M. Impact of the Hydration States of Polymers on Their Hemocompatibility for Medical Applications: A Review. *International Journal of Molecular Sciences*. MDPI AG August 3, 2017, p 1422. https://doi.org/10.3390/ijms18081422.

(57) Tsai, W. B.; Grunkemeier, J. M.; Horbett, T. A. Human Plasma Fibrinogen Adsorption and Platelet Adhesion to Polystyrene. *Journal of Biomedical Materials Research* **1999**, *44* (2), 130–139. https://doi.org/10.1002/(SICI)1097-4636(199902)44:2<130::AID-JBM2>3.0.CO;2-9.

(58) Murakami, D.; Segami, Y.; Ueda, T.; Tanaka, M. Control of Interfacial Structures and Anti-Platelet Adhesion Property of Blood-Compatible Random Copolymers. *Journal of Biomaterials Science, Polymer Edition* **2020**, *31* (2), 207–218. https://doi.org/10.1080/09205063.2019.1680930.

(59) Tanaka, M.; Mochizuki, A.; Ishii, N.; Motomura, T.; Hatakeyama, T. Study of Blood Compatibility with Poly(2-Methoxyethyl Acrylate). Relationship between Water Structure and Platelet Compatibility in Poly(2-Methoxyethylacrylate-Co-2-Hydroxyethylmethacrylate). *Biomacromolecules* **2002**, *3* (1), 36–41. https://doi.org/10.1021/bm010072y.

(60) Murakami, D.; Kitahara, Y.; Kobayashi, S.; Tanaka, M. Thermosensitive Polymer Biocompatibility Based on Interfacial Structure at Biointerface. *ACS Biomaterials Science and Engineering* **2018**, *4* (5), 1591–1597. https://doi.org/10.1021/acsbiomaterials.8b00081.

(61) Ueda, T.; Murakami, D.; Tanaka, M. Analysis of Interaction between Interfacial Structure and Fibrinogen at Blood-Compatible Polymer/Water Interface. *Frontiers in Chemistry* **2018**, *6*, 542. https://doi.org/10.3389/fchem.2018.00542.

(62) Murakami, D.; Mawatari, N.; Sonoda, T.; Kashiwazaki, A.; Tanaka, M. Effect of the Molecular Weight of Poly(2-Methoxyethyl Acrylate) on Interfacial Structure and Blood Compatibility. *Langmuir* **2019**, *35* (7), 2808–2813. https://doi.org/10.1021/acs.langmuir.8b02971.

(63) Hayashi, T.; Tanaka, M.; Yamamoto, S.; Shimomura, M.; Hara, M. Direct Observation of Interaction between Proteins and Blood-Compatible Polymer Surfaces. *Biointerphases* **2007**, *2* (4), 119–125. https://doi.org/10.1116/1.2794712.

(64) Hayashi, T.; Tanaka, Y.; Koide, Y.; Tanaka, M.; Hara, M. Mechanism Underlying Bioinertness of Self-Assembled Monolayers of Oligo(Ethyleneglycol)-Terminated Alkanethiols on Gold: Protein Adsorption, Platelet Adhesion, and Surface Forces. *Physical Chemistry Chemical Physics* **2012**, *14* (29), 10196–10206. https://doi.org/10.1039/c2cp41236e.

(65) Murakami, D.; Nishimura, S. nosuke; Tanaka, Y.; Tanaka, M. Observing the Repulsion Layers on Blood-Compatible Polymer-Grafted Interfaces by Frequency Modulation Atomic Force Microscopy. *Materials Science and Engineering C* **2021**, *133*, 112596. https://doi.org/10.1016/j.msec.2021.112596.

(66) Kobayashi, M.; Terayama, Y.; Yamaguchi, H.; Terada, M.; Murakami, D.; Ishihara, K.; Takahara, A. Wettability and Antifouling Behavior on the Surfaces of Superhydrophilic Polymer Brushes. *Langmuir* **2012**, *28* (18), 7212–7222. https://doi.

Supporting Information
of

Cell adhesion strength indicates the antithrombogenicity of Poly(2-methoxyethyl acrylate) (PMEA): Potential candidate for artificial small-diameter blood vessel

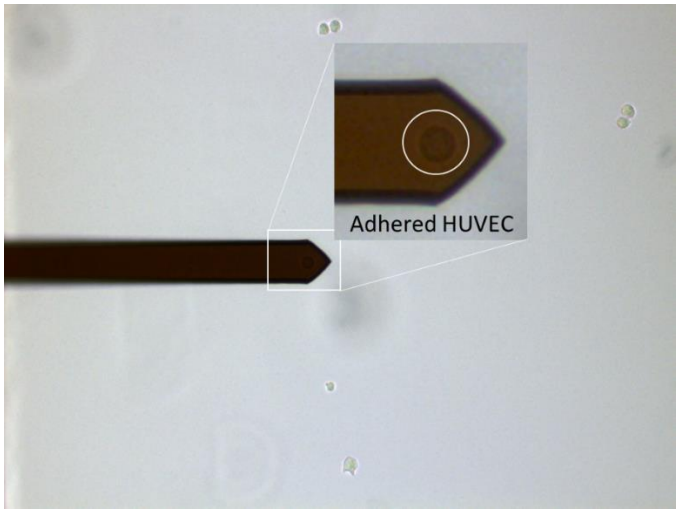

Figure. S1. HUVEC captured by tip-less cantilever TL-CONT (spring constant k = 0.2 N/m, Bruker) was treated with human fibronectin solution (1 mg/mL) for 20 min.

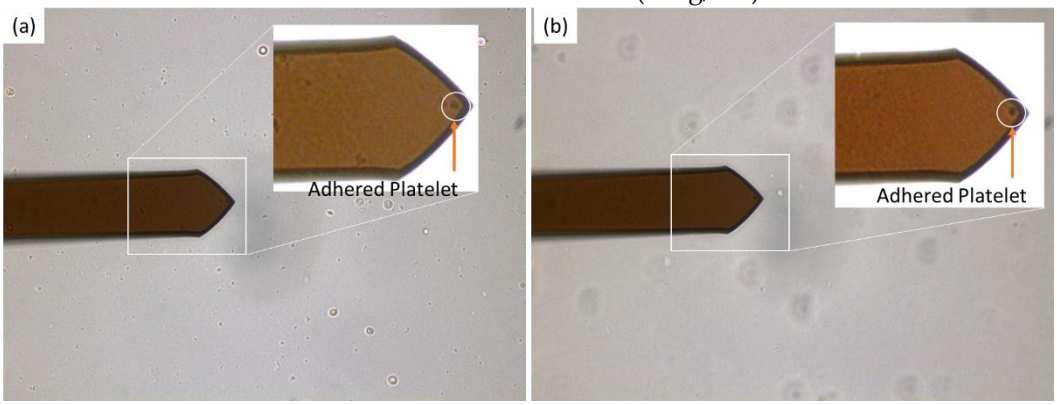

Figure. S2. Platelet captured by tip-less cantilever TL-CONT (spring constant k = 0.2 N/m, Bruker) was treated with human fibronectin solution (1 mg/mL) for 10 min. (a) During capture, (b) After captured

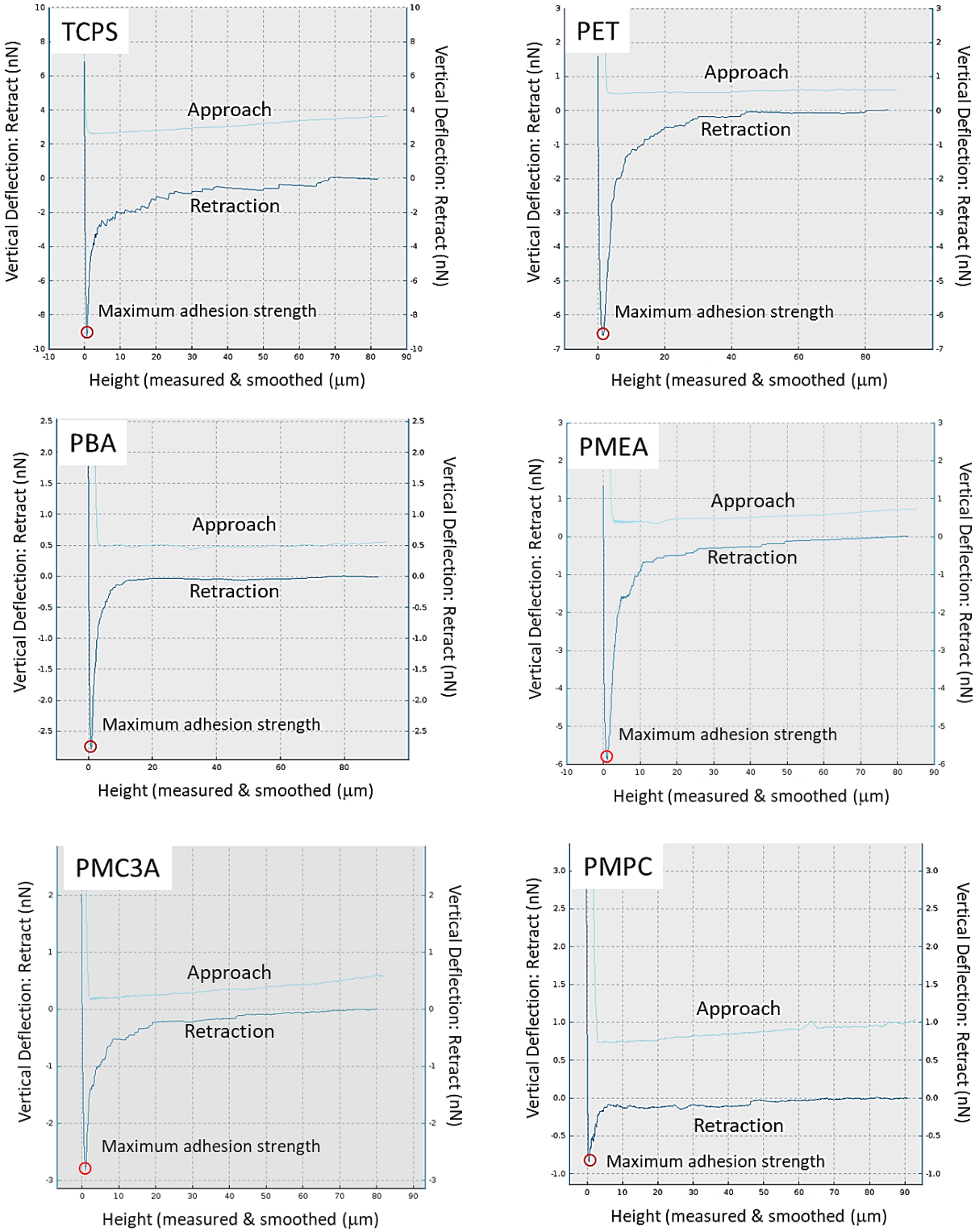

Figure. S3. Force curve of HUVEC–polymer interaction for TCPS, PET, PBA, PMEA, PMC3A, and PMPC. (Set point: 2 nN, approach rate: 5.0 µm/s, holding time: 120 s, retraction time: 15 µm/s).

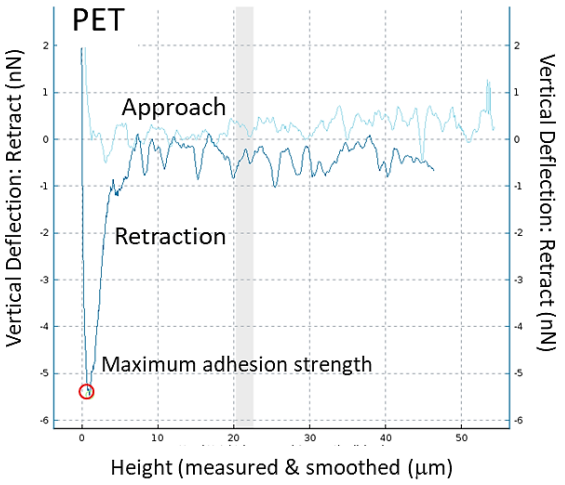
PET
Approach
Retraction
Maximum adhesion strength
Vertical Deflection: Retract (nN)
Vertical Deflection: Retract (nN)
Height (measured & smoothed (µm)

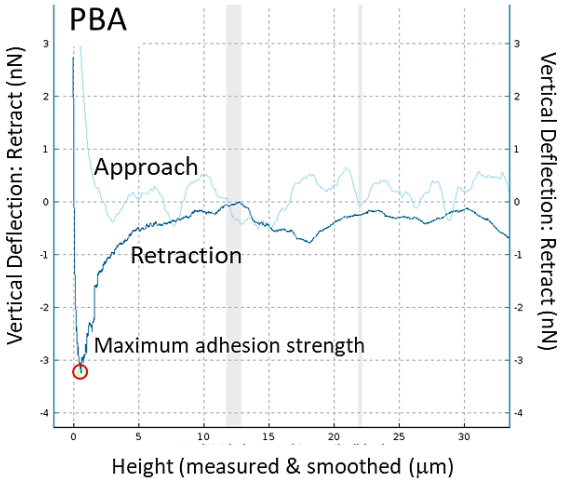
PBA
Approach
Retraction
Maximum adhesion strength
Vertical Deflection: Retract (nN)
Vertical Deflection: Retract (nN)
Height (measured & smoothed (µm)

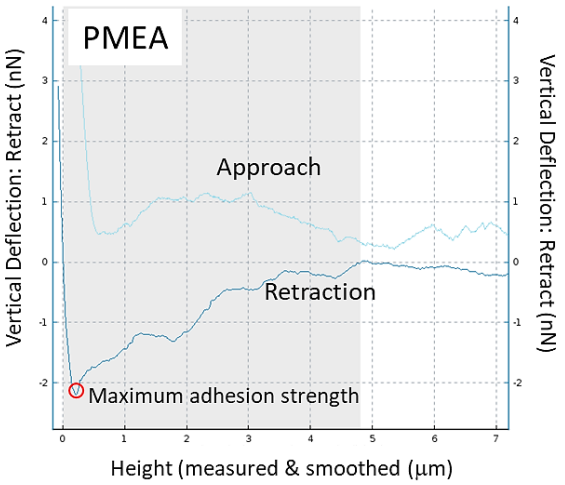
PMEA
Approach
Retraction
Maximum adhesion strength
Vertical Deflection: Retract (nN)
Vertical Deflection: Retract (nN)
Height (measured & smoothed (µm)

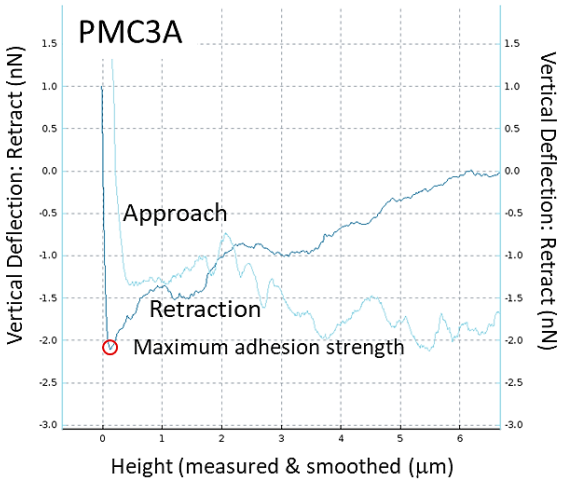
PMC3A
Approach
Retraction
Maximum adhesion strength
Vertical Deflection: Retract (nN)
Vertical Deflection: Retract (nN)
Height (measured & smoothed (µm)

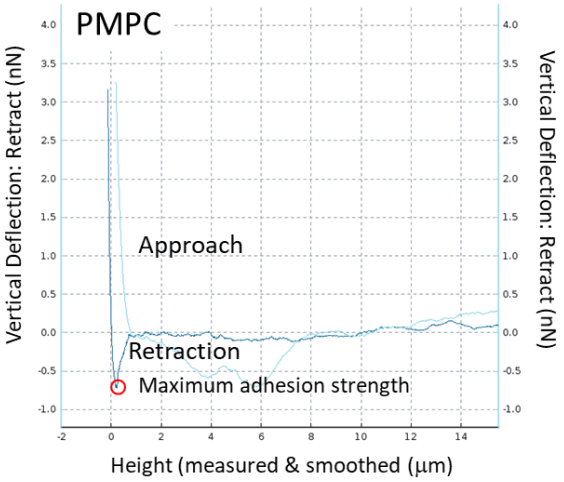
PMPC
Approach
Retraction
Maximum adhesion strength
Vertical Deflection: Retract (nN)
Vertical Deflection: Retract (nN)
Height (measured & smoothed (µm)

Figure. S4. Force curve of platelet–polymer interaction for PET, PBA, PMEA, PMC3A, and PMPC. (Set point: 2 nN, approach rate: 1.0 μm/s, holding time: 10 s, retraction time: 5 μm/s).

Chapter 3

Poly(2-methoxyethyl acrylate) (PMEA)-coated anti-platelet adhesive surfaces to mimic native blood vessels through HUVECs attachment, migration, and monolayer formation

Graphical Abstract

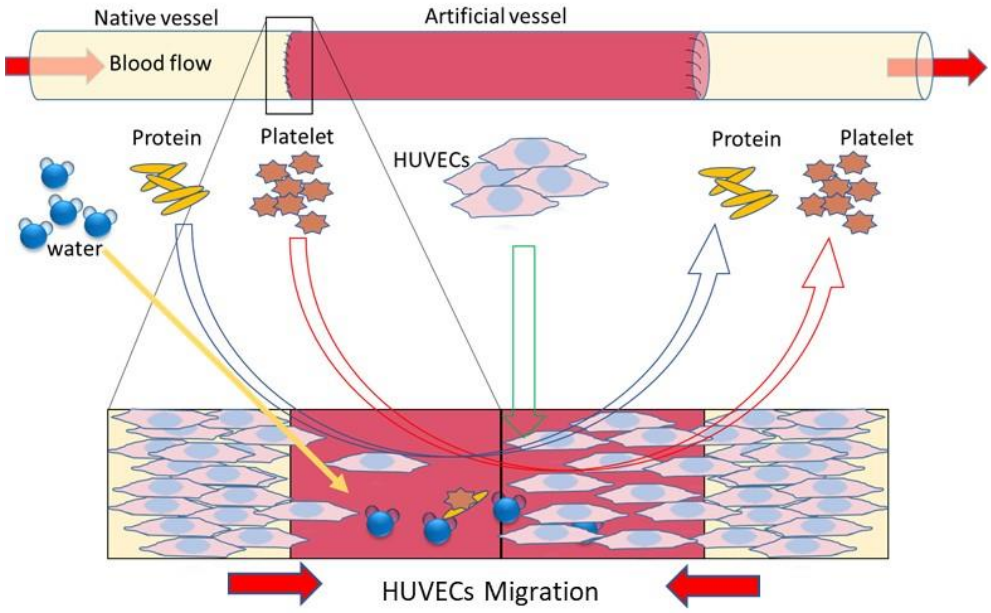

Abstract:

Confluent monolayers of human umbilical vein endothelial cells (HUVECs) on a poly(2-methoxyethyl acrylate) (PMEA) antithrombogenic surface play a major role in mimicking the inner surface of native blood vessels. In this study, we extensively investigated the behavior of cell-polymer and cell-cell interactions by measuring adhesion strength using single-cell force spectroscopy. In addition, attachment and migration of HUVECs on PMEA-analogous substrates were detected, and the migration rate was estimated. Moreover, the bilateral migration of HUVECs between two adjacent surfaces was observed. Furthermore, the outer surface of HUVEC was examined using frequency-modulation atomic force microscopy (FM-AFM). Hydration was found to be an indication of a healthy glycocalyx layer. The results were compared with the hydration states of individual PMEA-analogous polymers to understand the adhesion mechanism between the cells and substrates in the interface region. HUVECs could attach and spread on the PMEA surface with stronger adhesion strength than self-adhesion strength, and migration occurred over the surface of analogue polymers. We confirmed that platelets could not adhere to HUVEC monolayers cultured on the PMEA surface. FM-AFM images revealed a hydration layer on the HUVEC surfaces, indicating the presence of components of the glycocalyx layer in the presence of intermediate water. Our findings show that PMEA can mimic original blood vessels through an antithrombogenic HUVEC monolayer and is thus suitable for the construction of artificial small-diameter blood vessels.

Keywords: poly(2-methoxyethyl acrylate) (PMEA); human umbilical vein endothelial cell (HUVEC); cell-cell interaction; cell adhesion strength; cell migration; frequency-modulation atomic force microscopy (FM-AFM); hydration; artificial small-diameter blood vessel

3.1 Introduction

According to the World Health Organization (WHO), due to the rapid increase in cardiovascular diseases (CVDs) and the associated number of deaths, the 17.9 million deaths from CVDs in 2019 is estimated to increase to 23.6 million by 2030 [1,2]. Approximately 32% of total deaths worldwide are caused by the diverse categories of CVDs, such as coronary heart disease (CHD) and peripheral artery disease (PAD). Currently, researchers are focusing on obtaining the most suitable treatments for CVDs. To date, angioplasty, atherectomy, stent insertion, and bypass of the injured vessels are the most well-known treatments [3]. Bypass of injured vessels is an effective treatment, and autologous saphenous vessels are generally selected; however, there is a risk of secondary trauma. Therefore, synthetic artificial vascular grafts can be suitable alternatives to autologous saphenous vessels. To date, polyethylene terephthalate (PET) and expanded polytetrafluoroethylene (ePTFE) have been used as synthetic grafts for large-diameter vessels; however, these grafts show poor patency for small-diameter blood vessels due to thrombus formation inside them [4]. PET and ePTFE are unable to promote endothelialization and induce thrombosis and inflammation due to platelet and neutrophil activation[5]. Therefore, vascular graft diameter smaller than 6 mm showed high risk of thrombus formation. In addition, protein adsorption boosts up the platelet adhesion in surface induced clotting[6].

Many methods have been implemented to improve the surface of synthetic grafts through surface modification, new polymer development, and cell-substrate interaction investigation using mechanobiology assessments. Various surface modification techniques have been used to functionalize the substrate interface for cell attachment, growth, migration, rapid endothelization, and long-term anticoagulation[7–9]. Polymer coating is an effective approach to functionalize biomaterial surfaces. Functionalization with poly(ethylene glycol) and zwitterionic polymers,

including poly(2-methacryloyloxyethyl phosphorylcholine) (PMPC), suppresses biofilm formation, immune responses to biomaterial surfaces, and adhesion of platelets [10–16]. Moreover, there are several approaches have been introducing to get the smart or responsive surfaces. Temperature-responsive grafted polymer brushes based on LCST opens opportunities for fabrication of responsive surfaces[17]. On the other hand, stimuli-responsive macromolecules significantly impacted new developments in polymeric coatings where surface shows responsiveness to bacterial attacks, ice or fog formation, anti-fouling properties, autonomous self-cleaning and self-healing, or drug delivery systems[18].

A stable confluent endothelium lining may act as completely antithrombogenic surface. However, such an endothelial cells (ECs) layer does not form spontaneously at the surface of a vascular implant in humans i*n vivo*. Subsequently, researcher has proposed pre-seeding of ECs or progenitor cells prior to implantation in order to increase the patency of synthetic vascular graft[19,20]. However, poor cells adhesion ability under flow condition indicates low compatibility[21]. Consequently, polymers with antifouling and antithrombogenic properties with strong endothelial cell attachment abilities are desirable for researchers to develop artificial small-diameter blood vessels (ASDBVs) that can mimic native blood vessels.

In this regard, poly(2-methoxyethyl acrylate) (PMEA), an antithrombogenic synthetic polymer, is a suitable alternative to ePTFE and PET because of its intermediate water (IW, loosely bound water) content, which is a measure of biocompatibility and blood compatibility[22,23]. It was found that IW is present in natural biocompatible polymers such as DNA (and RNA), heparin, and chondroitin sulfate [24]. PMEA is a US Food and Drug Administration (FDA)-approved biocompatible polymer used in artificial lungs, catheters, and stents as an antithrombogenic coating material. PMEA is a water insoluble and hydrophobic in nature. It makes thin film coatings

on substrates such as PET or others surface where coating need to be performed. When the biomaterials contact with the body fluids, the primary interaction happens on the biomaterials-fluids interface at hydrated state; first, proteins are adsorbed and then denatured on the hydrated material surface. Cell adherent proteins adsorption depends on the wettability, polymer rich and poor region as well as microphase separation of a homopolymer at an interface. The amount and degree of denaturation of adsorbed proteins affect subsequent cell behavior, including cell adhesion, migration, proliferation, and differentiation. The modification in the chemical structure of PMEA shows distinct morphological and interaction behavior with blood component[25,26]. The polymer with similar chemical and structural properties of PMEA named as PMEA analogous polymer. Our recent investigation reveals PMEA-analogous polymers suppress platelet adhesion and the degree of suppression depends on the amount of IW present in each polymer [22,26]. In particular, a polymer with high IW content (e.g., PMPC, IW = 11.11% w) suppresses platelets more effectively than a polymer with low IW content [27]. However, PMPC does not allow the attachment of cells, proteins, or any other blood components on its surface.

A monolayer of ECs can effectively protect surfaces from the adhesion of blood components (platelets, white blood cells, red blood cells, and proteins), thus suppressing platelet coagulation and thrombus formation [28]. Alternatively, PMEA, a blood-compatible polymer, does not activate leukocytes, erythrocytes, or platelets, *in vitro* [22]. Furthermore, because PMEA and analogous polymers promote the attachment of non-blood cells, they are believed to facilitate endothelization [29]. Therefore, endothelization over the polymer surface may play a major role in surface antithrombogenic properties.

In recent years, the human umbilical vein endothelial cells (HUVEC) model is using to cardiovascular and clinical research as compared to animal models. *In vitro* HUVEC models have

been convenient to study platelet adhesion to the endothelium, endothelial dysfunctions, the potential effect of atherosclerosis in initial stages and atherosclerosis progression[30,31]. On the other hand, EC activation, migration, and proliferation responsible for the formation and organization of tubular structures to form new blood vessels through angiogenesis process[32,33]. Finally, HUVEC as a model to study the endothelium has greatly facilitated the study of cardiovascular disease. In contrast, the glycocalyx is a combination of a hydrated sugar-rich molecules (heparin sulfate, chondroitin sulfate, and hyaluronic acid) coating the surface of ECs lining the inside of blood vessels. Our previous study showed that promoting the glycocalyx of HUVECs with transforming growth factor-β1(TGF-β1) decreased platelet adhesion, while degrading the glycocalyx with heparinase I increased platelet adhesion. These results suggested that the glycocalyx of cultured HUVECs modulates platelet compatibility, and the amount of glycocalyx secreted by HUVECs depends on the chemical structure and cross-linker concentration of the scaffolds [34]. Matrix stiffness is also known to affect the expression of the glycocalyx in cultured ECs [35].

In the present study, we aim to find the best polymer from PMEA analogous polymers that can be used to construct artificial small diameter vascular graft as a coating material. For this purpose, the polymer should have fulfil the basic needs such as, antithrombogenic surface, good HUVECs attachment, growth, proleferation, migration, monolayer formation and strong adhesion strength to the surface. We used HUVECs to measure cell-cell and cell-substrate interactions using single-cell force spectroscopy (SCFS). We found a possible mechanism of HUVECs monolayer formation over a biocompatible polymer surface by comparing the strength of cell-cell and cell-substrate interactions. We then evaluated the migration behavior of HUVECs on the PMEA polymer analogs. In addition, bilateral migration of HUVECs between two adjacent polymer surfaces was observed, indicating migration of HUVECs from native blood vessels to artificial

implants in vitro. Furthermore, a platelet adhesion test was performed on HUVECs monolayers cultured on PMEA and PET. Finally, the upper surface of a single HUVEC was investigated using frequency-modulation atomic force microscopy (FM-AFM) to determine the hydration states of the HUVEC surface to verify the expression of the glycocalyx layer as well as IW states.

3.2 Materials and Methods

3.2.1 Chemicals and materials

Hydrophilized PET sheet (thickness = 120 μm) was purchased from Mitsubishi Plastic Inc. (Tokyo, Japan). PMEA (M_n = 26.9 kg/mol, M_w/M_n = 2.73), poly(3-methoxypropyl acrylate) (PMC3A, M_n = 20.8 kg/mol, M_w/M_n = 3.83), and poly(*n*-butyl acrylate) (PBA, M_n = 62.8 kg/mol, M_w/M_n = 1.41) were synthesized as previously reported [26]. Poly(*n*-butyl mathacrylate-*co*-2-methacryloyloxyethyl phosphorylcholine) (BMA 70 mol%, MPC 30 mol%) (PMPC, Mw=600 kg/mol) was a gift from the NOF Corporation, Japan. Tissue culture polystyrene (TCPS) was purchased from IWATA, Japan. The chemical structures of the polymers used in the present study are shown in **Figure 3.1**. Fibronectin was collected from Wako Pure Chemical Industries (Osaka, Japan). Platelet adhesion test was performed using human whole blood which was purchased from Tennessee Blood Services (Memphis, TN, USA). Human whole blood was collected from healthy doner and stored in a vacuum blood collection tube (Venoject II; Terumo Co., Tokyo, Japan) containing 3.2% sodium citrate as an anticoagulant. Blood was used within a week after collection. Blocking reagent was purchased from Nacalai Tesque (Kyoto, Japan). All other reagents and solvents were obtained from Kanto Chemical Co. (Tokyo, Japan).

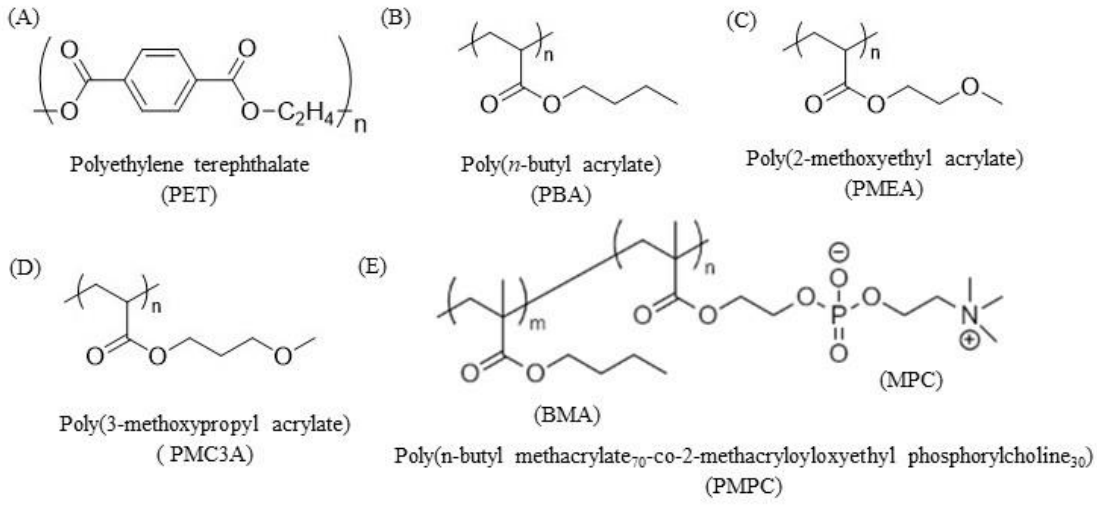

Figure 3.1. Chemical structure of (A) polyethylene terephthalate (PET); (B) poly(n-butyl acrylate) (PBA); (C) poly(2-methoxyethyl acrylate) (PMEA); (D) poly(3-methoxypropyl acrylate) (PMC3A), and (E) poly(*n*-butyl mathacrylate-*co*-2-methacryloyloxyethyl phosphorylcholine) (BMA 70 mol%, MPC 30 mol%) (PMPC).

3.2.2 Fabrication of polymer-coated substrates

PET was used as a substrate for the polymer coating. Initially, the PET sheet was cut into a circular shape with a diameter of 14 mm using a hand press cutter and cleaned by washing with toluene. PMEA, PMC3A, and PBA were dissolved in toluene (0.5% w/v) to obtain the polymer solution. PMPC was dissolved in methanol at the same concentration. The PMEA analogous polymer solutions of 40 µLwere charged on the PET substrates for spin-coating using a Spin Coater (Mikasa MS-A100) at a constant speed of 3000 rpm for 40 s, ramped down for 4 s, and then dried for at least for 24 h in a vacuum dryer at 25 °C. Bare PET was used as the positive control and TCPS was used as the cell culture dish. The morphologies of the polymer-coated surfaces were observed by atomic force microscopy (AFM) and the thickness was estimated around 100 nm using transmission electron microscopy[25,36]. The surface roughness of all polymer coatings was almost the same within 10-20 nm. However, AFM observation showed that the interfacial

structures of the PMEA and PMC3A were highly ordered with homogeneous and compactly dispersed in nanometer scale, although the low-blood-compatible polymer PBA interface had irregular structure [25].

3.2.3 Contact angle

Contact angle measurements were conducted using milli Q water. Two methods (sessile drop and air bubble) were used to measure the contact angle values of PMEA analogues surfaces at 25°C using a DropMaster DMo-501SA (Kyowa Interface Science Co., Tokyo, Japan (shown in Table 1). 1. Sessile drop method: 2 μL of water droplet was dropped on the polymer surface for 60 s, and the contact angles were calculated from the photograph. On the captive bubble method, PMEA analogues substrates were immersed in Milli-Q water for 24 h. Then, 2 μL of air bubble was injected beneath the substrate surfaces located in water, and the contact angles were also measured using photographic images. Finally, the contact angle at 30s was counted as the contact angle of that substrate.

Table 3.1: Contact angle* and water content of studied polymers

Polymers	Contact angle [deg]			
	Sessile water drops	Captive air bubble		IW
	(30 s)	(30 s)	24 h	(wt.%)
PET	73.3 (±0.9)	125.5 (±2.2)	125.4 (±0.5)	0
PBA	83.8 (±1.9)	126.7 (±2.8)	125.0 (±1.7)	0.31
PMEA	44.3 (±2.1)	134.0 (±0.9)	132.9 (±1.8)	3.7
PMC3A	52.1 (±0.5)	126.9 (±1.0)	127.8 (±0.7)	2.8
PMPC	108.9 (±0.5)	152.4 (±2.9)	150.0 (±3.8)	11.11

* 2 μL water droplet in air (sessile drop) and 2 μL air bubble in water (Captive bubble). The data represent the means ± SD (n = 5)

3.2.4 HUVECs culture

ECs were solely used for all experiments described in this article. Commercially available HUVECs (Lonza, Cologne, Germany) were cultured under static cell culture conditions (37 °C, 5% CO_2) in polystyrene-based cell culture flasks. Cells were used for four to six passages and cultured in endothelial basal medium (EBM-2) supplemented with endothelial growth medium (EGM-2) Single Quots® kit and 2% fetal calf serum (FCS; Lonza). Before starting the experiments, cells were detached using 0.25% trypsin/EDTA solution (Thermo Fisher Scientific, Rockford, IL, USA) from the culture dish. Then HUVECs solution was centrifugated for 3 min at 1200 rpm to isolate HUVECs from the medium. Initial cell counting was performed using a hemocytometer to adjust the cell density.

3.2.5 Cell attachment, proliferation, and immunocytochemical analysis

Cell attachment and proliferation assays were performed using a 24-well plate (IWATA). The 24-well plate was first coated with PMPC (0.5% w/v) and allowed to dry. The pre-coated polymer substrates were then fixed onto the 24-well plate using glue on the back side of each substrate and cured under UV light for 30 min. Phosphate-buffered saline (PBS) was then added to the wells and incubated for 1 h at 37 °C. Afterwards, culture media were added and incubated for another hour at 37 °C. HUVECs were seeded on the substrates at 1 x 10^4 cells/cm^2 in serum-containing media and allowed to adhere and proliferate on the surface of the substrates for 1 h, 1 day, or 3 days. After cultivation at these specific time intervals, the cells were analyzed using ImageJ software (version 1.53C; National Institutes of Health, Bethesda, MD, USA).

In addition, before starting the immunocytochemical analysis the prepared substrates were preconditioned, as in the cell attachment and proliferation assays. HUVECs were seeded (5×10^3 cells/cm^2) on polymer-coated PET substrates and incubated for 1, 24, or 72 h. After culturing for

specific times, the cells were fixed using preheated (37 °C) 4% (w/v) paraformaldehyde (Fujifilm Wako Pure Chemical Co., Ltd., Osaka, Japan) and stored outside for 10 min. Thereafter, 1% (v/v) Triton X-100 (Fujifilm Wako Pure Chemicals Co., Ltd.) in PBS (−) was added to increase plasma membrane permeability. After washing, the sections were blocked for 30 min. Then the substrates were stained with mouse monoclonal anti-human vinculin antibody (VIN-11-5; Sigma-Aldrich, St. Louis, MO, USA) (1:200) diluted in PBS (−) for 90 min at room temperature (RT), and subsequently stained with Alexa Fluor 568-conjugated anti-mouse immunoglobulin G (IgG) (H + L) antibody (1:1000 dilution), Alexa Fluor 488-conjugated phalloidin (1:1000 diluted), and 4,6-diamidino-2-phenylindole (DAPI, 1:1000 dilution) (all from Thermo Fisher Scientific, Waltham, MA, USA), all diluted in 10% blocking solution in PBS, treated for 1 h at RT. After performing these steps, stained cells were fixed on glass slides. Fluorescence photographs were taken using a confocal laser-scanning microscope (CLSM) (FV-3000; Olympus, Tokyo, Japan). The HUVEC morphology were quantitatively assessed using ImageJ.

3.2.6 HUVECs migration analysis

HUVECs migration analyses were executed in six-well plates. Initially, one half of the PET substrate (φ = 30 mm) was coated with a PMEA-analogous polymer and the other half was exposed to bare PET. First, HUVECs were cultured on all studied substrates placed into six-well plates with seeding density 1×10^4 cells/cm^2 and incubated at 37 °C until full confluency. After confluency, the cell monolayer surface was scratched using a 4 mm wide rubber cell scraper in the PET-polymer interface region and kept in incubator for migration. Finally, cell migration towards the scratched area was observed at 0, 24, and 48 h of scratching, and time-laps images were taken using a phase-contrast microscope. The migrated area was quantified using ImageJ software and denoted as $A_0 - A_t$, where A_0 is the initial area before migration, and A_t is the area at the certain time

t (i.e., o, 24, or 48 h). The migration rate was then plotted against the types of substrates where migration happened.

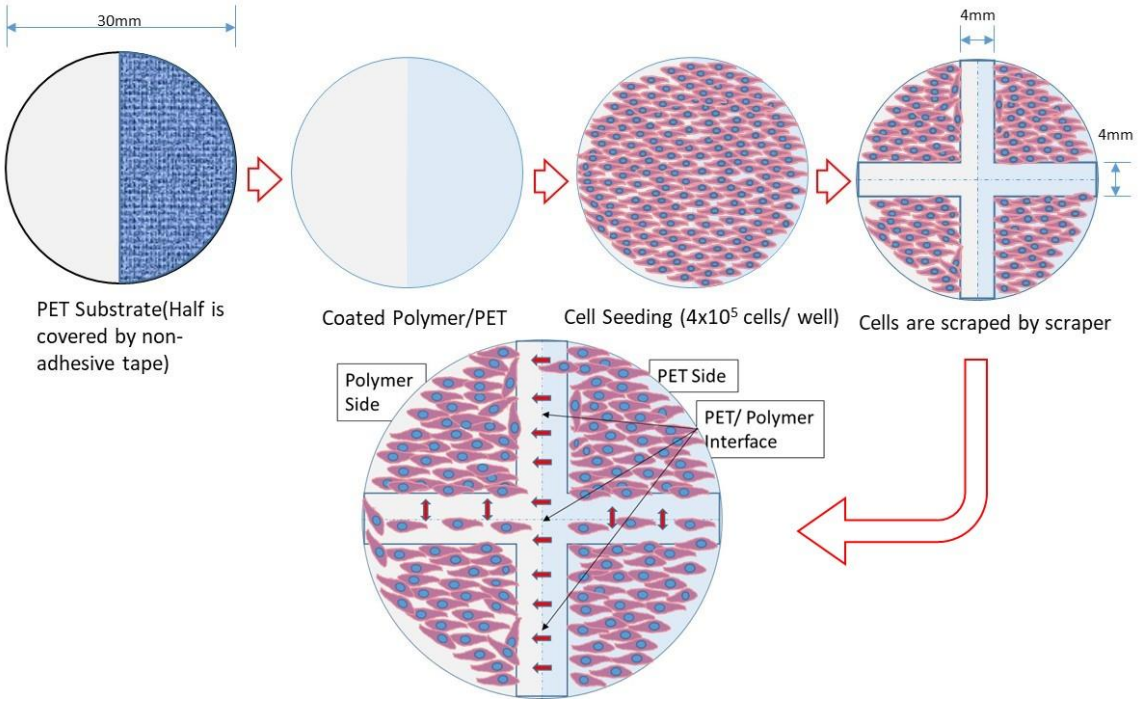

Figure 3.2. Schematic representation of the HUVECs migration rate measurements and observation of HUVECs migration through the coated polymer-PET interface.

3.2.7. HUVEC-PMEA and HUVEC-HUVEC interaction determined by SCFS

Prior to the HUVEC-PMEA interaction measurement, the PMEA-coated substrates were placed under UV light for 30 min and then poured the PBS and placed in incubator for 1 h at 37 °C. Subsequently, EGM-2 medium was added to the substrate and freshly detached cells (five to six passages) were injected into it. In addition, the tipless cantilever named TL-CONT (spring constant k = 0.2 N/m; Bruker, Billerica, MA, USA) was coated with fibronectin solution (1 mg/mL)and kept for around 20 min to dry. Then a single HUVEC was captured with a tipless cantilever for 10 min with set point: 2 nN. The force-distance curves between the cells and the substrates were measured using an AFM (CellHesion JPK; Bruker) equipped with a tipless cantilever (set point: 2

nN, approaching rate: 5.0 μm/s, holding time: 120 s, retraction rate: 15 μm/s). The value of set point for the measurement of HUVEC adhesion strength was used from our previous report where the relationship between the set points and the cell adhesion strength of HeLa cells were evaluated [37]. In this investigation, the maximum force for cell detachment from the substrate is denoted as adhesion force, which is indicated in lowest point of retraction curve. Adhesion work was estimated as the amount of work required to detach the cell from the substrate, corresponding to the area enclosed by the baseline and retraction curve [38]. The same experimental conditions were used to determine HUVEC-HUVEC interactions. The only exception was that HUVECs were cultured on both the PMEA-coated PET substrate and TCPS. HUVEC adhesion strength was measured on the attached HUVECs using the same procedure as described earlier in this section.

3.2.8 Platelet adhesion test on cultured HUVECs monolayer

The platelet adhesion test was performed under static conditions as previously described [22,34,39]. In brief, fresh blood was centrifuged at 400 ×g for 5 min to obtain platelet-rich plasma (PRP), and the remaining blood was centrifuged at 2500 ×g for 10 min to obtain platelet-poor plasma (PPP). The platelet concentration was determined using a hemocytometer. Cell density (4 x 10^7 cells /cm^2) was adjusted by mixing PPP and PRP. Prior to this experiment, HUVECs were cultured on the PMEA-coated and bare PET substrates. Before loading the platelet suspension, the cultured HUVECs layer was washed with PBS (−). Then, 450 μL of platelet suspension was loaded onto HUVECs proliferated on the confluent layer and incubated for 1 h at 37 °C. After 1 h of incubation, the weakly adhered platelets were rinsed three times with PBS. Adhered platelets were then fixed using 1% glutaraldehyde for 2 h at 37 °C. After this period, samples were rinsed with PBS, 50% PBS, and Milli-Q water. Finally, the samples were dried at RT for 1-2 days before being subjected to sputter gold coating for scanning electron microscopy (SEM) observation. Then, the

number of adhered platelets was counted from SEM image using ImageJ software (n=15 of each substrate).

3.2.9 FM-AFM of single HUVEC surface

FM-AFM was conducted using an SPM-8100FM (Shimadzu Co., Kyoto, Japan) in water at 23 °C. A PPP-NCHAuD cantilever (typical spring constant, k = 42 N/m, NanoWorld AG, Neuchâtel, Switzerland) was used. The resonance frequency in water was approximately 140 kHz, and the scan in the z-direction was performed with a force limit of 2.5 V which corresponds to a frequency shift of approximately 500 Hz. The amplitude of the cantilever oscillation was maintained constant at approximately 2 nm.

3.2.10 Statistical analyses

At least three independent trials data were used in calculation of mean ± standard deviation (SD). The significance differences were assessed using one-way analysis of variance (ANOVA) (Tukey-Kramer multiple comparison test) of Origin Pro (version 2019b; OriginLab Co., Northampton, MA, USA). $P < 0.05$ was set to evaluate statistical significance.

3.3 Results and Discussion

3.3.1 HUVECs cultured on PMEA-analogous polymers

The formation of confluent EC monolayers on implanted materials has been identified as a method to avoid thrombus formation [28,40]. PMEA polymer analogs (PMEA, PMC3A, and PBA) and PMPC were coated on PET substrates to culture HUVECs and investigate HUVECs adhesion ability. The physical properties of studied polymer have shown in Table 3.1. HUVECs attachment ability depends on the surface type, morphology, and biomechanical interaction in the interface. In our previous study, we have mentioned the surface morphology of our studied polymer by AFM observation[25]. **Figure 3.3** shows the phase-contrast micrographs of the sub-confluent to confluent

layer of HUVECs attached to the PMEA polymers at 120 h. Bare PET and PMPC were used as the positive and negative controls, respectively. It was found that HUVECs can attach to PMEA polymer analogs and form a confluent monolayer. This confirms our previous findings that ECs can attach, proliferate, and form a layer on PMEA-coated surfaces compared with other analogous polymers. The proliferation of HUVECs on the various substrates decreased in the following order: TCPS > PET≈ PMEA > PMC3A≈PBA > PMPC. No considerable number of HUVECs was found on PMPC at 120 h. HUVECs could not survive on PMPC because of their strong antithrombogenic properties. These results agree with those of our previous study in which HUVECs and aorta smooth muscle cells (AoSMCs) were cultured on PET, PMEA, and PMPC [41].

The different attachment behaviors of HUVECs on PMEA-analogous polymers depend on the hydration state, surface morphology, and stiffness of each polymer [35,40,42]. Generally, cells adhere to a polymeric surface via cell-binding proteins, such as fibronectin or fibrinogen, through integrin [43]. HUVECs are more likely to adhere to fibronectin than fibrinogen through the RGD sequence, which is a universal binding site [44]. It has been proven that cells can attach to PMEA in an integrin-dependent and-independent manner through direct interaction between the cell membrane and the polymer interface [45]. In this study, we found a more confluent HUVECs monolayer on PMEA-coated substrates than on other analogous polymers. This can be attributed to the selective protein adsorption and integrin-independent and -dependent adhesion mechanism of PMEA, which is regulated by the IW content [41].

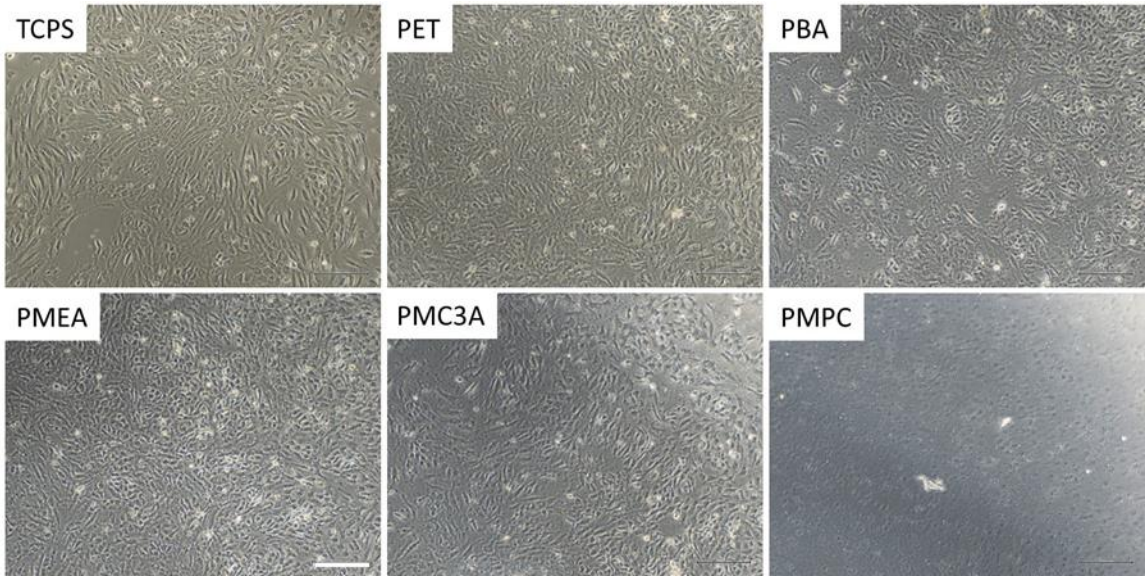

Figure 3.3. Phase-contrast micrographs of the HUVECs cultured for 120 h on PMEA-analogous polymers and on TCPS, PET, and PMPC as controls (scale bar = 200 μm).

3.3.2 Possible mechanism of HUVECs monolayer formation on PMEA (cell-cell interaction)

The initial interactions between individual HUVECs cultured on the PMEA surface were measured using the SCFS. **Figure 3.4** shows the HUVEC adhesion strength in nN, measured at three different places of the attached HUVEC on PMEA. We found that the adhesion strength was highest in the external cellular matrix (ECM) of the attached single HUVEC, lower on arbitrary positions of the monolayer, and lowest on the top of the cell where the nucleus is present. Therefore, variation in interaction strength can occur because of the concentration of adhesion proteins in the serum medium. Previous studies have shown that cell adhesion on PMEA in serum-free medium is similar to that on serum-containing medium[45]. In contrast, the adhesion energy differed among the various interaction locations of the attached HUVEC, which may be due to the dissimilar surface interaction area and number of focal adhesion points.

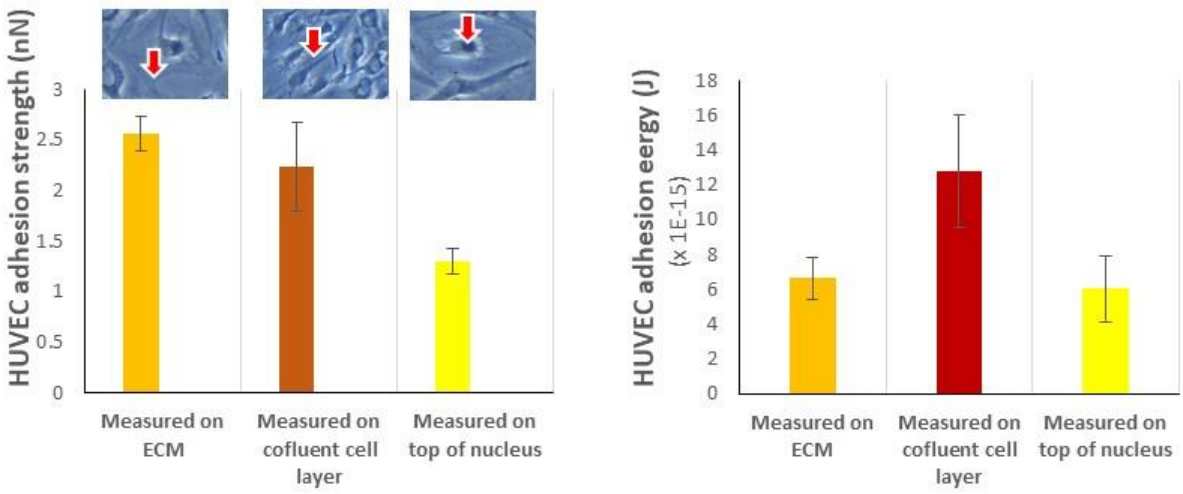

Figure 3.4. Cell-cell interaction strength measured in three positions (ECM, arbitrary point of confluent layer, top of nucleus) of confluent HUVECs monolayer. The data represent the mean ± SD (n = 4).

In contrast, intercellular adhesion plays a major role in tissue development and homeostasis [46]. Sancho et al. measured the cell adhesion forces of HUVECs on substrates in well-attached individual cells and monolayers. In the present study, we measured and compared the initial HUVEC adhesion strength between HUVEC-PMEA and HUVEC-HUVEC, where the HUVECs were cultured on both TCPS and PMEA surfaces, as shown in **Figure 3.5**. The average HUVEC-HUVEC interaction strength was calculated, as shown in Figure 3.4, and results revealed that there is no effect of culture substrates on cell-cell interaction strength. However, the HUVEC-PMEA adhesion strength was much higher than the cell-cell interaction. Therefore, initially, HUVECs seem to be more involved in attachment to the substrates than individual cells, even though a few portions of seeded cells were in a tri-dimensional (3D) aggregated form. After seeding, the cells spread and formed a two-dimensional (2D) layer. Therefore, the initial cell adhesion strength is a measure of monolayer formation. This result shows that the measurement of cell adhesion strength is vital for the development of endothelial monolayers for the construction of ASDBV. In addition,

ECs forming the inner wall of every blood vessel are constantly exposed to the mechanical forces generated by blood flow [47]. If the cell-substrate interaction is not sufficient to resist the force exerted by blood flow, then no cell can be attached or migrated to form a confluent layer of cells. Therefore, EC responses to these hemodynamic forces and interaction strength play a critical role in the homeostasis of the circulatory system in the development of ASDBV.

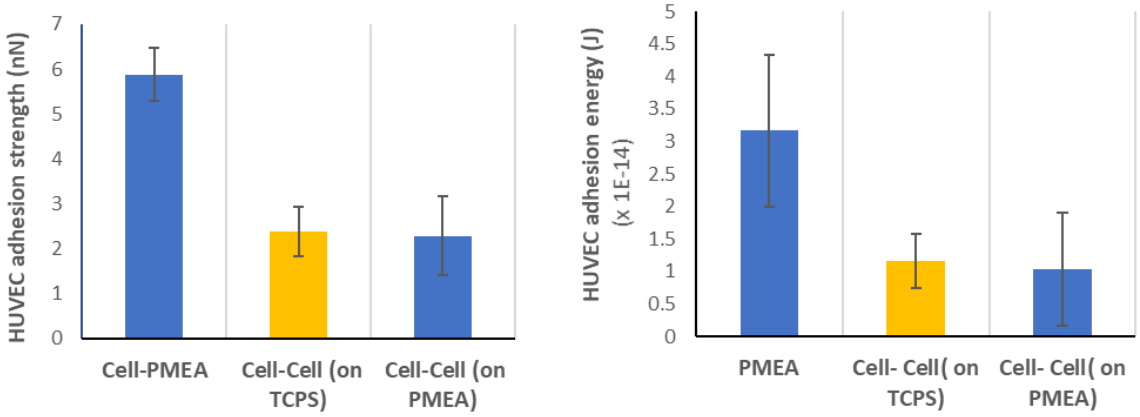

Figure 3.5. Comparison of HUVEC adhesion strength between cell-PMEA, cell-cell cultured on TCPS, and cell-cell cultured on PMEA. The data represent the mean ± SD (n > 4).

3.3.3 HUVECs migration analysis

HUVECs migration analysis was performed to evaluate the migration ability of HUVECs on the different polymeric surfaces. Figure 6 shows the HUVECs migration analysis on the PMEA, PMC3A, PBA, and PET. The left side of each substrate was coated on the polymer side, and the right side was always bare PET. The white dotted line in each image indicates the interface between the PMEA-analogous and bare PET. The migration time was recorded from 0 to 48 h using a time-lapse microscope. The red dotted line indicates the area occupied by HUVECs before and after migration at the various time intervals. In **Figure 3.2**, we demonstrated the HUVECs migration procedure, in which the layer of HUVECs was scratched in both the vertical and horizontal directions. After migration, five locations were selected for each substrate to calculate the

migration rate. From **Figure 3.6**, we can see those cultured monolayers of HUVECs were scratched using a rubber scraper to set the initial area of cultured HUVECs on PMEA-analogous polymer and PET surfaces. Then, images were taken every hour for 48 h.

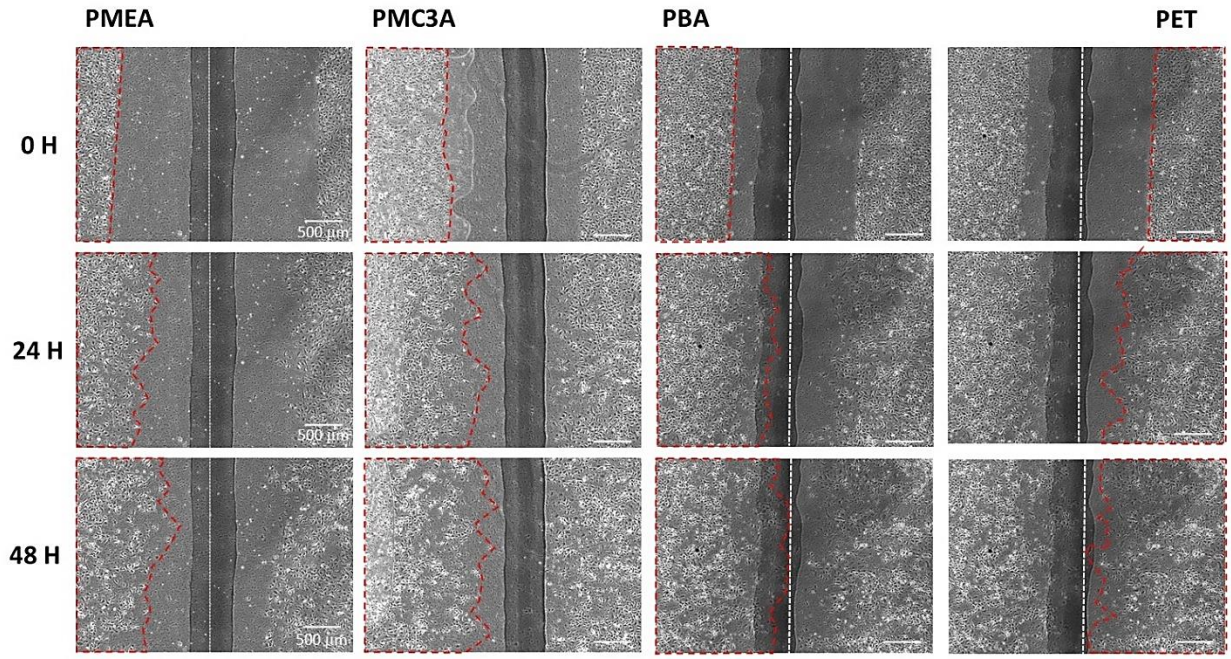

Figure 3.6. HUVECs migration analysis on PMEA, PMC3A, PBA, and PET (scale bar = 500 µm). The white dotted line indicates the interface between PMEA-analogous polymers and bare PET. Migration was recorded from 0 to 48 h. The red dotted line indicates the HUVECs occupied area before and after migration.

3.3.4 Observation of cell migration between surfaces

In addition, we observed HUVECs migration between the surfaces through the interface. Focusing on the interface (white dotted line) of each polymer, we identified the migration of HUVECs from the bare PET side to the PMEA side through the interface. The migration is marked by a red rectangle in **Figure 3.7**, and it increased with time. Furthermore, we calculated the HUVECS migration rate for all the substrates from the newly covered area after migration. We found that the migration rates were slightly different, although the differences were not statistically

significant (Figure 8). However, PMEA showed the highest averaged migration rate among all samples.

The most vital task of ECs is to protect the vascular system through the formation of a antithrombogenic monolayer that is periodically renewed to maintain proper endothelial functions [48,49]. To treat CVDs, after the implementation of cardiovascular devices or artificial blood vessels, the capacity to migrate ECs toward injured or foreign surfaces is crucial. Endothelization and migration of HUVECs are influenced by many factors, including the physical and chemical properties of polymers, surface characteristics, and adhesion of binding proteins on specific polymeric substrates. In the present study, PMEA analogs showed similar migration behavior, although PMEA-analogous polymers have dissimilar wet abilities, surface characteristics, and binding protein adsorption abilities, as already known from our previous study. These effects did not affect the migration rate of HUVECs. In addition, migration from the bare PET to the PMEA side confirmed the mimetic behavior of native blood vessels.

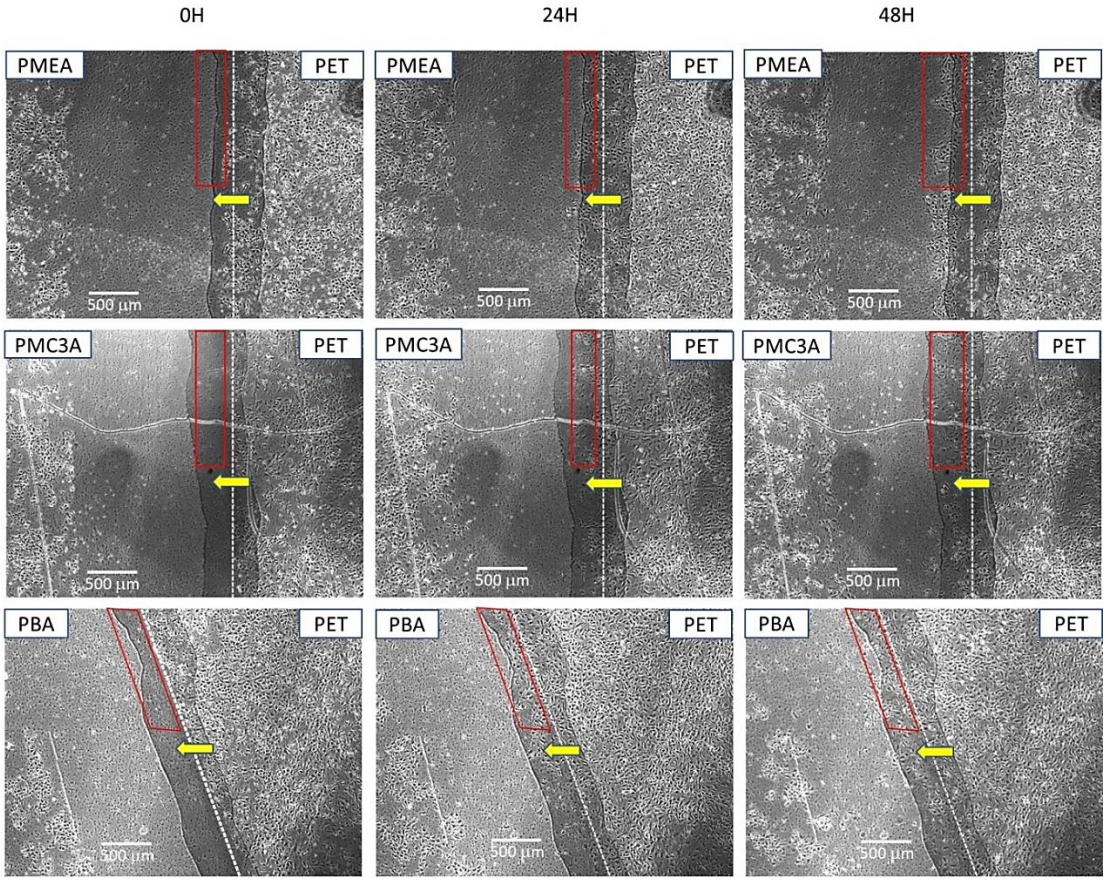

Figure 3.7. Observation of HUVECs migration between the substrate surfaces (scale bar = 500 µm). Time laps imaging confirmed the HUVECs migration from PET to polymers through the interface of PMEA-PET, PMC3A-PET, and PBA-PET. Migration was recorded from 0 to 48 h.

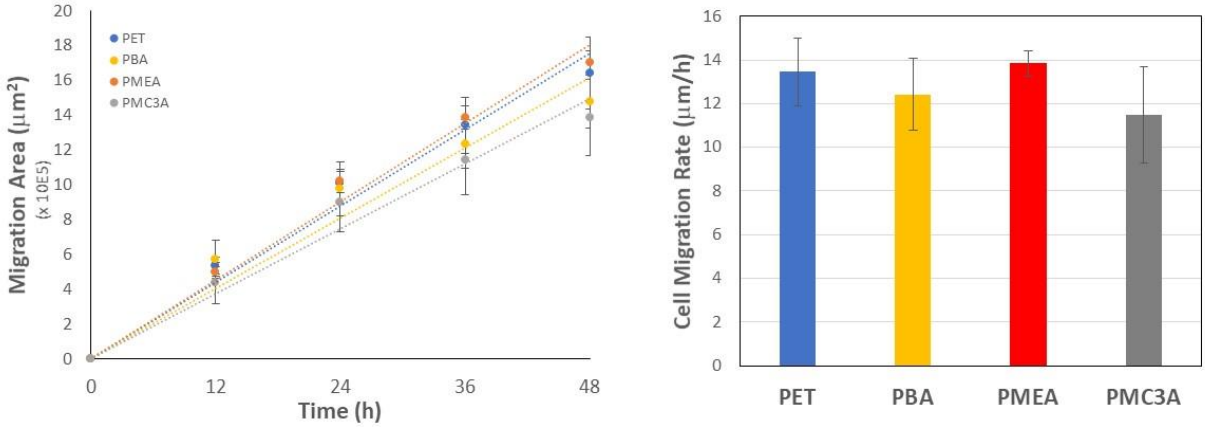

Figure 3.8. (a) Migration area **(b)** migration rate on PMEA-analogous polymers and bare PET. The data represent the mean ± SD (n = 5). $P < 0.05$ was used to define statistical significance.

3.3.5 Platelet adhesion on HUVECs monolayer cultured on polymers film

The biocompatibility and antithrombogenic behavior of PMEA-analogous polymers have already been studied based on different factors such as contact angle, protein adsorption, surface roughness, polymer chain length, platelet adhesion behavior, and IW content of each polymer. In the present study, we limited our investigation to only PMEA and PET because of the results of previous platelet adhesion tests under static conditions. PMEA showed an antithrombogenic surface compared with PET, where more platelets were adhered. In contrast, there is no significant study on platelet adhesion on a HUVECs monolayer that acts as an internal antithrombogenic surface of real blood vessels.

Figure 9 shows confocal images from the immunocytochemical analysis of HUVECs cultured on PMEA and PET. These CLSM images reveal that a similar type of HUVECs monolayer was formed on PET and PMEA. In addition, the shape of adhered HUVECs was comparable in both substrates. In our previous study we found that cell adhesion depends on the integrin-mediated binding protein adhesion to the specific surface, known as integrin-dependent adhesion [45]. However, cells can adhere to PMEA through direct physicochemical contact (integrin-independent contact) and via integrin-dependent adhesion. Furthermore, the HUVEC adhesion strength on PMEA was similar to that on PET. If the PET-based artificial vascular graft needs to be replaced because of thrombus formation after implementation, PMEA seems to offer the best alternative due to its proven antithrombogenicity. We observed that the number of platelets was much higher on bare PET (**Figure 3.10 a**) than bare PMEA (**Figure 3.10 e**), which agrees with our previous studies[23,41,50]. In contrast, few adhered platelets were found on the HUVECs monolayer on PET (Figure 10 b-d), and this was lower than in the bare PET. However, no significant number of platelets was found on the surfaces of HUVECs cultured on PMEA (**Figure 3.10 f-h**). Therefore,

PMEA seems to keep its antithrombogenic activity before and after HUVECs monolayer formation on PMEA. The summary of platelet adhesion test has shown in **Figure 3.10 (i)**. This antithrombogenic property of HUVECs monolayer on PMEA is essential information for the construction of ASDBVs. Further investigations are still needed in blood flow conditions, including in vivo experiments, for additional confirmation of this antithrombogenic property of PMEA.

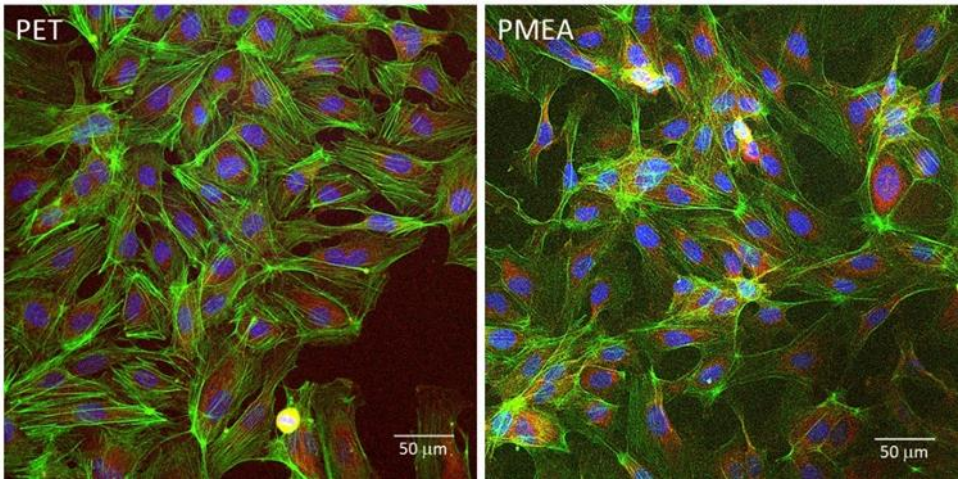

Figure 3.9. CLSM images of HUVECs cultured on PET and PMEA-coated surface. Blue: Cell nuclei; green: vinculin; red: actin fiber.

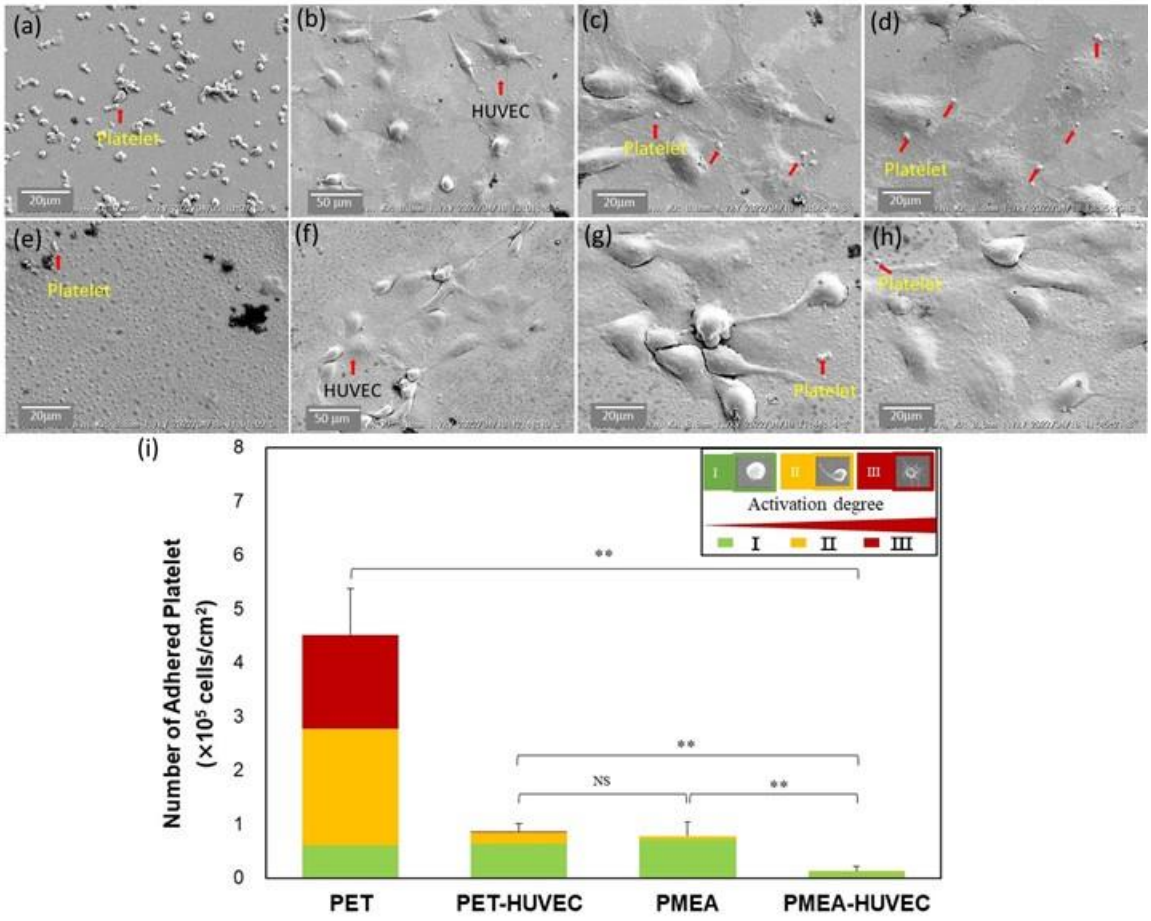

Figure 3.10. SEM image of (**a**) bare PET; (**b**) HUVEC monolayer on PET (scale bar = 50 μm); (**c**) and (**d**) HUVEC monolayer on PET (scale bar = 20 μm); (**e**) bare PMEA; (**f**) HUVEC monolayer on PMEA (scale bar = 50 μm); and (**g**) and (h) HUVEC monolayer on PMEA (scale bar = 20 μm). (i) Number of adhered platelets counted from SEM images. The data represent the means ± SD, n=15, **p < 0.05; *p < 0.01)

3.3.6 FM-AFM of HUVECs surface

To investigate the antithrombogenic activity of the HUVEC monolayer on PMEA from the hydration state perspective, FM-AFM was performed. **Figure 3.11** shows the results of the FM-AFM (z–x scan) on the HUVEC/PBS interface. The repulsive layer observed is marked in blue and white, demonstrating the degree of frequency shift. This repulsive layer may be attributed to the glycocalyx, which is composed of a hydrated sugar-rich layer. Our previous work demonstrated that such a hydrated polymer layer could contribute to the antithrombogenicity of the surfaces [51]. The repulsive layer on HUVEC was thicker than 10 nm. This is thicker than that observed on the PMEA spin-coated surface (approximately 5 nm) and thinner than that on the PMPC spin-coated surface (approximately 20 nm) on PET (see Supporting Information). Thus, the FM-AFM results corroborated the high antithrombogenic activity of the HUVEC monolayer on PMEA, as well as the platelet adhesion test results.

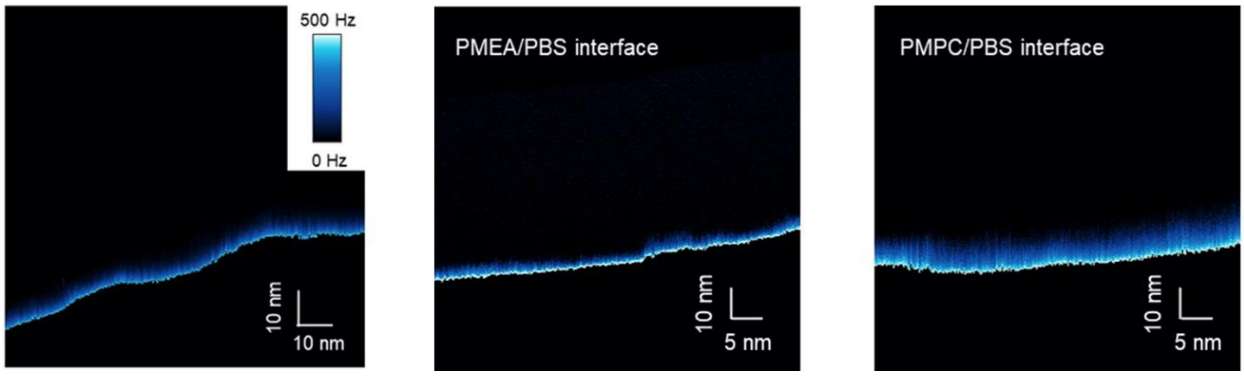

Figure 3.11. FM-AFM z-scan image on the HUVEC/PBS interface, PMEA/PBS and PMPC/PBS interface respectively.

3.4 Conclusions

In conclusion, the comparison study of HUVEC-substrate and HUVEC-HUVEC adhesion strength revealed the mechanism of HUVECs monolayer formation on PMEA-coated substrates. HUVECs attachment, proliferation, and migration indicated the blood compatibility of PMEA as a coating material. HUVECs migration from bare PET to the PMEA-coated side is a sign of cell migration from the native blood vessel to the artificial graft. In addition, the HUVECs monolayers effectively suppressed platelet adhesion. Finally, the FM-AFM observation of the hydration layer of HUVECs may be attributed to the presence of the glycocalyx layer. A healthy glycocalyx contributes to the antithrombogenic property of the PMEA-coated surface. Based on our results, a confluent monolayer of HUVECs can prevent platelet adsorption. Therefore, the PMEA coating can mimic the native blood vessel and can be used as a construction material for the development of ASDBVs for the antithrombogenic and confluent monolayer formation of ECs.

3.5 References

(1) WHO. Cardiovasculaer Diseases (CVDs)- World Health Organization. *available from www.who.int/news-room/fact-sheets/detail/cardiovascular-diseases-(cvds)* **2017**.

(2) Smith, S. C.; Collins, A.; Ferrari, R.; Holmes, D. R.; Logstrup, S.; McGhie, D. V.; Ralston, J.; Sacco, R. L.; Stam, H.; Taubert, K.; Wood, D. A.; Zoghbi, W. A. Our Time: A Call to Save Preventable Death from Cardiovascular Disease (Heart Disease and Stroke). *Global Heart* **2012**, *7* (4), 297–305. https://doi.org/10.1016/j.gheart.2012.08.002.

(3) Mallis, P.; Kostakis, A.; Stavropoulos-Giokas, C.; Michalopoulos, E. Future Perspectives in Small-Diameter Vascular Graft Engineering. *Bioengineering*. 2020, p 160. https://doi.org/10.3390/bioengineering7040160.

(4) Xue, L.; Greisler, H. P. Biomaterials in the Development and Future of Vascular Grafts.

Journal of Vascular Surgery. 2003, pp 472–480. https://doi.org/10.1067/mva.2003.88.

(5) Eckmann, D. M.; Tsai, I. Y.; Tomczyk, N.; Weisel, J. W.; Composto, R. J. Hyaluronan and Dextran Modified Tubes Resist Cellular Activation with Blood Contact. *Colloids and Surfaces B: Biointerfaces* **2013**, *108*, 44–51. https://doi.org/10.1016/j.colsurfb.2013.02.013.

(6) Thalla, P. K.; Fadlallah, H.; Liberelle, B.; Lequoy, P.; de Crescenzo, G.; Merhi, Y.; Lerouge, S. Chondroitin Sulfate Coatings Display Low Platelet but High Endothelial Cell Adhesive Properties Favorable for Vascular Implants. *Biomacromolecules* **2014**, *15* (7), 2512–2520. https://doi.org/10.1021/bm5003762.

(7) Gao, A.; Hang, R.; Li, W.; Zhang, W.; Li, P.; Wang, G.; Bai, L.; Yu, X. F.; Wang, H.; Tong, L.; Chu, P. K. Linker-Free Covalent Immobilization of Heparin, SDF-1α, and CD47 on PTFE Surface for Antithrombogenicity, Endothelialization and Anti-Inflammation. *Biomaterials* **2017**, *140*, 201–211. https://doi.org/10.1016/J.BIOMATERIALS.2017.06.023.

(8) Weidenbacher, L.; Müller, E.; Guex, A. G.; Zündel, M.; Schweizer, P.; Marina, V.; Adlhart, C.; Vejsadová, L.; Pauer, R.; Spiecker, E.; Maniura-Weber, K.; Ferguson, S. J.; Rossi, R. M.; Rottmar, M.; Fortunato, G. In Vitro Endothelialization of Surface-Integrated Nanofiber Networks for Stretchable Blood Interfaces. *ACS Applied Materials and Interfaces* **2019**, *11*, 5740–5751. https://doi.org/10.1021/acsami.8b18121.

(9) Radke, D.; Jia, W.; Sharma, D.; Fena, K.; Wang, G.; Goldman, J.; Zhao, F. Tissue Engineering at the Blood-Contacting Surface: A Review of Challenges and Strategies in Vascular Graft Development. *Advanced Healthcare Materials* **2018**, *7* (15), e1701461. https://doi.org/10.1002/adhm.201701461.

(10) Noy, J.-M.; Chen, F.; Akhter, D. T.; Houston, Z. H.; Fletcher, N. L.; Thurecht, K. J.; Stenzel, M. H. Direct Comparison of Poly(Ethylene Glycol) and Phosphorylcholine Drug-Loaded Nanoparticles In Vitro and In Vivo. *Biomacromolecules* **2020**, *21*, 2320–2333. https://doi.org/10.1021/acs.biomac.0c00257.

(11) Furuzono, T.; Ishihara, K.; Nakabayashi, N.; Tamada, Y. *Chemical Modifcation of Silk Fibroin with 2-Methacryloyloxyethyl Phosphorylcholine. II. Graft-Polymerization onto Fabric through 2-Methacryloyloxyethyl Isocyanate and Interaction between Fabric and Platelets*; 2000.

(12) Park, H. H.; Sun, K.; Seong, M.; Kang, M.; Park, S.; Hong, S.; Jung, H.; Jang, J.; Kim, J.; Jeong, H. E. Lipid-Hydrogel-Nanostructure Hybrids as Robust Biofilm-Resistant Polymeric Materials. *ACS Macro Letters* **2019**, *8* (1), 64–69. https://doi.org/10.1021/acsmacrolett.8b00888.

(13) Hoffmann, J.; Groll, J.; Heuts, J.; Rong, H.; Klee, D.; Ziemer, G.; Moeller, M.; Wendel, H. P. Blood Cell and Plasma Protein Repellent Properties of Star-PEG-Modified Surfaces. *Journal of Biomaterials Science, Polymer Edition* **2006**, *17* (9), 985–996.

(14) Zhang, M.; Desai, T.; Ferrari, M. *Proteins and Cells on PEG Immobilized Silicon Surfaces*; 1998; Vol. 19.

(15) Ratner Buddy, D. J. Blood Compatibility — a Perspective. *Journal of Biomaterials Science, Polymer Edition* **2000**, *11*, 1107–1119. https://doi.org/https://doi.org/10.1163/156856200744219.

(16) Kidane, A.; Lantz, G. C.; Jo, S.; Park, K. Surface Modification with PEO-Containing Triblock Copolymer for Improved Biocompatibility: In Vitro and Ex Vivo Studies. *Journal of Biomaterials Science, Polymer Edition* **1999**, *10* (10), 1089–1105.

(17) Stetsyshyn, Y.; Raczkowska, J.; Harhay, K.; Gajos, K.; Melnyk, Y.; Dąbczyński, P.; Shevtsova, T.; Budkowski, A. Temperature-Responsive and Multi-Responsive Grafted Polymer Brushes with Transitions Based on Critical Solution Temperature: Synthesis, Properties, and Applications. *Colloid and Polymer Science* **2021**, *299* (3), 363–383. https://doi.org/10.1007/s00396-020-04750-0.

(18) Liu, Q.; Urban, M. W. Stimulus-Responsive Macromolecules in Polymeric Coatings. *Polymer Reviews* **2022**, 1–35. https://doi.org/10.1080/15583724.2022.2065299.

(19) Bordenave, L.; Fernandez, Ph.; Rémy-Zolghadri, M.; Villars, S.; Daculsi, R.; Midy, D. In Vitro Endothelialized EPTFE Prostheses: Clinical Update 20 Years after the First Realization. *Clinical Hemorheology and Microcirculation* **2005**, *33* (3), 227–234.

(20) Deutsch, M.; Meinhart, J.; Fischlein, T.; Preiss, P.; Zilla, P. ,. Clinical Autologous in Vitro Endothelialization of Infrainguinal EPTFE Grafts in 100 Patients: A 9-Year Experience. *Surgery* **1999**, *126* (5), 847–855.

(21) Feugier, P.; Black, R. A.; Hunt, J. A.; How, T. v. Attachment, Morphology and Adherence of Human Endothelial Cells to Vascular Prosthesis Materials under the Action of Shear Stress. *Biomaterials* **2005**, *26* (13), 1457–1466. https://doi.org/10.1016/j.biomaterials.2004.04.050.

(22) Tanaka, M.; Motomura, T.; Kawada, M.; Anzai, T.; Yuu Kasori; Shiroya, T.; Shimura, K.; Onishi, M.; Akira Mochizuki. Blood Compatible Aspects of Poly(2-Methoxyethylacrylate) (PMEA)-Relationship between Protein Adsorption and Platelet Adhesion on PMEA Surface. *Biomaterials* **2000**, *21* (14), 1471–1481.

(23) Tanaka, M.; Mochizuki, A.; Ishii, N.; Motomura, T.; Hatakeyama, T. Study of Blood Compatibility with Poly(2-Methoxyethyl Acrylate). Relationship between Water Structure

and Platelet Compatibility in Poly(2-Methoxyethylacrylate-Co-2-Hydroxyethylmethacrylate). *Biomacromolecules* **2002**, *3* (1), 36–41. https://doi.org/10.1021/bm010072y.

(24) Hatakeyama, T.; Tanaka, M.; Hatakeyama, H. Thermal Properties of Freezing Bound Water Restrained by Polysaccharides. *Journal of Biomaterials Science, Polymer Edition*. Taylor and Francis Inc. October 1, 2010, pp 1865–1875. https://doi.org/10.1163/092050610X486946.

(25) Murakami, D.; Kobayashi, S.; Tanaka, M. Interfacial Structures and Fibrinogen Adsorption at Blood-Compatible Polymer/Water Interfaces. *ACS Biomaterials Science and Engineering* **2016**, *2* (12), 2122–2126. https://doi.org/10.1021/acsbiomaterials.6b00415.

(26) Kobayashi, S.; Wakui, M.; Iwata, Y.; Tanaka, M. Poly(ω-Methoxyalkyl Acrylate)s: Nonthrombogenic Polymer Family with Tunable Protein Adsorption. *Biomacromolecules* **2017**, *18* (12), 4214–4223. https://doi.org/10.1021/acs.biomac.7b01247.

(27) Hatakeyama, T.; Tanaka, M.; Hatakeyama, H. Studies on Bound Water Restrained by Poly(2-Methacryloyloxyethyl Phosphorylcholine): Comparison with Polysaccharide-Water Systems. *Acta Biomaterialia* **2010**, *6* (6), 2077–2082. https://doi.org/10.1016/j.actbio.2009.12.018.

(28) McGuigan, A. P.; Sefton, M. v. The Influence of Biomaterials on Endothelial Cell Thrombogenicity. *Biomaterials*. June 2007, pp 2547–2571. https://doi.org/10.1016/j.biomaterials.2007.01.039.

(29) Kitakami, E.; Aoki, M.; Sato, C.; Ishihata, H.; Tanaka, M. Adhesion and Proliferation of Human Periodontal Ligament Cells on Poly(2-Methoxyethyl Acrylate). *BioMed Research International* **2014**, *2014*. https://doi.org/10.1155/2014/102648.

(30) Fearon, I. M.; Gaça, M. D.; Nordskog, B. K. In Vitro Models for Assessing the Potential Cardiovascular Disease Risk Associated with Cigarette Smoking. *Toxicology in vitro : an international journal published in association with BIBRA*. 2013, pp 513–522. https://doi.org/10.1016/j.tiv.2012.08.018.

(31) Medina-Leyte, D. J.; Domínguez-Pérez, M.; Mercado, I.; Villarreal-Molina, M. T.; Jacobo-Albavera, L. Use of Human Umbilical Vein Endothelial Cells (HUVEC) as a Model to Study Cardiovascular Disease: A Review. *Applied Sciences (Switzerland)* **2020**, *10* (3). https://doi.org/10.3390/app10030938.

(32) Carmeliet, P.; Jain, R. K. Molecular Mechanisms and Clinical Applications of Angiogenesis. *Nature*. May 19, 2011, pp 298–307. https://doi.org/10.1038/nature10144.

(33) Zhao, Z.; Sun, W.; Guo, Z.; Zhang, J.; Yu, H.; Liu, B. Mechanisms of LncRNA/MicroRNA Interactions in Angiogenesis. *Life Sciences*. Elsevier Inc. August 1, 2020. https://doi.org/10.1016/j.lfs.2019.116900.

(34) Chen, Y. M.; Tanaka, M.; Gong, J. P.; Yasuda, K.; Yamamoto, S.; Shimomura, M.; Osada, Y. Platelet Adhesion to Human Umbilical Vein Endothelial Cells Cultured on Anionic Hydrogel Scaffolds. *Biomaterials* **2007**, *28* (10), 1752–1760. https://doi.org/10.1016/J.BIOMATERIALS.2006.12.005.

(35) Mahmoud, M.; Cancel, L.; Tarbell, J. M. Matrix Stiffness Affects Glycocalyx Expression in Cultured Endothelial Cells. *Frontiers in Cell and Developmental Biology* **2021**, *9*. https://doi.org/10.3389/fcell.2021.731666.

(36) Hoshiba, T.; Orui, T.; Endo, C.; Sato, K.; Yoshihiro, A.; Minagawa, Y.; Tanaka, M. Adhesion-Based Simple Capture and Recovery of Circulating Tumor Cells Using a Blood-Compatible and Thermo-Responsive Polymer-Coated Substrate. *RSC Advances* **2016**, *6*

(92), 89103–89112. https://doi.org/10.1039/c6ra15229e.

(37) Nishida, K.; Anada, T.; Kobayashi, S.; Ueda, T.; Tanaka, M. Effect of Bound Water Content on Cell Adhesion Strength to Water-Insoluble Polymers. *Acta Biomaterialia* **2021**. https://doi.org/10.1016/j.actbio.2021.07.058.

(38) Friedrichs, J.; Legate, K. R.; Schubert, R.; Bharadwaj, M.; Werner, C.; Müller, D. J.; Benoit, M. A Practical Guide to Quantify Cell Adhesion Using Single-Cell Force Spectroscopy. *Methods* **2013**, *60* (2), 169–178. https://doi.org/10.1016/j.ymeth.2013.01.006.

(39) Tanaka, M.; Motomura, T.; Kawada, M.; Anzai, T.; Kasori, Y.; Shimura, K.; Onishi, M.; Mochizuki, A.; Okahata, Y. A New Blood-Compatible Surface Prepared by Poly (2-Methoxyethylacrylate) (PMEA) Coating -Protein Adsorption on PMEA Surface. *Japanese Journal of Artificial Organs* **2000**, *29* (1), 209–216. https://doi.org/doi.org/10.11392/jsao1972.29.209.

(40) Krüger-Genge, A.; Hauser, S.; Neffe, A. T.; Liu, Y.; Lendlein, A.; Pietzsch, J.; Jung, F. Response of Endothelial Cells to Gelatin-Based Hydrogels. *ACS Biomaterials Science and Engineering* **2021**, *7* (2), 527–540. https://doi.org/10.1021/acsbiomaterials.0c01432.

(41) Sato, C.; Aoki, M.; Tanaka, M. Blood-Compatible Poly(2-Methoxyethyl Acrylate) for the Adhesion and Proliferation of Endothelial and Smooth Muscle Cells. *Colloids and Surfaces B: Biointerfaces* **2016**, *145*, 586–596. https://doi.org/10.1016/J.COLSURFB.2016.05.057.

(42) Kono, K.; Hiruma, H.; Kobayashi, S.; Sato, Y.; Tanaka, M.; Sawada, R.; Niimi, S. In Vitro Endothelialization Test of Biomaterials Using Immortalized Endothelial Cells. *PLoS ONE* **2016**, *11* (6). https://doi.org/10.1371/journal.pone.0158289.

(43) Hozumi, K.; Otagiri, D.; Yamada, Y.; Sasaki, A.; Fujimori, C.; Wakai, Y.; Uchida, T.;

Katagiri, F.; Kikkawa, Y.; Nomizu, M. Cell Surface Receptor-Specific Scaffold Requirements for Adhesion to Laminin-Derived Peptide-Chitosan Membranes. *Biomaterials* **2010**, *31* (12), 3237–3243. https://doi.org/10.1016/j.biomaterials.2010.01.043.

(44) Hersel, U.; Dahmen, C.; Kessler, H. RGD Modified Polymers: Biomaterials for Stimulated Cell Adhesion and Beyond. *Biomaterials* **2003**, *24* (24), 4385–4415. https://doi.org/10.1016/S0142-9612(03)00343-0.

(45) Hoshiba, T.; Yoshihiro, A.; Tanaka, M. Evaluation of Initial Cell Adhesion on Poly (2-Methoxyethyl Acrylate) (PMEA) Analogous Polymers. *Journal of Biomaterials Science, Polymer Edition* **2017**, *28* (10–12), 986–999. https://doi.org/10.1080/09205063.2017.1312738.

(46) Sancho, A.; Vandersmissen, I.; Craps, S.; Luttun, A.; Groll, J. A New Strategy to Measure Intercellular Adhesion Forces in Mature Cell-Cell Contacts. *Scientific Reports* **2017**, *7*, 46152. https://doi.org/10.1038/srep46152.

(47) Zeng, Y.; Zhang, X. F.; Fu, B. M.; Tarbell, J. M. The Role of Endothelial Surface Glycocalyx in Mechanosensing and Transduction. In *Advances in Experimental Medicine and Biology*; Springer New York LLC, 2018; Vol. 1097, pp 1–27. https://doi.org/10.1007/978-3-319-96445-4_1.

(48) Félétou, M. The Endothelium, Part I: Multiple Functions of the Endothelial Cells -- Focus on Endothelium-Derived Vasoactive Mediators. *Colloquium Series on Integrated Systems Physiology: From Molecule to Function* **2011**, *3* (4), 1–306. https://doi.org/10.4199/c00031ed1v01y201105isp019.

(49) Gori, T.; von Henning, U.; Muxel, S.; Schaefer, S.; Fasola, F.; Vosseler, M.; Schnorbus, B.;

Binder, H.; Parker, J. D.; Münzel, T. Both Flow-Mediated Dilation and Constriction Are Associated with Changes in Blood Flow and Shear Stress: Two Complementary Perspectives on Endothelial Function. *Clinical Hemorheology and Microcirculation*. IOS Press 2016, pp 255–266. https://doi.org/10.3233/CH-168102.

(50) Murakami, D.; Kitahara, Y.; Kobayashi, S.; Tanaka, M. Thermosensitive Polymer Biocompatibility Based on Interfacial Structure at Biointerface. *ACS Biomaterials Science and Engineering* **2018**, *4* (5), 1591–1597. https://doi.org/10.1021/acsbiomaterials.8b00081.

(51) Murakami, D.; Nishimura, S. nosuke; Tanaka, Y.; Tanaka, M. Observing the Repulsion Layers on Blood-Compatible Polymer-Grafted Interfaces by Frequency Modulation Atomic Force Microscopy. *Materials Science and Engineering C* **2021**, *133*, 112596. https://doi.org/10.1016/j.msec.2021.112596.

Chapter 4

Endothelial cell adhesion, proliferation, and cytoskeleton on grafted polymer surfaces of poly(2-methoxyethyl acrylate) (PMEA) analogs

Graphical Abstract

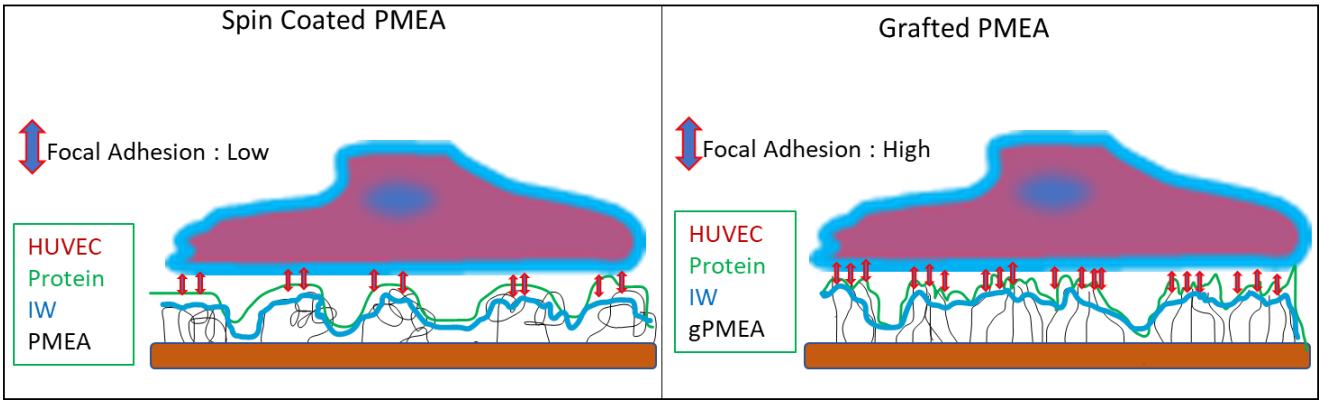

Abstract:

Cell attachment behavior on biocompatible polymer brush surfaces is more reliable than the coating methods. In this study, we have investigated the HUVECs attachment ability, proliferation, and growth on grafted PMEA analogous brush system and bare gold surfaces. Immunocytochemical analysis represents the cell morphology such as cell area, circularity, aspect ratio and number of focal adhesions. In addition, HUVECs adhesion strength also measured. It was found that the polymer brush system increases the cell adhesion strength for some PMEA analogues compared to coating. We found that the elevation of adhesion strength comes due to the controlled height and grafting density (σ =0.1 chain/nm2) of brush system and more focal adhesion formation of attached cells. Therefore, it can be said that polymer brush is an alternative of polymer coating in order to use it as a blood contacting surface.

Keywords: PMEA; HUVEC; Polymer brush, Cell adhesion strength

4.1 Introduction

Small-diameter artificial blood vessels with inner diameters of smaller than 6 mm have not been used widely because of early thrombus formation, graft occlusion and low patency rate[1–4]. To date, it is in developing stage and researchers are trying to overcome the limitations by incorporating different techniques and strategies. To develop small-diameter artificial blood vessels with anti-thrombus property and long-term patency, one of the promising approaches is endothelialization of the lumen by surface modification approaches of tissue engineering scaffolds[5]. Among of many approaches, biocompatible polymer coating has been widely used as an antithrombogenic coating on various sophisticated medical devices such as artificial hearts and lungs, stents, catheters, and dialyzers etc[6–9]. However, the conventional polymer coating methods, such as spin coating have not yet reached in technological maturity because of some limitations. Therefore, the perfect coating should satisfy many requirements: such as even surface thickness, surface roughness, long-term stability, high effectiveness, durability, biocompatibility, large-scale applicability, platelet adhesion suppuration, strong adhesion of endothelial cells and more.

Similarly, modification of the biochemical surface properties by polymer coating is one of the most common methods of improving endothelial cell adhesion on polymer surfaces[10]. Coating polymer surfaces with proteins, such as fibronectin and collagen, has been reported to promote cellular adhesion and proliferation. Fibronectin enhances adhesion at cell boundaries, whereas collagen produces extracellular matrix contacts[11,12].

Poly(2-methoxyethyl acrylate) (PMEA) is a water-insoluble homopolymer which is identified as a promising biocompatible and blood-compatible polymer by FDA. PMEA is easily synthesized, low toxic and suppresses protein adsorption and denaturation, platelet adhesion, and activation[13]. In addition, PMEA showed integrin dependent and independent cell adhesion

ability[14]. Our earlier report showed three types of water named 1) free water (scarcely bound water), 2) freezing-bound water (loosely bound water, intermediate water; IW), and 3) non-freezing water (tightly bound water) interacting with PMEA[15] . It was observed that an adhesion of blood component such as serum protein and platelet on PMEA analogs are inhibited with increasing of IW of PMEA and its analogs[16]. Furthermore, our group recently reported the observation of the interface of PMEA analogous and phosphate-buffered saline (PBS) using atomic force microscopy (AFM). This result revealed that spontaneous and homogeneous nanometer-scale protrusions appeared at the interface of PMEA which indicates the nanometer-scale phase-separated structures at the interface with water or PBS[17]. This kind of phase- separated structures suppressed fibrinogen adsorption as well as platelet adhesion, especially on the water-rich region. Ueda et al. showed that grafting density of PMEA affects the interfacial structure and plays an important role in the blood compatibility of the material. On the other hand, it has been revealed that PMEA surface can adsorb cell adhesion protein such as fibronectin which can increase the cell adhesion ability[18]. In contrast, there is not enough research on endothelial cell adhesion on polymer grafted system of PMEA analogs. In order to construct the small diameter blood vessel or vascular graft, endothelial cell adhesion behavior need be investigated on biocompatible polymer grafted systems.

Endothelial cell seeding on polymeric surface is an effective method of preventing thromboembolism on surfaces of cardio-vascular implants and medical devices because endothelial cells resist proteins adsorption that suppress platelet adhesion and fibrin formation[19–22]. Seeding of artificial vascular graft with endothelial cells before implantation significantly increases graft patency and survival[11,23,24]. From this point of view, studies in human umbilical vein endothelial cells (HUVECs) have been acknowledged as a suitable model for research on

human endothelium. HUVECs are an excellent model for the study of vascular endothelium properties and the main biological pathways involved in endothelium function[25].

In this study, we have used thiol terminated PMEA analogous polymers to graft them onto gold substrates. PMEA analogous polymers were grafted with fixed grafting density (σ=0.1 chain/nm^2) investigate the HUVECs adhesion behavior such as number of attached cells, cell area, circularity, aspect ratio, and cell adhesion strength on it at serum condition. According to our recent report on AFM measurement of the gPMEA/water interfaces, in-plane phase separation of the polymer surfaces developed gradually as polymer-rich and polymer-poor domains in hydrate condition. We are hoping that this phase separated surface will regulate the HUVECs adhesion capacity towards construction of small-diameter blood vessel.

4.2 Materials and Methods

4.2.1 Synthesis of grafted PMEA analogous polymer substrate

The polymer-grafted layers of poly(2-methoxyethyl acrylate) (gPMEA), poly(3-methoxypropylacrylate) (gPMC3A), poly(*n*-butyl acrylate) (gPBA), and poly(2-methoxyethylmethacrylate) (gPMEMA) were prepared involving S-Au interactions on the gold surfaces i.e., Au-sputtered (thickness≈10 nm) glass wafers (d=14 mm) for HUVECs attachment assay and adhesion strength measurements. The polymer-grafted surfaces were prepared by grafting-to method described previously[26–28]. We have recently reported that the biocompatibility of gPMEA was significantly affected by the grafting density and showed the highest performance at approximately 0.1 chains nm^{-2} [28]. So, the all samples in this work were prepared to be the grafting density of 0.1 chains nm^{-2}. The grafting densities were confirmed by quartz crystalline microbalance method. The chain length of polymers was adjusted as almost same as PMEA. The details of the synthesis, and polymer properties are provided in the Supplementary material in the

previous work[28,29]. The molecular weight (Mn), molecular weight distribution (Mw/Mn), and grafting density (σ) of each prepared polymer-grafted surface are listed in Table 1

4.2.2 Immobilization of PMEA analogous-SH on gold surface

The thiol-terminated PMEA analogous polymer (PMEA-SH, PMC3A-SH, PBA-SH and PMEMA-SH) was immobilized on the gold coated glass substrates. First, the glass wafers were cleaned with methanol by sonication for 10 minutes then coated with Titanium (Ti) and Gold respectively by using vacuum depositor. After that the gold coated glass substrates were cleaned with UV O_3/O_2 and then immersed in the thiol terminated PMEA analogous polymer solutions as listed in Table 1. The grafting density (σ) was controlled by the reaction time (Table 1) during the grafting process. After the reaction occurred, the samples were washed with acetone and methanol respectively at least five times, blow-dried in air, and placed under conditions of relative humidity <10%.

Table 4.1. Immobilization of thiol terminated PMEA analogous polymer

Polymer	M_n/g mol^{-1}	M_w/M_n	Grafting density (σ=chains/nm^2)	Solvent	Conc. (μM)	Temperature (˚C)	Time (Min)
PMEA	38,000	1.17	0.1	MeOH	1	Room temp (25)	20
PMC3A	42,000	1.19		MeOH	10	40	30
PBA	38,000	1.07		MeOH: EtOH=1:1	10	40	60
PMEMA	40,000	1.15		MeOH: Water=9:1	10	Room temp (25)	30

4.2.3 Endothelial cell culture on grafted polymers

Endothelial cells were used for all experiments described in this article. Commercially available human umbilical vein endothelial cells (HUVEC, Lonza, Cologne, Germany) were cultured under static cell culture conditions (37 °C, 5 vol% CO_2) in polystyrene-based cell culture flasks. Cells were used for 4 to 6 passages and cultured in endothelial basal medium (EBM-2)

supplemented with endothelial growth medium (EGM-2) Single Quots® kit and 2 vol% FCS (Lonza, Cologne, Germany). Prior to the experiments, 0.25% trypsin/EDTA solution (Thermo Fisher Scientific, Rockford, IL, USA) was used to detach the cells from the culture dish. The HUVECs solution was centrifuged at 1200 rpm for 3 min to isolate HUVECs from the old medium. Quantification of initial cell number was performed using a haemocytometer to adjust the cell density.

4.2.4 Cell attachment and proliferation assay

Cell attachment and proliferation assays were performed using 24 well plate (IWATA, Japan). Initially, the 24 well plate was coated with PMPC (0.5 wt/vol%) and stored for drying. The thiol terminated PMEA analogous polymer substrate were thereafter placed in 24 well plate. The substrates were then cured under ultraviolet (UV) light for 30 min. Phosphate-Buffered Saline (PBS) was then added to the well and stored it in incubator for 1 h at 37 °C. Afterwards, culture media were added and incubated under the same conditions for another 1 h at 37 °C. HUVECs were seeded on the substrates at 1 x 10^4 cells/cm^2 in serum-containing media and allowed to adhere and proliferate on the surface of the substrates for 1 h, 1 day and 3 days. After cell cultivation, at specific time intervals, the cells were fixed with 4% paraformaldehyde (Fujifilm Wako Pure Chemical Corporation, Osaka, Japan) and image was captured using microscope. The number of cells were counted using ImageJ software (version 1.53C, Bethesda, MD, USA).

4.2.5 Immunostaining Assessment of Cell Morphology

Before starting the experiment, the prepared substrates were preconditioned, as in the cell attachment and proliferation assays. HUVECs (1×10^4 cells/cm^2) were thereafter seeded on the grafted substrate ($\varphi = 14$ mm) and incubated for 1, 24, and 72 h. After culturing for specific times, the cells were fixed using preheated (37 ˚C) 4% (w/v) paraformaldehyde (Fujifilm Wako Pure

Chemical Corporation, Osaka, Japan) and stored outside for 10 min. Thereafter, 1% (v/v) Triton X-100 (Fujifilm Wako Pure Chemicals Co., Ltd., Osaka, Japan) in PBS (−) was added to increase plasma membrane permeability. After washing, the sections were blocked for 30 min. The substrates were thereafter treated with mouse monoclonal anti-human vinculin antibody (VIN-11-5; Sigma-Aldrich, St. Louis, MO, USA)(1:200) diluted in PBS (−) for 90 min at room temperature, and subsequently treated with Alexa Fluor 568-conjugated anti-mouse IgG (H + L) antibody(1:1000 dilution), Alexa Fluor 488-conjugated phalloidin (1:1000 diluted), DAPI (4,6-diamidino-2-phenylindole (1:1000 diluted)) (all from Thermo Fisher Scientific, Waltham, MA, USA), and all diluted in 10% blocking solution in PBS, treated for 1 h at room temperature. After performing these steps, stained cells were fixed on glass slides. Fluorescence images were captured using a confocal laser scanning microscope (CLSM) (FV-3000; Olympus, Tokyo, Japan). The cell area and circularity were evaluated quantitatively using ImageJ software (version 1.53C, Bethesda, MD, USA).

4.2.6 HUVECs- polymer brush surface interaction by SCFS

The thiol terminated PMEA analogous polymer substrates were exposed under UV for 30 min and thereafter incubated with PBS for 1 h at 37 °C. Subsequently, EGM-2 medium was added to the substrate and freshly detached cells (passage: 5–6) were injected. In contrast, the tip-less cantilever TL-CONT (spring constant k = 0.2 N/m, Bruker) was treated with human fibronectin solution (1 mg/mL) for 20 min. A single HUVEC was captured with a tipless cantilever for 10 min of holding time (set point: 2 nN). The force curves between the cell and the substrate were recorded using an atomic force microscope AFM (CellHesion, JPK) equipped with a cell-attached tipless cantilever (set point: 2 nN, approach rate: 5.0 μm/s, holding time: 120 s, retraction time: 15 μm/s). The adhesion force was defined as the maximum force for the detachment of the cell from the

substrate, corresponding to the force at the minimum point of the retraction curve. Adhesion work was estimated as the amount of work required to detach the cell from the substrate, corresponding to the area enclosed by the baseline and retraction curve[30].

4.2.7 Cell Area, Circularity and Aspect Ratio Calculation.

The cell length, width, spreading area, and perimeter were measured optically using ImageJ, cell circularity and aspect ratio were calculated as the following equation

$$Circularity = \frac{4\pi + \text{spreading area}}{(\text{perimeter})^2} \quad (1)$$

$$Aspect\ ratio = \frac{L_{cell}}{W_{cell}} \quad (2)$$

Where, L_{cell} and W_{Cell} are the cell length and width, respectively.

4.2.8 Statistical analysis

Data are expressed as mean ± standard deviation (SD) of at least three independent trials. The significance of the differences between the means of the individual groups was assessed by one-way analysis of variance followed by the Tukey–Kramer multiple comparison test using Origin Pro ver. 2019b (Northampton, MA, USA). Statistical significance was set at $p < 0.05$. Curve fitting was performed using the Origin Pro ver. 2019b (Northampton, MA, USA).

4.3 Results and Discussion

4.3.1 Cell attachment behavior on polymer grafted surface

In the field of artificial vascular graft designing and improving, the capacity for endothelial cell attachment, proliferation and other quantitative and qualitative analyses are considered as significant factors. Cultivation of HUVECs was performed on bare gold, gPMEA, gPMC3A, gPBA and gPMEMA respectively. The number of attached HUVECs on them at 1, 24, and 72 h were presented in **Figure 4.1.** These results show that the HUVECs densities on the grafted PMEA

analogous are different from each other. The seeding density was 1×10^4 cells/ cm^2. We found, HUVECs attached around 55% on bare gold, 70% on gPMEA, 40% on gPMC3A, 11% on gPBA and 30% on gPMEMA of its seeding density at 1 hour. With increasing time, the HUVECs proliferated to 179%, 180%, 131%, 48% and 129% respectively at 72 h of incubation compared to the seeding density.

Figure 4.2 shows the densities of the HUVECs cultured on bare gold, gPMEA, gPMC3A, gPBA and gPMEMA substrates as a function of time. HUVECs proliferation rate on gPMEA is higher than that on bare gold at 24 h but, nearly same at 72 h. gPMC3A and gPMEMA show similar increasing trend as gPMEA but the total number of HUVECs are lower than gPMEA at 72 h. However, we have seen the different trend for gPBA surface. Indeed, initial cell adhesion number on gPBA is very low, around 11% which indicated that the gPBA is not suitable for HUVECs survival due to its high hydrophobicity.

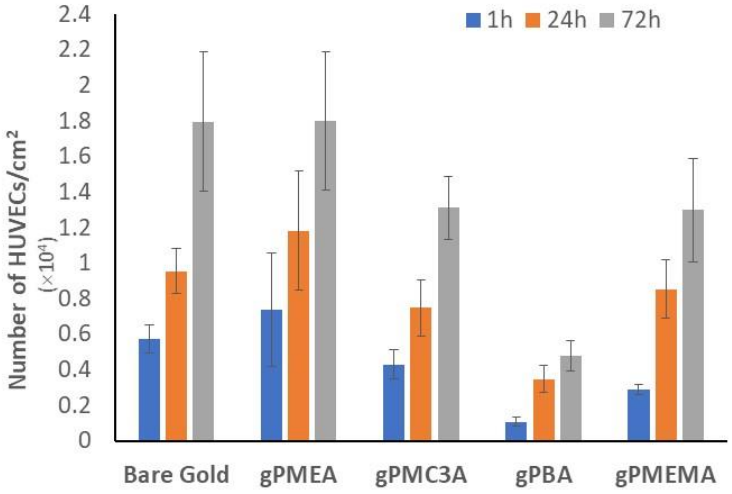

Figure 4.1. The number of adhered HUVECs on Bare gold, gPMEA, gPMC3A, gPBA and gPMEMA substrates at 1, 24, and 72 hours. The data represent the mean ±SD (n=3).

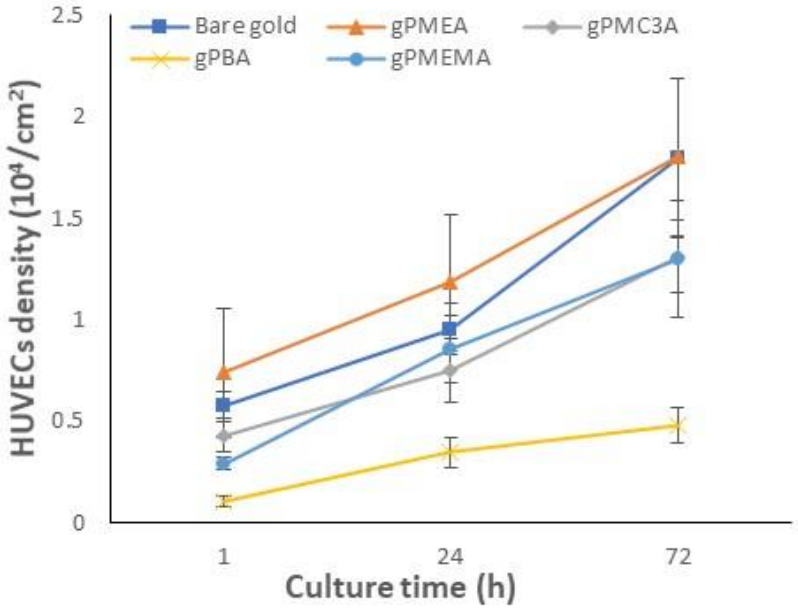

Figure 4.2. Densities of the HUVECs cultured on Bare gold, gPMEA, gPMC3A, gPBA and gPMEMA substrates as a function of time. The data represent the mean ±SD (n=3).

For further investigation, the CLSM image of adherent cell may be helpful to describe the surface morphology of HUVECs on each grafted polymer. The CLSM images of adherent HUVECs were taken at 72 h and shown in **Figure 4.3**. CLSM images of HUVECs on grafted PMEA analogous substrates are stained as blue: cell nuclei (DAPI); green: vinculin; red: actin fibers and the final image is the marge of all previous three stained images. From this study, it is clear that the spreading of HUVECs are higher on gPMEA than on the others. The number of focal adhesion and actin fibers are more significant on gPMEA. In addition, the attachment among cells was remarkable on gPMEA, meaning that HUVECs on gPMEA easily form a confluent monolayer. gPMC3A and gPMEMA shows similar morphology in shape and focal adhesion. In contrast, attached HUVECs on gPBA showed very unusual shape. Here, cells are loosely attached, and the spreading is extremely low even at 72 h. It is difficult to distinguish the cell nuclei and

ECM. This may be happened due to low anchoring point and more hydrophobic interaction between ECM and gPBA surface.

Figure 4.4 shows the quantitative analysis of attached HUVECs on each substrate. We have quantified the area, circularity and aspect ratio of attached HUVECs. We found that cell area on gPMEA is higher than that on other surfaces at initial stage. Similar trend is also visible at 24 h and 72 h. We reported previously that PMEA coating shows both integrin independent and dependent interaction[14]. It is expected that the integrin independent interaction promoted spreading and migration of HUVECs on gPMEA as well as integrin dependent interaction. In terms of circularity, cells are more circular on gPBA than the others. Circularity became lower on all substrates with increasing culturing time. On the other hand, the aspect ratio of HUVECs on all substrate shows similar leaning even though on gPMC3A and gPMEMA exhibited little elongation at higher culture time. Therefore, to explain the cell-surface interaction more closely, we have performed further investigations using SCFS as a more quantitative and short-time investigation.

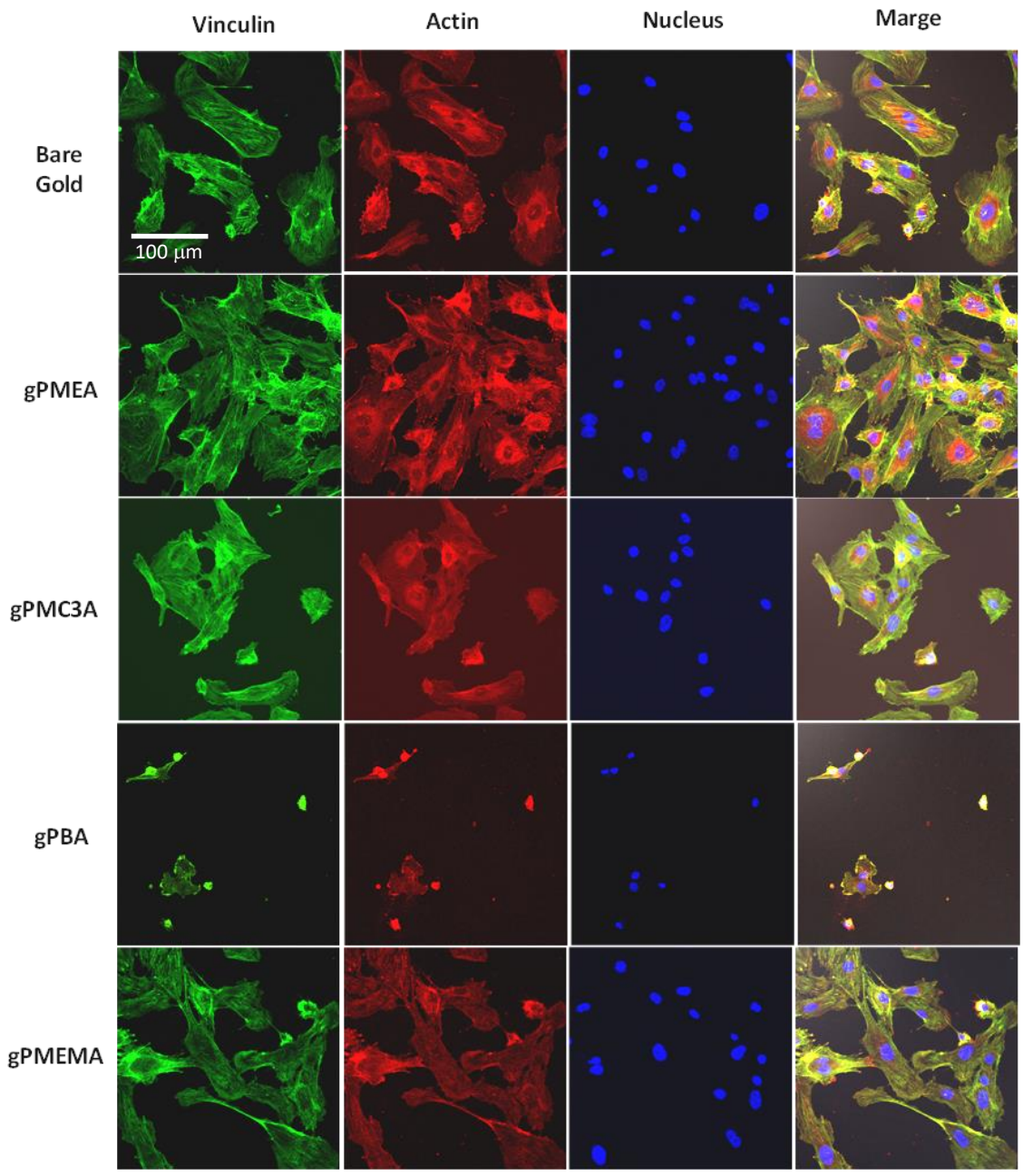

Figure 4.3. CLSM images of HUVECs on grafted PMEA analogous (polymer brush) substrates. Blue: cell nuclei (DAPI); green: vinculin; red: actin fibers. Image presented after 72 h of culture. Scale bar: 100 µm.

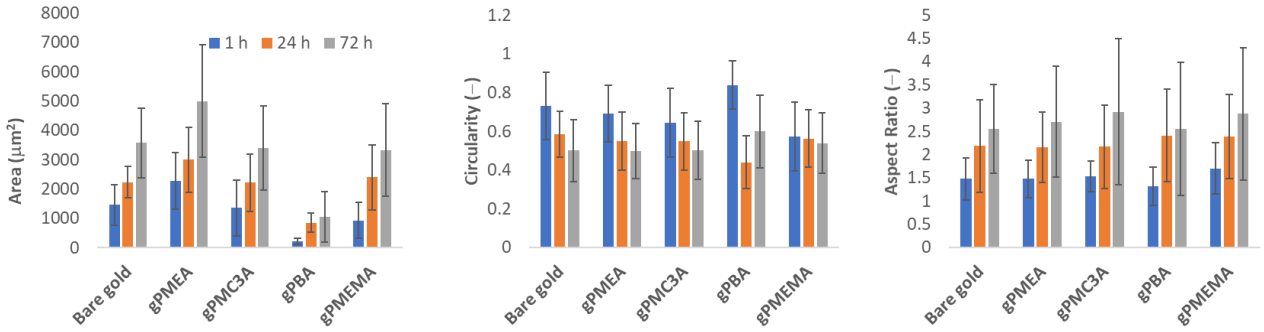

Figure 4.4. Evaluation of attached HUVECs morphology (area, circularity and aspect ratio) on Bare gold, gPMEA, gPMC3A, gPBA and gPMEMA at 1, 24 and 72 h of culture. The data represent the mean ±SD (n=25).

4.3.2 Evaluation of cell-substrate interaction r by SCFS

HUVECs-substrate interactions were measured quantitively using SCFS to explain the close relationship at the interface between cells and substrates during initial attachment. **Figure 4.5 (Upper)** shows the CLSM images of HUVECs cultured on bare gold, gPMEA, gPMC3A, gPBA and gPMEMA substrates respectively at 1h of incubation and **(Lower)** force-distance curve of HUVECs adhesion on substrates measured at 10s. In CLSM image, we observed that the HUVECs are more circular and spreading wider on gPMEA than the others. Similar tendency was found in the HUVECs adhesion strength and adhesion area measurement shown in **Figure 4.6**. HUVECs adhesion strength (nN) is presented in **Figure 4.7 (a)** and adhesion energy (J) is in **Figure 4.7 (b)** for various polymer substrates. These results shows that HUVECs adhesion strength on gPMEA is much higher than that of bare gold, gPBA and gPMEMA, although statistically difference is not significant to gPMC3A. In case of HUVECs adhesion energy, we found statistical difference between gPMEA and gPMC3A. If we compare these results with images of initial adhesion, the corelation can be found as the adhesion strength increases due to wide spreading of cell area and

increased number of focal adhesions in gPMEA. Bare gold and gPMEMA show almost same adhesion strength and energy. In contrast, gPBA shows weak interaction among all.

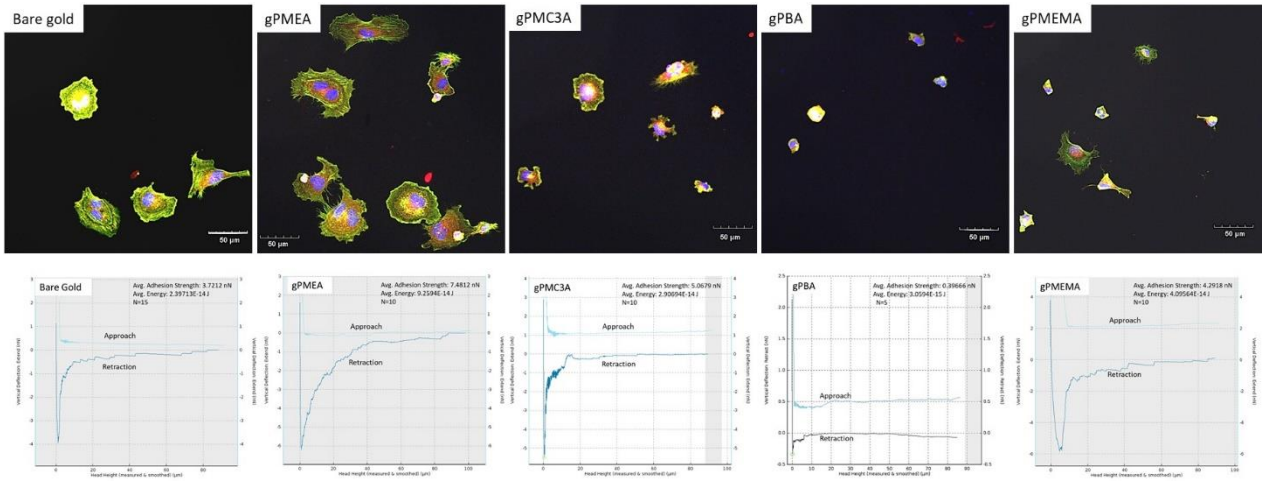

Figure 4.5. (Upper) CLSM images of HUVECs cultured on Bare gold, gPMEA, gPMC3A, gPBA and gPMEMA substrates respectively at 1h of incubation (initial attachment). Blue: cell nuclei (DAPI); green: vinculin; red: actin fibers. Scale bar: 50 μm. **(Lower)** Force-distance curve of HUVECs adhesion on equivalent substrate respectively.

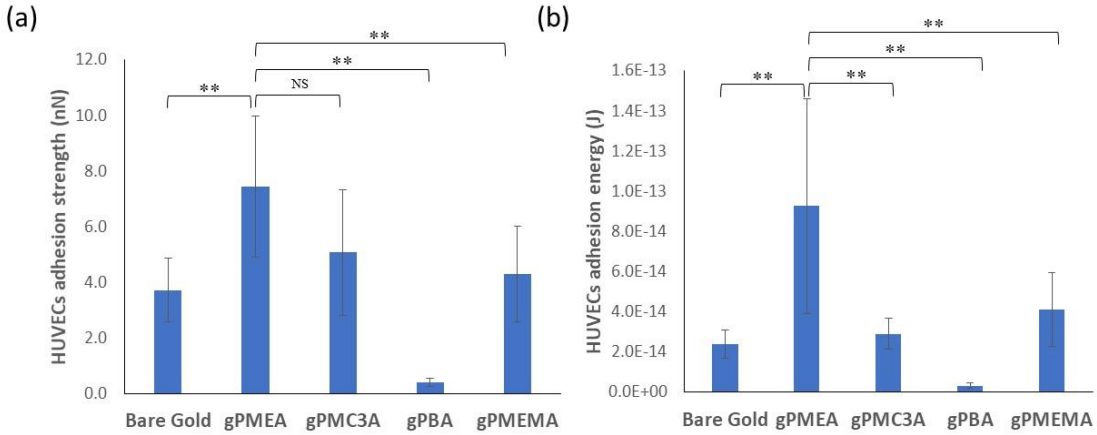

Figure 4.6. (a) HUVECs adhesion strength and (b) adhesion energy on various polymer substrate. The data represent the mean ± SD, n > 10**: $p < 0.05$.

4.3.3 Comparison between polymer coating and grafted systems

In this study, we have compared the surface interaction of HUVECs on PMEA analogous spin coating and polymer grafted systems in terms of HUVECs adhesion strength and adhesion energy. **Figure 4.7** represents the comparison of HUVECs adhesion strength and adhesion energy between (a) spin coated surface and (b) polymer grafted surface of PMEA analogous polymers. Here, we see dissimilar behavior in polymer grafted and spin coating systems. HUVECs adhesion strength is higher on gPMEA and gPMC3A than coating, whereas gPBA shows totally reverse tendency. HUVECs adhesion strength on gPBA is much lower than that on spin coated PBA. To explain this phenomenon, we need to go back our previous report, we showed that the AFM topographic images of polymer/PBS interfaces for PMEA, PMC3A, PBA, and PMEMA for both spin coated and grafted systems[17,29]. The spin-coated PMEA analogous polymer/water interfaces showed microphase separation into polymer-rich and water-rich domains, and the water-rich domains act to prevent the adsorption and activation of blood proteins such as fibrinogen[17]. Fibrinogen is responsible for platelet adhesion. On the other hand, polymer rich domains allowed fibrinogen adsorption. In addition to spin-coated PMEA analogs, grafted PMEA analogs were recently reported to exhibit phase separation in the in-plane direction[28]. Furthermore, the repulsive layers of hydrated polymer were clearly observed in the water-rich domains of gPMEA and gPMC3A by frequency modulation AFM (FM-AFM). From these works, gPBA exhibited phase separation similar to those of gPMEA and gPMC3A, but the water-rich domains scarcely generated on gPBA[29]. Actually, it was reported that the amount of adsorbed fibrinogen and exposure of the γ chain on a PBA surface were extremely higher than those on PMEA [28]. Therefore, more fibrinogen or hydrophobic proteins adhered on gPBA due to absent of repulsive layer which allowed platelet adhesion but decrease cell adhesion.

Furthermore, it was recently reported that fibronectin could easily adsorb both on polymer-rich and water-rich domains while fibrinogen mainly adsorbed on polymer-rich domains[18]. gPMEA used in this work was designed to be 0.1 chains/nm^2 of grafting density, at which the anti-thrombogenic performance of gPMEA is the highest. FM-AFM study clearly demonstrated that the gPMEA/PBS interface was occupied by higher ration of water-rich domains compared to that on spin-coated PMEA. The situation was similar also for gPMC3A. Thus, the adsorption of fibrinogen and other hydrophobic proteins are restricted more effectively on grafted surfaces than on spin-coated surfaces. In that case, the capacity for fibronectin adsorption increases, resulting in the increment of cell attachment ability. This may be attributed to the high HUVEC adhesion on gPMEA and gPMC3A compared to spin-coated surfaces. In order to construct artificial vascular graft, strong endothelial cell attachment is required. From our present study, we found that polymer grafted surfaces can be more suitable for endothelial cell adhesion, proliferation and as well as adhesion strength than spin coating surface, by adjusting the grafting density. Therefore, we can say that the grafted systems of PMEA analogous polymers are appropriate technique and possess high potential to be used for endothelialization during vascular graft preparation to achieve high performance small-diameter artificial blood vessels.

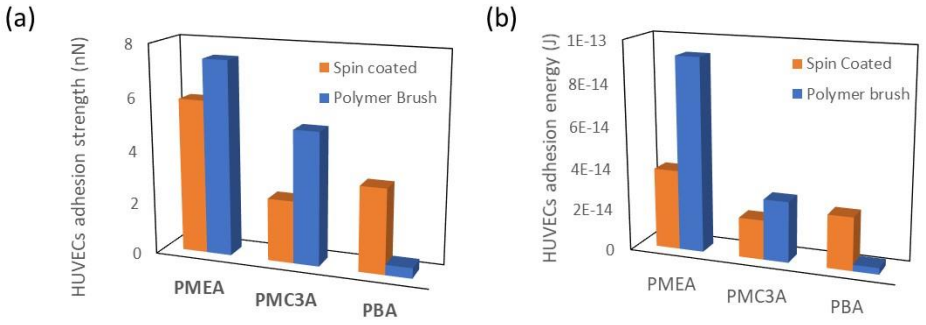

Figure 4.7. Comparison between spin coated polymer surface and grafted polymer surface (a) HUVECs adhesion strength and (b) HUVECs adhesion energy

4.4 Conclusion

In conclusion, based on the conducted experiments, results, and discussion, the surface interactions of HUVECs were measured extensively. We found that controlled PMEA analogous polymer brush system influences the HUVECs adhesion behavior such as the number of adhered HUVECs and cell adhesion strength. In addition, polymer brush also effects on cell area, circularity and aspect ratio. It can be said that gPMEA achieved the best outcomes among the other analogues in high HUVECs attachment, proliferation, and high adhesion strength at the initial stage. It can be suggested that PMEA can be used as a coating material through controlled grafting technique to develop surface for better endothelialisation of artificial vascular graft.

4.5 References

(1) Xue, L.; Greisler, H. P. Biomaterials in the Development and Future of Vascular Grafts. *Journal of Vascular Surgery*. 2003, pp 472–480. https://doi.org/10.1067/mva.2003.88.

(2) MacNeill, B. D.; Pomerantseva, I.; Lowe, H. C.; Oesterle, S. N.; Vacanti, J. P. Toward a New Blood Vessel. *Vascular Medicine* **2002**, *7* (3), 241–246.

(3) Isenberg, B. C.; Williams, C.; Tranquillo, R. T. Small-Diameter Artificial Arteries Engineered in Vitro. *Circ Res* **2006**, *98* (1), 25–35.

(4) Teebken, O. E.; Haverich, A. Tissue Engineering of Small Diameter Vascular Grafts. *European journal of vascular and endovascular surgery* **2002**, *23* (6), 475–485.

(5) Ohya, Y.; Nishimura, K.; Sumida, H.; Yoshizaki, Y.; Kuzuya, A.; Mahara, A.; Yamaoka, T. Cellular Attachment Behavior on Biodegradable Polymer Surface Immobilizing Endothelial Cell-Specific Peptide. *Journal of Biomaterials Science, Polymer Edition* **2020**, *31* (11), 1475–1488. https://doi.org/10.1080/09205063.2020.1762325.

(6) Mitra, D.; Kang, E. T.; Neoh, K. G. Polymer-Based Coatings with Integrated Antifouling

and Bactericidal Properties for Targeted Biomedical Applications. *ACS Applied Polymer Materials*. American Chemical Society May 14, 2021, pp 2233–2263. https://doi.org/10.1021/acsapm.1c00125.

(7) Thalla, P. K.; Fadlallah, H.; Liberelle, B.; Lequoy, P.; de Crescenzo, G.; Merhi, Y.; Lerouge, S. Chondroitin Sulfate Coatings Display Low Platelet but High Endothelial Cell Adhesive Properties Favorable for Vascular Implants. *Biomacromolecules* **2014**, *15* (7), 2512–2520. https://doi.org/10.1021/bm5003762.

(8) Tanaka, M.; Motomura, T.; Kawada, M.; Anzai, T.; Kasori, Y.; Shimura, K.; Onishi, M.; Mochizuki, A.; Okahata, Y. A New Blood-Compatible Surface Prepared by Poly (2-Methoxyethylacrylate) (PMEA) Coating -Protein Adsorption on PMEA Surface. *Japanese Journal of Artificial Organs* **2000**, *29* (1), 209–216. https://doi.org/doi.org/10.11392/jsao1972.29.209.

(9) Al-Khoury, H.; Espinosa-Cano, E.; Aguilar, M. R.; Román, J. S.; Syrowatka, F.; Schmidt, G.; Groth, T. Anti-Inflammatory Surface Coatings Based on Polyelectrolyte Multilayers of Heparin and Polycationic Nanoparticles of Naproxen-Bearing Polymeric Drugs. *Biomacromolecules* **2019**, *20* (10), 4015–4025. https://doi.org/10.1021/acs.biomac.9b01098.

(10) Tajima, S.; Chu, J. S. F.; Li, S.; Komvopoulos, K. Differential Regulation of Endothelial Cell Adhesion, Spreading, and Cytoskeleton on Low-Density Polyethylene by Nanotopography and Surface Chemistry Modification Induced by Argon Plasma Treatment. *Journal of Biomedical Materials Research - Part A* **2008**, *84* (3), 828–836. https://doi.org/10.1002/jbm.a.31539.

(11) Pratt, K. J.; Williams, S. K.; Jarrell, B. E. Enhanced Adherence of Human Adult Endothelial

Cells to Plasma Discharge Modified Polyethylene Terephthalate. *J Biomed Mater Res* **1989**, *23* (10), 1131–1147.

(12) Breithaupt-Faloppa, A. C.; Kleinheinz, J.; Crivello Jr, O. Endothelial Cell Reaction on a Biological Material. *Journal of Biomedical Materials Research Part B: Applied Biomaterials: An Official Journal of The Society for Biomaterials, The Japanese Society for Biomaterials, and The Australian Society for Biomaterials and the Korean Society for Biomaterials* **2006**, *76* (1), 49–55.

(13) Tanaka, M.; Motomura, T.; Kawada, M.; Anzai, T.; Yuu Kasori; Shiroya, T.; Shimura, K.; Onishi, M.; Akira Mochizuki. Blood Compatible Aspects of Poly(2-Methoxyethylacrylate) (PMEA)-Relationship between Protein Adsorption and Platelet Adhesion on PMEA Surface. *Biomaterials* **2000**, *21* (14), 1471–1481.

(14) Hoshiba, T.; Yoshihiro, A.; Tanaka, M. Evaluation of Initial Cell Adhesion on Poly (2-Methoxyethyl Acrylate) (PMEA) Analogous Polymers. *Journal of Biomaterials Science, Polymer Edition* **2017**, *28* (10–12), 986–999. https://doi.org/10.1080/09205063.2017.1312738.

(15) Tanaka, M.; Motomura, T.; Ishii, N.; Shimura, K.; Onishi, M.; Mochizuki, A.; Hatakeyama, T. Cold Crystallization of Water in Hydrated Poly(2-Methoxyethyl Acrylate) (PMEA). *Polymer International* **2000**, *49*, 1709–1713.

(16) Sato, K.; Kobayashi, S.; Kusakari, M.; Watahiki, S.; Oikawa, M.; Hoshiba, T.; Tanaka, M. The Relationship between Water Structure and Blood Compatibility in Poly(2-Methoxyethyl Acrylate) (PMEA) Analogues. *Macromolecular Bioscience* **2015**, *15* (9), 1296–1303. https://doi.org/10.1002/mabi.201500078.

(17) Murakami, D.; Kobayashi, S.; Tanaka, M. Interfacial Structures and Fibrinogen Adsorption

at Blood-Compatible Polymer/Water Interfaces. *ACS Biomaterials Science and Engineering* **2016**, *2* (12), 2122–2126. https://doi.org/10.1021/acsbiomaterials.6b00415.

(18) Nishida, K.; Baba, K.; Murakami, D.; Tanaka, M. Nanoscopic Analyses of Cell-Adhesive Protein Adsorption on Poly(2-Methoxyethyl Acrylate) Surfaces. *Biomaterials Science* **2022**, *10* (11), 2953–2963. https://doi.org/10.1039/D2BM00093H.

(19) Sterpetti, A. v; Schultz, R. D.; Bailey, R. T. Endothelial Cell Seeding after Carotid Endarterectomy in a Canine Model Reduces Platelet Uptake. *European Journal of Vascular Surgery* **1992**, *6* (4), 390–394.

(20) Stansby, G.; Berwanger, C.; Shukla, N.; Hamilton, G. Endothelial Cell Seeding of Vascular Grafts: Status and Prospects. *Cardiovascular Surgery* **1994**, *2* (5), 543–548.

(21) Kono, K.; Hiruma, H.; Kobayashi, S.; Sato, Y.; Tanaka, M.; Sawada, R.; Niimi, S. In Vitro Endothelialization Test of Biomaterials Using Immortalized Endothelial Cells. *PLoS ONE* **2016**, *11* (6). https://doi.org/10.1371/journal.pone.0158289.

(22) Chen, Y. M.; Tanaka, M.; Gong, J. P.; Yasuda, K.; Yamamoto, S.; Shimomura, M.; Osada, Y. Platelet Adhesion to Human Umbilical Vein Endothelial Cells Cultured on Anionic Hydrogel Scaffolds. *Biomaterials* **2007**, *28* (10), 1752–1760. https://doi.org/10.1016/J.BIOMATERIALS.2006.12.005.

(23) Zhuang, Y.; Zhang, C.; Cheng, M.; Huang, J.; Liu, Q.; Yuan, G.; Lin, K.; Yu, H. Challenges and Strategies for in Situ Endothelialization and Long-Term Lumen Patency of Vascular Grafts. *Bioactive Materials* **2021**, *6* (6), 1791–1809.

(24) Pawlowski, K. J.; Rittgers, S. E.; Schmidt, S. P.; Bowlin, G. L. Endothelial Cell Seeding of Polymeric Vascular Grafts. *Front biosci* **2004**, *9* (1–3), 1412.

(25) Baudin, B.; Bruneel, A.; Bosselut, N.; Vaubourdolle, M. A Protocol for Isolation and Culture

of Human Umbilical Vein Endothelial Cells. *Nature Protocols* **2007**, *2* (3), 481–485. https://doi.org/10.1038/nprot.2007.54.

(26) Biggs, C. I.; Walker, M.; Gibson, M. I. "Grafting to" of RAFTed Responsive Polymers to Glass Substrates by Thiol–Ene and Critical Comparison to Thiol–Gold Coupling. *Biomacromolecules* **2016**, *17* (8), 2626–2633.

(27) Zdyrko, B.; Luzinov, I. Polymer Brushes by the "Grafting to" Method. *Macromol Rapid Commun* **2011**, *32* (12), 859–869.

(28) Ueda, T.; Murakami, D.; Tanaka, M. Effect of Interfacial Structure Based on Grafting Density of Poly(2-Methoxyethyl Acrylate) on Blood Compatibility. *Colloids and Surfaces B: Biointerfaces* **2021**, *199*. https://doi.org/10.1016/j.colsurfb.2020.111517.

(29) Murakami, D.; Nishimura, S. nosuke; Tanaka, Y.; Tanaka, M. Observing the Repulsion Layers on Blood-Compatible Polymer-Grafted Interfaces by Frequency Modulation Atomic Force Microscopy. *Materials Science and Engineering C* **2021**, *133*, 112596. https://doi.org/10.1016/j.msec.2021.112596.

(30) Friedrichs, J.; Legate, K. R.; Schubert, R.; Bharadwaj, M.; Werner, C.; Müller, D. J.; Benoit, M. A Practical Guide to Quantify Cell Adhesion Using Single-Cell Force Spectroscopy. *Methods* **2013**, *60* (2), 169–178. https://doi.org/10.1016/j.ymeth.2013.01.006.

Chapter 5

Conclusion: Summary and Future research

5.1 Summary

An effective and functionating artificial small diameter artificial blood vessels can be designated as the second life carrier for millions of cardiovascular patients around the world. With the rapid increasing of cardiovascular risk factors such as unhealthy lifestyle, huge working load, suppression of happiness, lack of love and smoking trigger the diabetes and obesity which are considered the origin of heart disease. Nowadays, CVD is not only threatened for aged people, but also young individuals are affecting day by day. One of the applied therapeutic approaches that are currently followed is the replacement of damaged vessels with autologous vascular grafts which is usually collated from patients' body, but it causes secondary trauma. Therefore, development of artificial small diameter blood vessels is very urgent. Consequently, due to the fast growing of these disease, the necessity of artificial blood vessels is mounting so faster. Although there are some large diameter vascular grafts already invented and performed in clinical trial, but it shows poor patency rate which is beyond the basic requirements. Long term patency still the core problem. On the other hand, the performance of small diameter blood vascular grafts is more critical than that of large diameter graft. Reduction of thrombus formation is one of the main challenges for small diameter blood vessel. Researchers are trying to solve this problem by incorporating various techniques including invention of biocompatible biomaterial, blood compatible polymer, changing the fabrication methods and surface modification methods to improving mechanical properties and blood compatibility.

According to the above circumstances, we have started our research to develop artificial small diameter blood vessels using PMEA analogous polymer. PMEA is a clinically approved and used

antithrombogenic water insoluble polymer which has been used as a coating material for several medical devices. So, we aimed to investigate the PMEA analogous polymers through endothelial cell adhesion ability and antiplatelet property. It is known that healthy and confluent endothelium layer can suppress the platelet adhesion. Therefore, we had fixed our strategy in this way. We focused on the polymer that can allow endothelial cell to attach strongly, migrate and proliferate throughout the surface. In addition, it should be acted as anti-platelet surface until the confluent endothelium formation. We have used HUVECs throughout my thesis as our endothelial model cells. The findings of my research have been presented in three different chapters in the earlier sections. The summary of each chapter is presented in following the parts in brief.

In chapter 2, based on the conducted experiments, results, and discussion, the surface interactions of HUVECs were measured extensively. The IW content of PMEA analogous polymers influences the HUVEC adhesion strength and the number of adhered HUVECs and platelets on each substrate. It can be said that PMEA achieves the best outcomes among the analogues, such as low platelet adhesion and adhesion strength, high HUVECs attachment, proliferation, and high adhesion strength at the initial time. It can be suggested that PMEA can be used as a construction material to develop ASDBV because of its nonthrombogenic behavior and strong adhesion of endothelial cells.

Chapter 3 shows the comparison study of HUVEC-substrate and HUVEC-HUVEC adhesion strength revealed the mechanism of HUVECs monolayer formation on PMEA-coated substrates. HUVECs attachment, proliferation, and migration indicated the blood compatibility of PMEA as a coating material. HUVECs migration from bare PET to the PMEA-coated side is a sign of cell migration from the native blood vessel to the artificial graft. In addition, the HUVECs monolayers effectively suppressed platelet adhesion. Finally, the FM-AFM observation of the hydration layer

of HUVECs may be attributed to the presence of the glycocalyx layer. A healthy glycocalyx contributes to the antithrombogenic property of the PMEA-coated surface. Based on our results, a confluent monolayer of HUVECs can prevent platelet adsorption. Therefore, the PMEA coating can mimic the native blood vessel and can be used as a construction material for the development of ASDBVs for the antithrombogenic and confluent monolayer formation of ECs.

In chapter 4, the surface interactions of HUVECs on polymer grafted surfaces were measured extensively. We found that controlled PMEA analogous polymer grafted system influence the HUVECs adhesion behavior such as the number of adhered HUVECs and cell adhesion strength. In addition, polymer grafted surfaces also effect on cell area, circularity and aspect ratio. It can be said that grafted PMEA achieved the best outcomes among the other analogues in high HUVECs attachment, proliferation, and high adhesion strength at the initial stage. It can be suggested that PMEA can be used as a coating material through controlled grafting technique to develop surface for better endothelialisation of artificial vascular graft.

Finally, it can be said that PMEA showed the best outcomes in order to HUVECs adhesion, migration and proliferation. The cells morphology after attachment reveals the strong adhesion strength to the PMEA substrates which was measured by SCFS. HUVECs monolayer formation and suppression of platelet adhesion on confluent HUVECs reveals the candidacy of PMEA as coating material in lumen side of vascular graft for the construction of artificial small diameter blood vessel.

5.2 Future research

According to the purpose of this study, we have already achieved the primary goal by finding the suitable polymer, PMEA, through the several investigations specially HUVECs adhesion strength and adhesion energy measurement by SCFS, polymer surface and HUVECs surface hydration state observation by FM-AFM, HUVECs attachment test, and platelet adhesion number test. Now we are confirmed that PMEA can suppress the platelets adhesion and increase the HUVECs adhesion, monolayer formation. At this moment, it can be said that PMEA can be used as only coating material using grafting technique. Although the journey to construction of artificial small diameter blood vessel just started. We have to overcome many challenges and need to go forward. In near future, we have to do several intensive investigations on HUVECs, platelets and polymer surface. We have to clarify the effect of glycocalyx on platelet adhesion and activation, study on platelet surface, hydration state of platelets surface. So, we have set our extended goal such as elucidation of the mechanism of polymer-HUVECs-glycocalyx-platelet interaction at static as well as blood flow condition and how to make tough PMEA with required mechanical and physicochemical properties. Then, preparation of tubelike structure for in-vitro and in-vivo experiment.

PMEA is dense liquid like amorphous polymer. Making of tube-like structure is quite difficult with PMEA and the mechanical property of PMEA still uncertain for direct construction of blood vessels. Therefore, we are aiming to make comparatively hard PMEA by making copolymer of PMEA or making composites with incorporating other biocompatible materials or grafting with cellulose nanoparticles to get new shape without losing the excellent biocompatible property of PMEA polymer.

ACKNOWLEDGEMENTS

بِسْمِ اللَّهِ الرَّحْمَنِ الرَّحِيم

Alhamdulillah, all praises go to Allah the Almighty, the Most Gracious, and the Most Merciful for His blessing given to me during my study and in completing this doctoral thesis.

I would like to acknowledge my indebtedness and render my warmest thanks to my supervisor, Professor Masaru Tanaka, who made this work possible. His cordial guidance, expert advice and kind support have been invaluable throughout all stages of the work. I have learnt idea generating, critical and creative thinking and how to keep going forward to the goal by defending the unavoidable obstacles through his way of teaching, motivation, and encouragement. I am always delighted and feel blessed to become a member of the Tanaka Lab. Hopefully this knowledge will act as the key factors of my future success as a researcher.

I would like to express my sincere gratitude to my co-supervisor, Dr. Daiki Murakami, Assistant Professor, for his for his keen supervision, guidance, co-operation, inspiration, and continuous support throughout PhD journey. I am grateful to him and appreciate his serenity, friendliness, and expertise. I would be unable to progress in this field without his assistance. His care for the students is truly commendable. I am truly thankful for placing your trust and confidence in my abilities to carry out this research project.

I am also heartily grateful to Prof. Takahisa Anada for his patient, agreeable, suggestion and kind support. I learn how to become active from him. I would also wish to express my gratitude to Prof. Shingo Kobayashi for extended discussions and valuable suggestions which have contributed greatly to conducting my research. I always found him kind, cordial, and supportive with a smile face.

I would like to express my sincere gratitude to the Japanese government for providing the MEXT scholarship to support me to complete the doctoral study. I would like to express my sincere gratitude to Professor Masahiro Goto and Professor Shigenori Fujikawa for agreeing to be the member of my

PhD thesis committee. I really appreciate for their constructive comments and invaluable advice.

I would also like to thank to Dr. Kei Nishida, Dr. Shinnosuke Nishimura and Dr. Shohei Shiomoto, post-doctoral research fellow, for their help and advice throughout my study in Kyushu University. I am thankful to lab secretary Ms. Kumiko Araki, Ms. Tomoko Matthews, Ms. Sumiko Nakayama, and technical staff Ms. Yukiko Tanaka and Ms. Aki Yamamoto, for their kindness, assistance, thoughtful, and caring support for my study and daily life.

I am very happy to acknowledge all past and present members of the Tanaka Lab for their help, cooperation, and friendship attitude. Particularly, Dr. Toshiki Sonoda, Dr. Ms. Shichen Liu, Dr. Ms. Rubaiya Anjum and Dr. Tomoya Ueda, for their useful advice and help in experiments and research. Special thanks to Dr. Md. Rafiqul Islam for his help and suggestions, and Yasuki Okazaki-San for his kindness in Japanese language support during my needs. I never forget the kindheartedness, support, and love of Japanese people.

Finally, I would like to submit my kind respect to my parents and family. I am extremely grateful to my parents for their love, prayers, caring and sacrifices for educating and preparing me for my future. I am very much thankful and indebted to my beloved wife Ms. Razia Sultana and my only little daughter Azayiz Razwaa (Azbah) for their love, understanding, prayers and continuing support to complete this research work. Specially, my daughter who sacrificed the infanthood and affectionate moments from her parents. Also, I express my thanks to all my relatives and best wishers for their remote support and valuable prayers. May Allah bless all of us.

Md. Azizul Haque

July 2022, Japan